COMPUTER AIDED DESIGN AND OPTIMIZATION OF TILLAGE TOOL: ROTAVATOR

DISSERTATION

submitted to

Marathwada Agricultural University
in partial fulfillment of the
requirement for the degree of

MASTER OF TECHNOLOGY

(Agricultural Engineering)

in

FARM POWER AND MACHINERY

by

Mr. BADGUJAR PARAG DEVIDAS

UNDER THE GUIDANCE OF

Prof. G. U. SHINDE

DEPARTMENT OF FARM POWER AND MACHINERY,
COLLEGE OF AGRICULTURAL ENGINEERING AND TECHNOLOGY,
MARATHWADA AGRICULTURAL UNIVERSITY,
PARBHANI – 431402 (M.S.), INDIA.

June-2009

DEDICATED TO

My

PARENTS,

&

BROTHER

CANDIDATE'S DECLARATION

I, here by declare that the dissertation or part there of has not been submitted by me to any other University or Institution for a degree or diploma.

Badgujar.

Place : **Parbhani** **(Mr. BADGUJAR P. D.)**

Date : 07 / 01 /2010

Prof. G. U. Shinde.
Assistant Professor,Mech Engg.
Department of Farm Power and Machinery,
College of Agricultural Engineering & Technology,
Marathwada Agricultural University,
Parbhani – 431 402 (M.S.)

CERTIFICATE-I

This is to certify that the dissertation entitled **"Computer Aided Design and optimization of tillage tool:Rotavator"** submitted to Marathwada Agricultural University, Parbhani in partial fulfillment of the requirement for the award of the degree of **Master of Technology (Agril. Engineering)** in **Farm Power and Machinery** embodied the results of the bonafied study carried by **Mr. BADGUJAR PARAG DEVIDAS** under my guidance and supervision. I also certify that the dissertation has not been previously submitted by him for the award of Degree or Diploma of any University or Institute.

Place : Parbhani.
Date : 07/01/2010

Prof. G. U. Shinde
(Research Guide)

CERTIFICATE-II

This is to certify that the dissertation entitled **"Computer Aided Design and optimization of tillage tool: Rotavator"** submitted by **Mr. BADGUJAR PARAG DEVIDAS** to the Marathwada Agricultural University, Parbhani in partial fulfillment of the requirement for the degree of **MASTER OF TECHNOLOGY (Agril. Engg.)** in the subject of **Farm Power and Machinery** has been approved by the students advisory committee after oral examination in collaboration with external examiner.

External Examiner
(Prof. D.D. Tekale)

Prof. G. U. Shinde
(Research Guide)

Advisory Committee

Dr. R.G. Nadre

Prof. J. M. Potekar

Prof. S. N. Solanki

Prof. P. A. Munde

Prof. V. M. Bhosle

Associate Dean & Principal
College of Agricultural Engineering & Technology M. A. U. Parbhani

Associate Dean & Principal
College Of Agril. Engineering & Technology, M.A.U., Parbhani

Head
Deptt. Of Farm Power & Machinery
College of Agril. Engg. & Tech.
M.A.U. Parbhani

HEAD
Department of Farm Machinery & Power
M.A.E.U., Parbhani

ACKNOWLEDGEMENT

It is exquisite ecstasy and matter of privilege as well as an immense pleasure to express my sincere feelings of profound gratitude and indebtedness, adorned by the showers of thanks towards my research guide and chairman of my advisory committee to Prof. G. U. Shinde Assistant Professor, Department of Farm Machinery and Power, College of Agricultural Engineering and Technology, M.A.U., Parbhani for nourishing incentive and inspiration within me along with the unending encouragement, excellent guidance and give valuable suggestions during the course of investigation, and preparation and presentation of dissertation. His valuable suggestion helped me not only in completing my research work but will prove as light house through out my future life

It is my proud privilege to record a deep sense of gratitude of Dr. R.G. Nadre, Associate Dean and Principal and Prof. J. M. Potekar, Head Department of Farm Power and Machinery, C.A.E. & T., M.A.U., Parbhani., for valuable suggestions, consistent efforts and strives to keep the progress of work genuine by providing the necessary facilities throughout the research work.

I have great pleasure in expressing my deep sense of gratitude, indebtedness and sincere thanks to the members of advisory committee, Prof. S.N. Solanki, Associate Professor, Department of Farm Machinery and Power, C.A.E.T., M.A.U. Parbhani, Prof. P. A. Munde, Assistant Professor, Department of Farm Machinery and Power, C.A.E.T., M.A.U. Parbhani, and Prof. V. M. Bhosle, Associate Professor, B. S. C. T. Deptt. C.A.E.T., M.A.U. Parbhani, his valuable guidance and creative suggestions during my research work.

My sincere thanks and gratitude's are extended to Mr. Sundaram Raout, Farzin Irani, Dhiraj Ghotekar, Ashish Narayan, Nilesh, Kiran, Ashish Satao, Chintan, Harsh and other all team member in Extencore Solution Pvt. Ltd. Pune for his valuable information and kind co-operation during research work.

I am also thankful to shri.Bhatcharya of Department of Farm Machinery and Power, C.A.E.T., M.A.U. Parbhani for their timely help rendered during the conduct of research work.

The personal thanks to my friends Mr. Niranjan, Kunal, Rajendra, Nilesh, Swati, Rajshri, Amit, Kiran, Vikram, Pramod, Aniket, Rahul, Kedar Yogesh, Avinash Gadekar, Avinash Gangurde, Tanaji, Sooraj I take this opportunity to thank them for their constant encouragement and help during the entire project work.

One uses the choicest words to measure the boundless love for someone. I express heartly feelings to my Father Mr. Devidas N. Badgujar, Mother Sushila D. Badgujar, Brother Mr. Niranjan D. Badgujar and Sister Yogita S. Badgujar for encouraging me throughout my education. The words with me are insufficient to express the feelings of my heart to acknowledge them for their difficult job of educating me in all comforts without which this work would not have seen the light of the day at all.

While traveling on this path of education many hands pushed me forth learned hearts put me on the right track enlightened by their knowledge and experience. I ever rest thanks to all if them.

Finally I owe my sincere thanks to all those whom I might have forgotten due to my short come.

Place: Parbhani
Date:07/01/2010

Badgujar.
(Badgujar P. D.)

ABBREVIATIONS

Agril. /Agric.	-	Agricultural.
ASAE	-	American Society of Agricultural Engineering
B-REP	-	Boundary representation
C	-	Carbon
CAD	-	Computer aided design
CAM	-	Computer aided modeling
cm	-	Centimeter.
cm^2	-	Centimeter square
cm^3 /cc	-	Centimeter cube
c/s	-	Cross section
CSG	-	Constructive solid geometry
d.b.	-	dry basis
B.C	-	Boundary condition
Deptt.	-	Department
dia.	-	Diameter
DOF	-	Degree of freedom
Dr.	-	Doctor
DVS	-	Displacement vector sum
e.g.	-	Example gratia
EFC	-	Effective field capacity
et. al.	-	and all
etc.	-	etceteras
FBM	-	Feature based modeling
FEA	-	Finite element analysis
FE	-	Finite element
F.S.	-	Factor of safety
fig.	-	Figure
F/M	-	Force/moment
g	-	grams

ha	-	Hectare.
hexes	-	Hexahedrons
hp	-	Horse power
hr	-	hour
i.e.	-	that is
ISAE	-	Indian Society of Agricultural Engineers
J	-	Journal
kg	-	Kilogram.
kg-m	-	Kilogram meter
km	-	Kilometer.
KN	-	Kilo-Newton
Kw	-	Kilo watt
lit	-	liter
M	-	Meter.
M.A.U.	-	Marathwada Agricultural University
m.c.	-	Moisture content
M.S.	-	Mild Steel
m/s	-	Meter per second
m^2	-	Meter square.
m^3	-	Meter cube
mm	-	Mili meter.
Mpa	-	Mega pascal
Max	-	Maximum
Min	-	Minimum
No.	-	Number
Pro-e	-	Pro-engineering
Prof.	-	Professor
PTO	-	Power take off
rpm	-	Revolutions per minute
Rs	-	Rupees
R_X	-	Rotation along X axis

Ry	-	Rotation along Y axis
Rz	-	Rotation along Z axis
Sci.	-	Science.
Sec	-	Second
Sr.No	-	Serial number.
Tech	-	Technology
TFC	-	Theoretical field capacity
tets	-	Tetrahedrons
U_X	-	Translation in X direction
U_Y	-	Translation in Y direction
Uz	-	Translation in Z direction
VMS	-	Von mises stress
viz.	-	Namely
Wt	-	Weight
%	-	Per cent
&	-	and
θ	-	Angle
1-d	-	One dimensional
2-d	-	Two dimensional
3-d	-	Three dimensional

LIST OF TABLES

LIST OF FIGURES

CONTENTS

INTRODUCTION

CHAPTER I

INTRODUCTION

Mechanization plays an important role in agriculture for increased production, productivity and profitability through timeliness in operation. During Fourth and fifth plan more sophisticated implements were introduced. The major thrust of agriculture mechanization is to reduce drudgery in the field operation and provide better quality of life to rural people who are always subjected to arduous labour and drudgery. Tillage play an important role in increasing of farm mechanization. Tillage is a "mechanical manipulation of soil, to provide favorable condition for crop production".

Preparation of seedbed includes operation such as ploughing, disking, cultivating, harrowing and planting etc. These operations give better-pulverized soil leading to friable and properly aerated soil ideal for better germination of seed. However these tillage operations need more labour, time and money. Many seedbed preparations implement such as rotavator, M.B. plough, disc plough for primary tillage and harrows and cultivators are used for secondary tillage tools.

1.1 Rotavator

Rotary tiller is a tillage machine designed for preparing land suitable for sowing seeds (without overturning of the soil), for eradicating weeds, mixing manure or fertilizer into soil, to break up and renovate pastures for crushing clods etc. It offers an advantage of rapid seedbed preparation and reduced draft compared to

conventional tillage. It saved 30-35 % of time and 20-25 % in the cost of operation as compared to tillage by cultivator. It gave higher quality of work (25-30 %) than tillage by cultivator. The Rotavator is the most efficient means of transmitting engine power directly to the soil with no wheel slip and a major reduction in transmission power loss.

Tillage is a major operation for seedbed preparation. It is one of the major items of energy and cost expenditure in crop production. The energy input in soil manipulation is exceeded only by the level of energy input in irrigation (Singh *et. al,* 2000).

During the Design of new Rotavator, you should check all the boundary condition of Rotavator for their safety. Different type of forces act on Rotavator, due to that the failure occur and stresses developed on different part of Rotavator. this failure of rotavator can be avoided by using Finite Element Analysis (FEA)

Since the last decade advent of powerful **Finite element analysis** (FEA) packages have proven good tool to accurately analysis. The complicated geometry of the rotavator and load transfer by the soil make their analysis difficult; but optimized meshing and accurate simulation of boundary conditions along with ability to apply complex load, provided by various FEM packages have helped the designer to carry Modeling and Dynamic analysis with the investigation of critical stresses.

1.2 Extencore Solution pvt. Ltd. Pune.

Extencore solution is a global engineering services company, they provide CAD, CAE, CFD and other allied engineering solution. Company work on following areas,

1. Automobile
2. Aerospace
3. Oil and Gas
4. Agriculture
5. Surgical Equipment etc.

Extencore is well equipped with the latest design and testing facilities-utilizing the latest available hardware and software tool for CAD/CAM/CFD

1.2.1 Software tools:

CAE: Ansys, Nastran, Abaqus, Hypermesh, Cosmos, Adams

CAD: Catia, unigraphix, Solidwork, Solidedge, AutoCAD

CFD: Fluent, Ansys CFX, ICEM-CFD,

1.2.2 Design Services: Extencore provide top of the line CAD/CAM design services for aircraft components, industrial equipment, agricultural implement and machine tool

1.2.3 Engineering Analysis: Extencore offer engineering analysis and use of CAE based solutions to customers with product development initiatives, to develop word class and reliable products. The design (Modeling , Meshing and Analysis) was carried out at the "Extencore Solution Pvt. Ltd,".

The main motivation behind the work was to go for complete Finite Element Analysis of rotavator tillage tool.

1.3 OBJECTIVES:

1. To prepare a geometric solid model of rotavator by using Pro-E/CATIA software

2. To make the meshing by using Hypermesh software.

3. To generate a CAD-analysis report of rotavator for specifically von-mises stress and deformation with ideal loading and boundry conditions by using ANSYS Software.

REVIEW OF LITERATURE

CHAPTER-II

REVIEW OF LITERATURE

This main focus of the study was to Design and Analysis of Rotavator. In this chapter, the past work done on computer aided design and analysis of rotavato. While scanning through the literature on rotavator, rotavator designs, modeling and analysis. It was observed that practically little work has been done all over the world. The review has been arranged as follows.

1. Power operated rotavator
2. Rotavator blade
3. Effect of blade angle of draft
4. Operational parameters
    - 4.1. Speed of operation
    - 4.2. Depth of operation
    - 4.3. Forces acting on rotavator
    - 4.4. Lift angle of tool
5. Rotavator design consideration
6. CAD/CAM
7. Finite Element Analysis
    - 7.1. Static analysis
    - 7.2. Dynamic analysis

2.1 Tractor operated rotavator

Teruo Takahashi (1981) studied the dynamic behavior of rotary tiller attached to tractor. The motion of rotary tiller attached to tractor without slip of tires in order to analyze the behavior of the rotary tiller on farm soil. The equation of motion of the rotary tiller was composed of every equation of engine power, forward speed of tractor , the relation of the co-ordinates and the force equilibrium of the rotary tiller body. The cutting resistance of the rotary tiller blade was represented by using such factors as thickness of soil slice and angle of the tangent to the path of the blade. The calculated results showed that on firm field, the depth of operation decreased as the tilling pitch increased, in the same manner as in actual operation.

Razzaq *et al.* (1991) studied the tractor operated rotavator increases the manipulation of soil up to an average depth of 12 cm but still leaves majority of roots uncut below the working profile. The effective and theoretical field capacities with rotavator (150 cm width) in clay soil covered with grass were 0.3 and 0.4 ha/h that with cultivator (206 cm width) are 0.8 and 0.6 ha/h respectively. The field efficiency of each these implements was 75%

Tanya *et. al.* (1993) studied the direction of rotation of rotor was down cut and it has a center drive type rotor. The C-shape blades were fixed on the rotor shaft. The width of rotor was 550 mm. The tests were conducted in a soil bin with the clay soil. The average soil moisture content was 23.9 per cent (db) and dry bulk density was 1.5 g/cc. The test were conducted at working depths of 12 and 18 cm, rotor speed of 140, 160, 180, 200 and 220 rpm and forward speed of 0.16, 0.23, 0.35, 0.64 and 1.25 m/s. The rotary tiller was driven by an electric motor. The data obtained include power requirement to

cut and throw soil away, the soil tilling pattern and the characteristics of tilled soil. The size of tilled soil was evaluated in terms of mean-mass diameter. The working depth should be 18 cm, the rotor speed should be in the range of 165-220 rpm and the forward speed of the implement should be in the range of 0.16-0.35 m/s. The power requirement used for cutting and throwing soil away was about 2.58-4.48 K.W. The mean-mass diameter of tilled soil was about 33-50 mm. For the optimum performance of the rotary tiller, the rotor speed should be 180 rpm and forward speed should be 0.35 m/s.

Niyamapa *et. al.* (1994) conducted a laboratory study in a soil bin to determine optimum parameters for the design of a rotary cultivator with clay soil at a moisture content of 23.26% (dry basis) and dry bulk density of 1.29 g/cm^2. Experiments were conducted at working depths of 12 and 18 cm, rotor speeds of 140, 15\60, 180, 200 and 220 r.p.m. and forward speeds of 0.16, 0.23, 0.35, 0.64 and 1.25 m/s. From the speed and rotor data, power consumption was calculated. The power requirement for cutting and throwing the soil increased with an increase in rotor speed, forward speed and tillage depth. These three parameters also affected the soil breakage. Larger clod sizes were found when tillage depth and forward speed were high and the rotor speed was low. Smaller clod sizes were found when tillage depth and forward speed were low and the rotor speed was high. The optimum parameters for the design of a rotary cultivator were found to be a tillage depth of 18 cm at a forward speed of 0.35 m/s and rotor speed of 165-220 r.p.m. At these operating conditions power consumption was 2.70-3.50 KW.

Anonymous (1997) carried out feasibility testing of tractor – mounted rotavator at HAU Hissar center. The size of the machine was 1250 mm. The rotavator was mounted on three point linkage system of 35 hp tractor. Testing of the rotavator was carried out for preparation of puddled seedbed for rice and seedbed for wheat and tomato crops. The field capacity obtained for preparation of puddled bed for wheat, rice and tomato was 0.224 ha/h for rotavating twice, 0.224 ha/h for disc harrowing once and rotavating once and 0.137 ha/h for once disc harrowing and twice rotavating.

The seedbed quality obtained with rotavator was better than conventional practice. The rotavator was recommended for large scale popularization.

Anon (1998) reported the development of rotary weeder to eradicate the weeds growing in between and around the sugarcane plants with the operating speed of about 4.8 km/h at first or second low gear with 1500 Vm (rotor velocity). And also found that the implement's field capacity was about 0.6 ha/hr.

Ben Yahia, *et. al.* (1999) studied the optimum settings for rotary tools. He conducted experiments to determine the effect of travel speed (3.0 to 9.0 kph), operating depth (12.7 to 63.5 mm) and orientation of rotary tool axis relative to the travel direction (0 to 30^0) and the thickness of the tilled soil layer projected on the crop rows. They concluded that the travel speed, operational depth and relative orientation of the rotary tool also have linear effect on the thickness of the projected soil layer and found that the rotary tool operated at 9.0 kph at a depth of 12.7 mm and rolling in a direction parallel to the direction of travel of the machine to provide adequate soil coverage on the maize rows to control weeds.

Salokhe V. M. and N. Ramalingam (2003) Conducted Experiments in a clay soil to evaluate the performance of a rotary tiller equipped with reverse or conventional blades. The conventional rotary tiller was equipped with C-type blades whereas the reverse-rotary tiller had new types of blades. Tests were conducted on wet land as well as in dry land. Tests were conducted at tractor forward speeds of 1.0, 1.5 and 2.0 km/h. A power-take-off. (PTO) power consumed was calculated from the PTO torque and speed. The results indicated that the PTO power consumption was less for the reverse-rotary tiller compared to the conventional tiller for all passes and forward speeds. For both rotary tillers, power consumption decreased as the number of passes increased, whereas power consumption increased when the forward speed was increased. At all forward speeds, the power consumption was the highest during the first pass and lowest during the third pass. The maximum diference of PTO power requirement was after the first pass at 1.0 km/h forward speed. The reverse-rotary tiller consumed about 34% less PTO power underthis condition.

Sharma and S. Mukesh (2008) reported that the tractor drawn rotavator is an excellent rotary secondary tillage implement and it is especially designed for wet land cultivation in paddy crop. It consists of a steel frame, a rotary shaft on which blades are mounted, power transmission system and gear box. The blade are of L type, made from medium carbon steel or alloy steel, hardened and tempered to suitable hardness. The PTO of tractor drives the rotavator. Rotary motion of the PTO is transmitted to the shaft carrying the blade through gear box and transmission system. A good seedbed and pulverization of the soil is achieved a single pass of the rotavator

2.2 Rotavator blade

Salokhe and Chuenpakaranant (1999) studied a rotavator equipped with uncoated and enamel-coated tines was evaluated in clay soil at an average soil moisture content of 21.6% (db). The power required and quality of work was compared for uncoated and enamel-coated tines under similar working conditions. The enamel coating alerted the power requirement. A maximum saving in power of 22% was obtained at 1.5 km/h speed during the rest pass of enamel-coated tines compared to that of uncoated tines. The power requirement of the enamel-coated tines was higher than the uncoated tines in the second pass, but it gave better soil inversion. The quality of work in terms of bulk density, cone index and mean weight diameter of soil mass were almost the same for both tines. Soil inversion by enamel-coated tines was higher than the uncoated tines by 30 and 50% during the second and third pass, respectively. This might be the reason for the slightly higher power requirement for the enamel-coated tines during the second and third passes. The rate of wear of enamel-coated tines was found to be less than that of the uncoated tines.

Dr S. Singh and Sharda, (2000) reported that Preparation of an optimum seedbed condition by minimizing the time, cost and energy. These requirements has assumed considerable significance for the paddy-wheat farming system widely practiced in northern part of India. In order to study the effect of various parameters on the performance under actual field conditions, a rotary tiller was selected. Two types of the blades, namely, L-type and C-type were used. The rear shield position was adjusted at full down and full up positions and two different rotor speeds 185 rpm and 210 rpm were used for

the study. The studies were conducted under four different field conditions, namely, manually and combine harvested paddy and wheat fields. It was found that the draft (negative) for the two types of blades L-shaped and C-shaped, decreased (163 kgf to 63 kgf). As the rotor speed increased (185 rpm to 210 rpm) for the shield kept in the lowered (down) position. While operating the rotary tiller (Rotavator) under different field conditions. It was observed that at a given rotary speed, the rotary power requirement of C-shaped blades was 19% less as compared to L-shaped blades. But C-shaped blades required 13% less power because draft was about two and a half times more due to reduction in the rotor thrust. The power requirement of 24.2 kW was found to be the highest while operating the rotavator in the combine harvested paddy fields. Soil break up resulting from the action of L-shaped and C-shaped blades under selected field conditions was the lowest at 210 rpm of rotor speed, While operating the rotavator in manually harvested wheat fields. The extent of residue incorporation was the maximum (99%) while operating the rotavator with the shield in the lowered position for both types of blades and at both rotor speeds studied.

2.3 Effect of blade angle on draft in the design of soil engaging tools.

Thakur (1985) reported that draft increased with the increase in angle but the rate of increase in draft became greater at angles more than 50^0. For angles up to 45^0, there is a downward component of the resultant force, which will aid penetration. At angles greater than 45^0, the vertical force acts upward tending to lift the tool out of work.

Oni (1990) developed the appropriate technology for effective weed control by analysis of ridge profile rotary weeders. He concluded

that the optimum draft for maximum weed removal was attained at 60^0 angle of inclination to the horizontal.

Gupta and Pandey (1996) studied on performance of rotary tiller tynes under wet land condition. Four different shapes of L-type rotary tiller tine, namely; arichimedian spiral, logarithmic spiral, circular curvature and straight edge were tested and evaluated at four different rotor speeds (146, 211, 327 and 427 rpm) and 2 modes of operation (down-cut and up-cut). These tines were tested 1.33 km/h forward speed and 100 mm depth. The torque requirement, draft, vertical soil reaction forces and quality of puddling were recorded. Based on these data, the specific energy requirement and puddling index were calculated. Based upon the experiment result, the performance of an L-type tine with an Archimedean spiral was found to be the best of the shapes tested.

2.4 Operational tool parameters.

The depth of operation, forward speed and length of travel are key operational parameters having dominant influence on tool wear.

2.4.1 Speed of operation

Davies (1967) studied the effect of speed on wear mechanism of different materials, on a laboratory wear machine. The analysis of the speed-wear loss indicated that the wear loss increased with increase in the speed of tool, which was primarily caused by increase in the unit of load on the test sample.

Richardson (1967) stated that the increase in speed over the range of 0.5-5.0 miles per hours increase the tool wear rate by 20 per cent.

Gupta and Pandey (1991) studied on performance of spiral and straight edge tynes of rotary tiller under wetland condition. Two types

of rotary tiller tine, a spiral cutting edge and a straight cutting edge, were tested in a soil bin to evaluate their performance. The study was conducted at four different rotor speeds with two modes of operation. The linear speed and working depth were kept constant at 1.33 km/h and 100 mm respectively. The performance criteria were specific energy requirement and puddling index. The results revealed that the spiral cutting edge tine gave about 9.13% higher performance index than the straight edge tine under wetland conditions.

Kosutic *et.al.* (1997) studied rotary cultivator energy requirement influenced by different constructional characteristics, velocity and depth of tillage. This paper deals with energy requirement of rotary cultivators with two tine arrangements (flat and steep spiral) and two tine shapes (L shaped and straight tines). The study took into account the influences of forward speed and depth of tillage on energy requirement. Results show that tine shape has a greater influence on energy requirement than does the arrangement of tines. Straight tines require 21.2-25.7% less energy than L tines. Forward speed and depth of tillage also influenced energy requirement. Increasing velocity from 0.68 to 1.40 m/s decreased energy requirement per unit volume of tilled soil by 23%, while increasing depth of tillage by 40% decreases the energy requirement per unit volume of tilled soil by 19.3%.

2.4.2 Depth of Operation

Hendrick and Gill (1971 a) developed the rotary tiller design parameters like direction of rotation, depth of tillage and ratio of peripheral and forward velocities. The reverse rotation of rotary-tiller blades appear to have 20 to 30 per cent general reduction in power requirement when the depth of operation greater than radius of rotor

and the vertical cutting component is reduced, the vertical stability is increased.

Hendrick and Gill (1971 b) studied the average depth of tillage will be governed by factors other than the ratio of rotor radius and depth, the factors are tilling pitch, peripheral velocities, lateral spacing of blades increase in the depth of operation of a rotary tiller, increase the power requirement.

Zheng *et al.* (1996) conducted experiment with rotary tillers blade and found that the amount of wear varied in proportion to depth of operation of the tyne.

2.4.3 Forces acting on rotavator

Fielke *et al.* (1993) studied the tillage forces were similar in magnitude for two types of soils viz. clay loam and sandy loam, however the wear rate was increased by 40 to 50 per cent in the sandy loam soil. He conducted experiments in the calcareous soils in tilled and untilled conditions and found that the previous tilling reduced the draft force by 55 percent and the wear rate by 73 per cent (pressed steel) and 55 per cent for cast steel shovel.

Papazov and Todorov (1996) made investigations on the process of soil loosening by rotary cultivator and carried out series of experiments were made to determine the effect of soil density, (1, 1.3 and 1.6 g/cm^2), soil moisture (8,15 and 22%), and pitch (40, 80 and 120 mm) on soil loosening with a rotary cultivator (mini-tiller). Results are tabulated, and show that soil density was the most influential factor, that soil m. c. and pitch were practically equal to their effect. A mathematical model was developed describing the effect of the three factors. Tests of rotary cultivators should be carried out on soil of density 1-1.59 g/cm^2 and 15.7-20% m.c.

Juanqin *et. al.* (2004). studied the traction method of analyzing forces acting on a trailed plough was evaluated, and the sources of the errors were studied in theory. The system of equations of forces acting on trailed plough was established, and the solution was found by the use of computer-aided analysis. In light of the equation, the influence of different values of parameters on the forces was forecast. These result provided theoretical basis for designing and optimizing the structure of a trailed plough.

2.4.4 Lift angle of tool

The lift angle or rake angle of tillage tool has a dominant influence on soil reaction there by it effects the wear rate of the tool.

Leachner and Mecolly (1959) studied the detailed investigation on influence of tool life angle on wear rate. They observed that the fastest wear was produced when the tools were moved through the soil at an angle of 75^0.

Biswas, *et. al.* (1993) studied the use of straight blades in mechanical weeder and evaluated in black soils. The draft force per unit working with (Du) was minimum for the rake angle of 22.01^0, the blade width of 15 to 40 mm may be selected with the thickness of 2 to 5 mm and the blade sharpness angle of 15^0 and below may be used. They also reported that the material strength of the tool is the major consideration because the spring steels and high-speed alloy steels have better mechanical strength.

2.5 Design consideration.

Godwin *et. al.* (1987) studied the design consideration and solutions for systems to measure the forces, displacements and angular position of soil-engaging implements where variation in both

soil shear strength and surface elevation occur are described. Specific reference is made to both mole and trench less drainage ploughs.

Sharma D. N. (2008) studied the step by step procedure for the design of tractor drowns rotavator. For design of rotavator it is necessary to take into account the maximum peripheral force of working blade sets, at the time design of rotary blade, required Byte length. Rotavator work on the principle of rotary motion. It takes it drive from tractor PTO shaft and transmits to the tynes through the reduction gear so that its tynes rotate at 250-350 rpm while in operation. The outer casing/cover ensures that the clods are brocken to small pieces and the soil is properly pulverized. It consists of a steel frame, a rotary shaft on which blades are mounted, power transmission system and gear box. The blades are L- type, made from High carbon steel and alloy steel, hardened and tempered to suitable hardness. The PTO of tractor drives the rotavator. Rotary motion of the PTO is transmitted to the shaft carrying the blades through gear box and transmission system.

2.6 CAD/CAM

Noguchi N. (1998) studied internal CAD (Computer Aided Design) system, which is proposed in this paper, will open and serve the technology of design for agricultural machinery and how to mechanize through the interactive communication on the internet. In this research, a CAD program applied to rotary blade which is the paddy rice field in Asia was constructed as an internet CAD System. The system may contribute to mechanization of Asian countries with diffusing for infrastructure of the computer network

Saimbhi1 *et. al.* (2004) Coordinate transformations were used to simulate the kinematics of a rotary tillage, C type blade. Using three

dimensional computer graphics, a Bezier surface of the rear surface of the blade was generated. The error in generating the surface remained below 1_2, 5 and 8 per cent for the x, y and z coordinates, respectively, joining multiple Bezier surface patches. The analysis was carried out at rotor speeds of 180, 200 and 220 min_1 and at tractor forward speeds of 3, 3_25 and 3_5kmh_1 and for two blade orientations: namely, 08 and 208. The interaction of the blade with soil during its operation was analyzed using a scan of trochoidal paths of the leading and trailing edges of the blade (LT scan) computer programmed in language C/C++. Interference of the trailing edges of the blade with uncut soil was eliminated by design changes and checked with LT scans for the range of selected rotor speeds and forward speeds. The rectified surface was manufactured using high carbon steel.

Nishiwaki *et. al.* (2008) studied the current automotive development, innovations to reduce development time and to use a virtual prototype have been numerous and progressive. Computer Aided Engineering (CAE) has played an important role in these innovations. CAE numerically estimates the performance of automobiles and proposes alternative ideas that lead to higher performance without building physical prototypes. However, current CAE is usually not used at the initial design phase due to its sophisticated, difficult to use, and complex functions and characteristics. They proposed a new type of CAE, First Order Analysis (FOA) in order to overcome these problems and quickly obtain optimal designs. In this method, the structural analysis mainly deals with beam and panel elements because they focused on an automotive body structure and suspension system. However, in order

to apply FOA to general mechanical systems; such as, machine tools and robotic system, we need to extend the concept of FOA. The important issue of this extension is to correctly model the system being analyzed since we use only beam and panel elements. It is very useful to link FOA with commercial software since this software includes other elements and functions. This is especially true with ANSYS which has a powerful solver for structural and multi-physical analyses, and can provide finite elements and analysis functions required for the FOA extensions. In this paper, first, they present the concept of FOA and examples. Then, they propose a way to develop FOA linked with ANSYS. In this hybrid system, ANSYS Parametric Design Language (APDL) is utilized to make analysis models and to set analysis conditions. Some prototypes are presented to depict the new concept and its availability for mechanical designs

2.7 Finite Element Analysis.

David Roylance (2001) studied the Finite element analysis (FEA) has become commonplace in recent years, and is now the basis of a multibillion dollar per year industry. Numerical solutions to even very complicated stress problems can now be obtained routinely using FEA, and the method is so important that even introductory treatments of Mechanics of Materials { such as these modules { should outline its principal features. In spite of the great power of FEA, the disadvantages of computer solutions must be kept in mind when using this and similar methods: they do not necessarily reveal how the stresses are influenced by important problem variables such as materials properties and geometrical features, and errors in input data can produce wildly incorrect results that may be overlooked by the analyst. Perhaps the most important function of theoretical

modeling is that of sharpening the designer's intuition; users of finite element codes should plan their strategy toward this end, supplementing the computer simulation with as much closed-form and experimental analysis as possible.

Mootaz Abo-Elnor (2004) studied the finite element analysis of the tillage of dry sandy soil, using the hypo plastic constitutive material model. In most earth moving machinery, such as bulldozers or tillage tools, the working tool is a blade. Hence for tillage systems, accurately predicting the forces acting on the blade is of prime importance in helping to enhance productivity. The initial conditions, such as blade geometry or soil type, and operating conditions, such as cutting speed and cutting depth, have been shown experimentally to have a great effect on machine productivity. Experimental studies give valuable insights but can be expensive and may be limited to certain cutting speeds and depths. Results are also highly dependent on the accuracy of the measuring devices. However with increasing computational power and the development of more sophisticated material models, finite element analysis shows more promise in analyzing the factors affecting soil–blade interaction. Most of the available finite element studies in the literature are two-dimensional however three-dimensional (3D), are limited to a certain blade displacement depending on the element distortion limit before the solution has convergence problems. In this study, a 3D finite element analysis of soil–blade interaction was carried out based on predefined horizontal and vertical failure surfaces, to investigate the behavior of the soil–blade interface and study the effect of blade-cutting width and lateral boundary width on predicted forces. Sandy soil was considered in this study and modeled using the hypo plastic

constitutive model implemented in a commercial finite code, 'ABAQUS'. Results reveal the validity of the concept of predefined failure surfaces in simulating soil–blade interaction and the significant effect of blade-cutting width, lateral boundary width and soil swelling on cutting forces.

Timoshenko (1994). Studied that Solid 45 is defined by eight nodes having three degrees of freedom at each node: translations in the nodal x, y, and z directions. The element has plasticity, creep, swelling, stress stiffening, large deflection, and large strain capabilities. and BEAM188 is a linear (2-node) beam element in 3-D. BEAM188 has six or seven degrees of freedom at each node, with the number of degrees of freedom. These include translations in the x, y, and z directions and rotations about the x, y, and z directions.

Mahanty *et. al.* (2007) studied that the redesign of tractor front axle for weight optimization and easy manufacturability. This led to five proposed designs of the front axle which were evolved based on the above objectives. The proposed designs were evaluated for selected worst load cases of the existing design. The finite element analysis of new models yielded displacements and stresses close to the existing design. The increase in stresses was close to 15 % for all five models. The increase in displacement was not significant but all the new designs conceived had met the structural requirement. It was also observed that for the proposed designs there was a significant reduction in weight (approximately 40 %) and the proposed models did not involve a lot of welding, thereby significant savings of manufacturing was observed. The components used in the assembly were also found to be cost effective like smaller diameters bearing, smaller knuckle size etc. The reduction in cost of production and

weight significantly reduced the cost of the new design of front axle. This analysis work showcases the use of finite element analysis as a method for reduction of cost in terms of materials and manufacturing.

Mehmet Topakci (2008) reported the tillage tools which gets own motion from tractor power take off (PTO) and it had been designed for blend to soil. Soil traffic is decreased to great extent with this tool by blending the soil. The use of rotary tiller is increasing nowadays in our country because of its many benefits. Rotary tiller construction has a gear box that changes motion direction with 90 degrees from tractor PTO, transmission gears for rotation velocity and a rotor shaft which placed as horizontal to soil for blending. There are cutter blades on rotor shaft for breaking into pieces and blend to soil. Especially, on cutter blade and transmission gears, deformations occur because of high vibration, pointless high power, impact effect of soil parts, design-manufacturing error and wrong using conditions. Especially for construction and transmission parts, stress distributions should be determined well for understand failure reasons. In this study, transmission gear train of a rotary tiller which was designed and manufactured by a local manufacturer was modeled as three-dimensional in parametric design software and structural stress distributions on transmission gears were simulated using finite element method software according to its operating condition. After evaluating of simulation results, stress distributions on gears show that gears working without failure according to yield stress of gear's materials. Additionally, working safety coefficient of gears calculated by reference simulation results.

2.7.1 Static analysis

Bechly M. E. and P. D. Clausent (1997) carried out preliminary work to optimize the use of material in a 2.5 m long fiberglass composite wind turbine blade. A program was written to create a detailed finite element mesh of the blade, using design data from blade element theory and panel code predictions, in a format suitable for direct input into a commercially available finite element software package. Finite element predictions compared well with static bending and twisting deflections of the blade and with the first two natural frequencies of vibration. The simulation of a rotating aerodynamically-loaded blade required a nonlinear analysis; The techniques for this analysis and the subsequent predictions are discussed. The best arrangement aligned elements using a previously developed translation scheme and rotated the elements about their centre of area to the twist angle determined by blade element theory.

2.7.2 Dynamic stress

Omprakash and Ramamurti (1989) studied the dynamic stress and deformation analysis of high pressure stage turbo-machinery bladed-disks. The analysis was carried out taking into account all the geometric complexities involved. The contributions due to initial stress and membrane behavior are included. Only one substructure was used for finite element modeling and analysis, taking advantage of rotational periodicity. A triangular shell element with six degrees of freedom per node was employed for this purpose. The blade and disk attachment was established by a set of constraint equations obtained by the Love-Kirchhoff hypothesis. The final set of equations is solved by an out of core sub matrices elimination method. The influence of

different levels of approximations and various geometric parameters on the stresses and deformations is discussed.

Koichi Iwasaki (1993) studied the measurement of stress on chain tightener. In order to reduce the noise and the vibration caused by the clutching of the chain and the sprocket, a chain tightener is generally used. A tightener is one of the small part of a rotary tiller, for it generally a commonly vended flat bar was used, but if it should be broken down, the performance of tiling work come to be impossible. Owing to the fact that repeated load acts inevitably on the tightener in the process of tillage work, the fatigue strength of the material should be considered in the stage of designing the chain tightener system leading to the whole structure of transmission system of rotary tiller.

THEROTICAL CONSIDERATION

CHAPTER III

THEROTICAL CONSIDERATION

Rotary tiller is a tillage machine which is used in arable field and fruit garden in agriculture. Rotary tiller has a huge capacity for cutting, mixing to topsoil and preparing the seedbed preparation directly. Additionally, a rotary tiller has more mixing capacity seven times than a plough (Ozmerzi, 2002). Thus, increasing the effectiveness of tillage tools, even by a small fraction, would amount to a huge saving in energy. It would be rather more economical to increase the productive rate of each machine rather than to increase the number of machines indiscriminately.. When a tillage operation is performed in the soil texture will be function of soil conditions, blade kinematics and soil dynamics. As the blades of a rotary tiller rotate, each point on a given blade traces a trochoidal path in the soil. On the forward part of the trochoidal path, the blade will cut or fracture untilled soil and on the return part of the blade will tend to mix and pulverize the soil slices. The power consumed, cutting action, the blade geometry, the path and the orientation of the blade relative to the path of the cutting edge of the blade will impudence soil texture and cultivation. The path of the cutting edge is a function of perpendicular distance from the cutting edge to the rotor axis of rotation, the rotor velocity and forward velocity of the machine (Koichi *et al.*, 1993). The proper design of the inter-related cutting and clearance angle of rotary tiller blades are essential for an efficient operation. As the effective cutting angle is increased from some

minimum value, the power requirements of the tiller and the amount of soil pulverizing, throwing and mixing are increases (Hendrick & Gill, 1974). Hendrick and Gill (1978) made a theoretical analysis of the motion of the rotary tiller blade. Equations of motion were used to analyze the characteristics of the trochoidal path. They used an instant centre technique to determine the direction of motion and the velocity at any point of the trochoidal path. A powered rotary chisel was designed and tested by Hendrick (1980). Singh (1996) found that the tools of the 'L' and 'C' shapes consumed minimum energy in comparison with other conventional rotary tillage tools. Noguchi *et. al.* (1992) developed an expert computer aided design (CAD) system to determine the arrangement of blade on a rotary cultivator. The system includes a database that contains 17 different blade of a cultivator with 24–56 blades. Sakurai *et. al.* (1989) developed a computer program to design and display selected passive tool shapes. The tool surface was represented by a multiplicity of quadrilateral faces limited by user selected bounding curves. The (x, y, z) face coordinates were generated by a FORTRAN program and read into AutoCAD using an Auto LISP program. The method permitted a complete study of the geometrical parameters upon the soil condition and energy requirement.

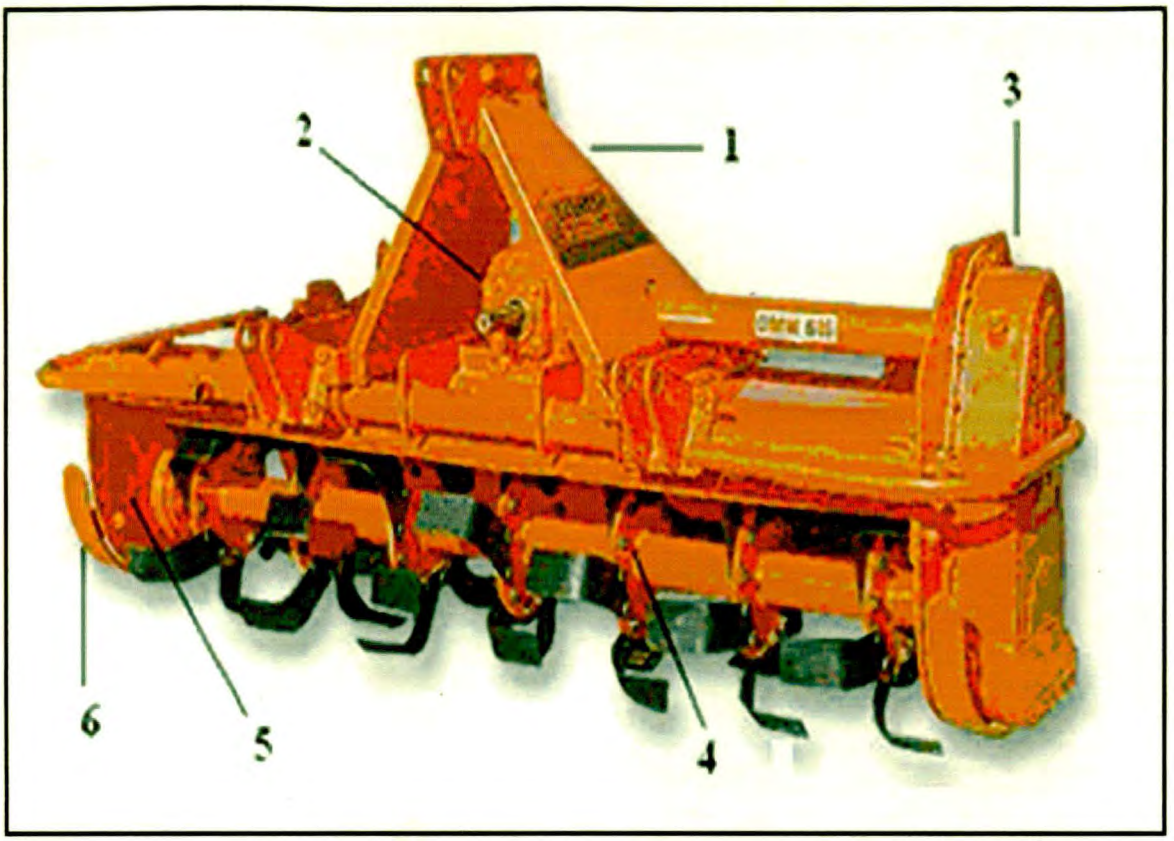

Fig 3.1: Parts of rotavator

1. Independent top mast

2. Single / Multi speed gear box

3. Chain / Gear drive

4. Six blades per flange

5. Adjustable depthskids

6.Central and offsetable positions with clevis mounting plates adjustable on a square tube

3.1 Rotavator assembly consists of following parts:

3.1.1 Telescopic shaft: one end of shaft will be connected to tractor P.T.O. and another end to rotavator. Thus it will be used to transmit power from tractor P.T.O. to input rotavator shaft.

3.1.2 Gear transmission: A gear box with bevel gears, main shaft, pinion shaft, heavy duty roller bearings combine to form a unit to reduce standard P.T.O. rpm 540 rpm to 204 rpm. It enables the rotor shaft to rotate in the direction of travel. This helps in throwing the material behind the rotavator, to facilities in preventing the clogging of rotavator.

3.1.3 Rotor assembly: It consists of a solid bar shaft, mounted on mainframe with the help of two ball bearings at its ends. On this shaft 36, L shape tines are mounted with the help of bracket placed equidistant

3.1.4 Shoes: The shoes are provided below the rotating shaft on both sides, for adjusting the depth of operation.

3.1.5 Rear cover: By adjusting the position of rear cover; the degree of pulverization of soil will be controlled. If the cover kept wide open, the clods are thrown away from the rotor. The closed position of cover facilities the clods to get further pulverized by the action of rotating blades and fine tilth will be obtained.

3.1.6 Tines: Two types of the tines, namely, L-type and C-type were used. The L shaped tine will be most common. The material composition of tine is generally carbon (0.52 %), manganese (0.72 %), and silicon (1.56 %).

3 .2 FEM Approach:

3.2.1 Introduction about FEM:

It is not always possible to obtain the exact analytical solution at any location in the body, especially for those elements having complex shapes or geometries. The boundary conditions and material properties, are the analytical solution that satisfies the governing equation and gives extreme values for the governing functional is difficult to obtain. Hence for most of the practical problems, the engineers resort to numerical methods like the finite element method to obtain approximate but most probable solutions. Finite element procedures are at present very widely used in engineering analysis. The procedures are employed extensively in the analysis of solids and structures and of heat transfer and fluids, and indeed, finite element methods are useful in virtually every field of engineering analysis

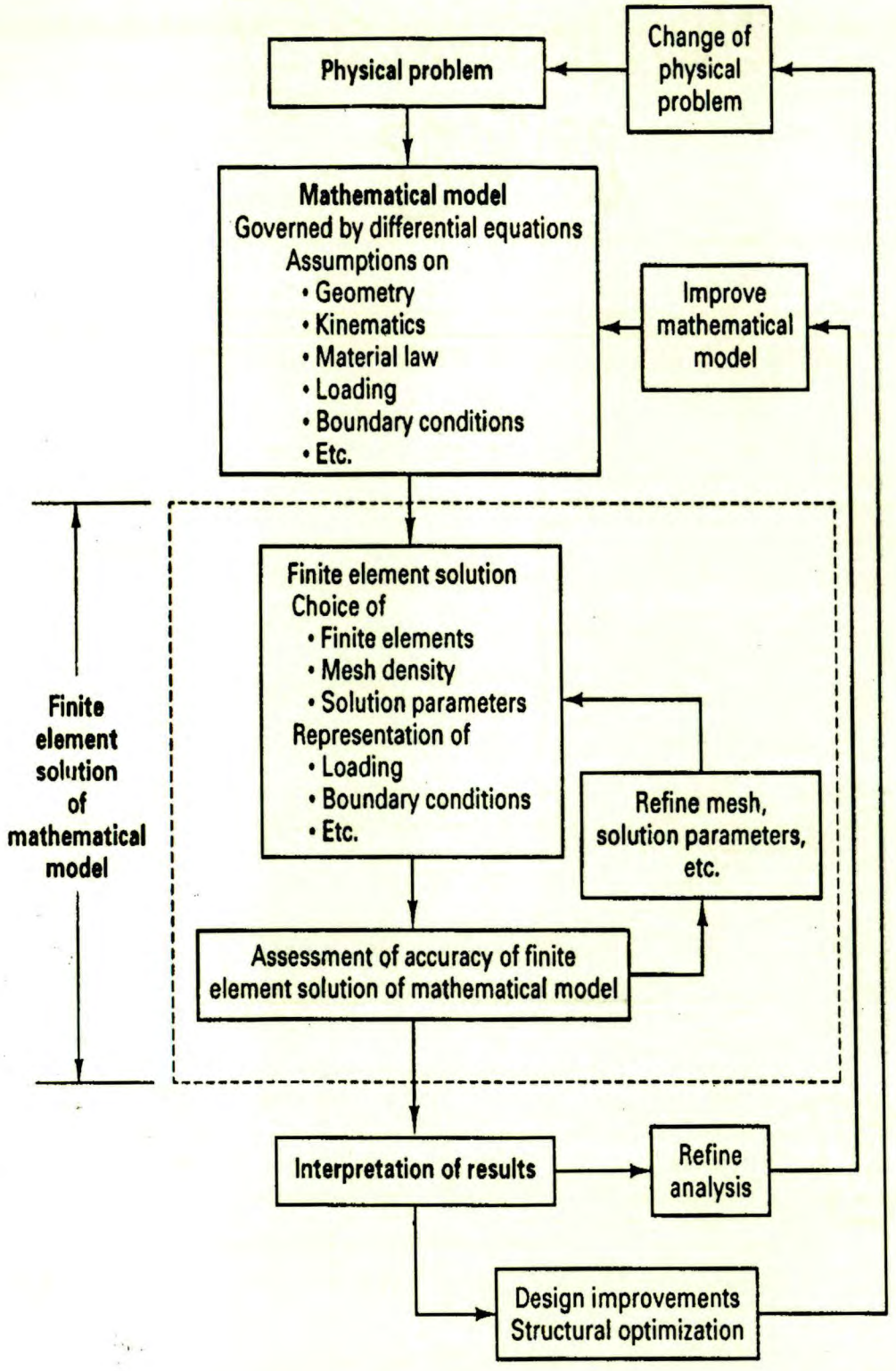

Fig3.2- Finite element process

3.2.2 Important features of Finite Element Method:

The finite element method is a technique in which a given domain is represented as a collection of simple domains, called finite elements. The following are the three basic features of the finite element method.

a) Division of whole into parts; which allows representation of geometrically complex domains as collection of simple domains that enable a systematic derivation of the approximation functions.

b) Derivation of approximations functions over each element; the approximation functions are often algebraic polynomials that are derived using interpolation theory.

c) Assembly of elements, which is based on continuity of the solution and balance of internal fluxes.

The basic equation used to solve the static analysis problem is:

$$\{Q\} = [K]\{\delta\}$$

where, $\{Q\}$ = the equivalent vector which is obtained by lumping the element and edge loads at the nodes,

$[K]$ = the global stiffness matrix of the system, and

$\{\delta\}$ = the unknown nodal displacement vector.

3.2.3 Steps followed in ANSYS programmed:

The three important steps in ANSYS programming are:

a) Preprocessing

b) Solution

c) Post processing

a) Preprocessing: This phase consists of making available the input data such as geometry, material properties, meshing of the model and boundary conditions. It has following steps:

1) Set up: In this step one can enter the analysis type, the material properties, and the geometry (i.e. prepare the model). The model may be built parametrically or a model from other software package can be imported.

2) Create FE model: In this step the total volume is divided into small simple regular volumes, which can be easily meshed. Then we define the mesh size for each small volume by virtually dividing all the edges of the small volume into same divisions.

3) Loading: In this step the boundary conditions are imposed, i.e. forces and constraints, on the model are defined.

b) Solution: In this phase a solver is used to solve the basic equation for the analysis type and to compute the results. This phase is taken care by the software programmed. In the solution process, the solver goes through following steps to compute the solution for a steady state analysis,

1) Formulate element matrices,

2) Assembly and triangularise the overall stiffness matrix,

3) calculate the solution by back substitution,

4) Compute the stresses, displacements, etc.

c) Post processing: This is the phase where the results are reviewed for the analysis done, by obtaining graphic displays, vector-plots and tabular reports of stress and displacement, etc.

3.3 Modeling

To carry out Finite Element Modeling analysis of any component, the solid model of the same is essential. So the solid model of rotavator is required and this can be done by using "CATIA V5" software which is available at CAD/CAM lab. M.A.U. Parbhani

3.4 Mesh Generation (Meshing)

After validation of the model next step is generation of Finite Element Mesh. For the Rotavator SOLID45 elements are used for meshing. A very fine mesh creates the hardware space problem because the computations become voluminous. As the number of nodes increases, the total degrees of freedom of the model increases Hence a designer has to model it optimally i.e. placing fine mesh only at critical area; and coarse mesh at other. So that the run time is less and also the accuracy is not much affected. Following types of element used for meshing

3.4.1 1-d Element: Used for geometries having one of the dimensions very large in comparison to rest of two. Shape of 1-d element is line. When the element is created by connecting two nodes,

software comes to know about only one of 3 dimensions. Remaining two dimensions i.e. area of c/s must be defined by the user as additional input and assigned to respective element.

3.4.2 2-d Element: used when two of the dimensions are very large in comparison to third one. 2-d meshing is carried out on mid surface of the part. 2-d element are planer just like paper

3.4.3 3-d Element: used when all the three dimension are comparable.

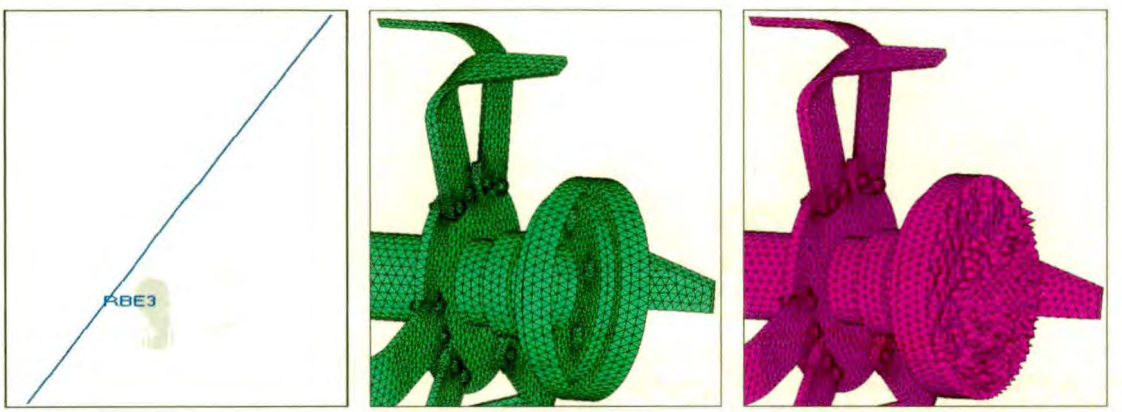

1-d Meshing 2-d Meshing 3-d Meshing

Fig 3.3: 1-d, 2-d and 3-d Meshing

3.5 Mesh Density:

The art of using FEM lies in choosing the correct mesh density required to solve a problem. If the mesh is too coarse, then the element will not allow a correct solution to be obtained. Alternatively, if the mesh is too fine, the cost of analysis in computing time can be out of proportion to the results obtained. In order to define a relevant mesh, some idea of parameter distributions (stress, temperature, pressure, etc.) within the component is required. If the answer is known, then a good mesh can

be defined. A fine mesh is required where there are high parameter gradients and strain and a course mesh is sufficient in areas that have result contours of reasonably constant slope.

3.5.1 Quality checks:

Different quality parameters like skew, aspect ratio, included angles, Jacobean etc. are the measures of how far a given element deviated from ideal shape Following are general definition of various quality checks. Through the names sound same but exact definition may differ from software to software.

3.5.1.1 Warp angle: Warp angle is not applicable for triangular element. It is defined as angle between normal's to two planes formed by splitting the quad element along diagonal. Max. angle out of the two possibilities is reported as warp angle.

Ideal value=0^0 (Acceptable<10^0)

3.5.1.2 Aspect: it is a ratio of max. Element edge length to minimum element edge length.

Ideal value=1 (Acceptable<5)

3.5.1.3 Skew: Skew for quadrilateral element=90^0 minus minimum angle between two lines joining opposite mid-side of the element. Skew for triangular element=90^0 minus minimum angle between the lines from each node to the opposing mid-side and between the two adjacent mid-sides at each node of the element.

ideal value=0 (Acceptable<45)

3.5.1.4 Jacobean: It is a scale factor arising because of transformation of co-ordinate system. Element are transformed from global co-ordinates to local co-ordinate from faster analysis point of view.

Ideal value=1.0 (Acceptable>0.6)

3.5.1.5 Included angle: skew is based on overall shape of element and does not take in to account individual angles of quadrilateral or triangular element. Included or interior angle check is applied for individual angle.

Quad ideal value=90^0 (Acceptable=$45^0 < \theta < 120^0$)

Tria ideal value=60^0 (Acceptable=$20^0 < \theta < 120^0$)

MATERIAL AND METHODS

CHAPTER IV

MATERIAL AND METHODS

In this chapter the materials and methods adopted in design of the tractor drawn rotavator has been outlined. The evaluation procedures have also been discussed.

4.1 Selection of material

The selection of material is now easier and faster, because of the availability of computerized and extensive databases. The choice of the material is firstly governed by the requirements, concerning the function, stressing and the life of the component. In addition the requirement concerning the shape and manufacturer are to be considered next. Lastly the cost of the material in relation to the manufacturing price of the component is to be considered.

There is hardly a product on the market today for which substitution of materials has not played a major role in helping companies maintain their competitive positions.

There are several regions for substituting materials in existing products:

1) Reduce the cost of material and processing
2) Improve manufacturing and assembly, installation and conversion to automated assembly.
3) Increase the stiffness-to-weight and strength-to-weight ratios of structure.
4) Reduce the need for maintenance and repair
5) Improve the perceived aesthetics of a product.

Table 4.1 Material Properties:

Sr No.	Material Name	Material Properties		
		Elastic Modulus (N/mm^2)	Poisson Ratio	Density ($Tonne/mm^3$)
1	High Carbon Steel	$1.97 \times e^{11}$	0.29	$7.48 \times e^{-9}$
2	Cast Iron	$1.20 \times e^{5}$	0.28	$7.20 \times e^{-9}$
3	Mild steel	$2.10 \times e^{5}$	0.3	$7.89 \times e^{-9}$

4.2. Soil parameters

The soil properties relevant to the design of rotavator were identified as soil type, moisture, bulk density and cone index. The manners of measurement and characterization of these properties are discussed in the following sections.

4.2.1. Soil type

The type of soil affects on the implements and draft required to it. Soil resistance for different soils is given in table 4.2

Table 4.2: soil resistance for various soils

Sr. No.	Type of soil	Soil resistance (kg/cm^2)
1.	Sandy soil	0.2
2.	Sandy loam	0.3
3.	Silt loam	0.35-0.5
4.	Clay	0.4-0.56
5.	Heavy loam	0.5-0.7

4.2.2. Soil moisture

Moisture content of soil will affect draft of implement and slip. Soils having more moisture content give more slip and hence increase the draft. Table 4.3 gives the optimum moisture content of different soils.

Table 4.3 : Optimum moisture of different soils

Sr. No.	Type of soil	Optimum moisture Content (%)
1.	Sandy soil	3.5
2.	Sandy or silt loam soils	5.8
3.	Clay loam soils	7.18
4.	Heavy soils	13.30

Moisture content of soil plays an important role for the growth of the crop

4.2.3. Bulk density

Bulk density of the soil is a measure of compaction of soil condition influencing the tool parameters. Hence it was measured to define the soil condition.

4.2.4. Cone Index

Cone index is measure of penetration resistance of the soil; hence it is necessary to define the soil condition

4.3. Design of Rotavator

Rotavator consist the following main part.

1) Independent top mast
2) Rotor with blade
3) Side gear box and Gear box housing

4) Frame and Cover

5) Right side frame

6) Left side frame

4.3.1. Independent top mast:

A standard three-point hitch arrangement was design from 50x 10 mm M.S. flat for mounting the frame to the tractor three-point linkage.

The plate thickness for top link is kept as 10 mm and two plates are spaced at 50 mm spacing attached to each other with a spacer in between them. This arrangement was decided by considering hitching system of different 35 HP tractors

4.3.2. Power transmission systems:

The power train of the power transmission system is shown in Fig 4.5. The speed from the tractor PTO was reduced from 540 rpm to 337 rpm with the help of a bevel gear arrangement, which was having a gear ratio of 1.6:1, which transmit power to the main shaft with speed ratio of 1.07:1. Again speed from main shaft reduced at a ratio of 1.21:1 and the power transmitted to rotary weeding assembly by chain and sprocket arrangement. The final speed of the blade was set to be 257 rpm.

4.3.3. Rotary blade assembly:

The blade assembly consisted of a on the periphery of the flange, high carbone steel blades of uniformly tapered edges were positioned such that it projects outwards with an inclination angle of 50^0 to horizontal as shown in Fig.4.2 and 4.3. Similarly another shaft was fitted on antifriction bearings horizontally on a suitable framework. Another two sets of weeding units were fabricated within between 200 mm clearance. These three units were assembled in a specially constructed framework. The rotary

weeding blade assembly was supported by a triangular supporting frame. It consisted of flanges, cutting blade and rotor shaft.

4.3.4. Rotor shaft :

The rotor shaft was used to mount the flanges with 'L' shaped blades. It receives power from main shaft by means of chain and sprocket arrangement. This shaft was supported on the journal bearings. The bearings were provided to the inner side of the channel.

4.3.5. Flanges :

Flange or circular metal plates are used for structural component for the cutting blades. In order to mount the blades, flanges are used.

Flanges are made of 10 mm thick mild steel sheet and 180 mm diameter. A pair of flanges with cutting blades were fabricated and mounted on a each rotor shaft. The clearance between the two flanges or discs were 220 mm with a blade overlapping of 20 mm.

4.3.6. Cutting blades

L shaped rotary blades are selected and mounted on flange. The "L" shaped cutting edge has been sharpened for easy cutting and fixed at an optimum angle of inclination of 50^0 to horizontal. The cutting blade was used as an inclined plane for elevating and converging the soil to the rotating blades to perform cutting the weeds and pulverizing the soil. The cutting blades of high carbon steel material were used.

Material	=	High carbon steel
Shape	=	L Type
Length	=	125 mm
Angle Between two blade	=	45^0
Angle of orientation	=	50^0
Byte length	=	20 mm

No. of blades per flange = 6

Total no. of blades = 36

4.4. Design Procedure for Tractor drawn Rotavators:

Tractor drawn rotavator is an excellent rotary secondary tillage implement. It is especially designed for wet land cultivation (puddling) in Paddy crop. It churns mixes and disperses the finer particles in muddy condition so that silt and clay particles are settled on the surface and restricts the infiltration of irrigation water. Thus it provides conditions conducive to the growth of paddy crop.

Rotavator can very effectively be used for dry cultivation as secondary tillage implement for the dry preparation of seedbed. It gives excellent pulverization of soil and mixes the trash, crop residues, weeds etc. into the soil for their rapid decay. It cuts the trash and crop residue to fine pieces and buries them into the soil. The planking attachment given behind the equipment ensures breakage of big clods, leveling of field and packing of soil moisture with the result that only 12 operations with the rotavator can make a very fine seed bed suitable for effective planting of crop. Rotavator work on the principle of rotary motion. It takes drive from tractor PTO shaft and transmits to the tynes through the reduction gear so that its tynes rotate at 250-350 rpm while in operation. The outer casing/cover ensures that the clods are broken to small pieces and the soil is properly pulverized.

It consists of a steel frame, a rotary shaft on which blades are mounted, power transmission system and gear box. The blades are L- type, made from high carbon steel and alloy steel, hardened and tempered to suitable hardness. The PTO of tractor drives the rotavator. Rotary motion of the PTO is transmitted to the shaft carrying the blades through gear box and transmission system.

The step by step procedure for the design of tractor drowns rotavator follows:

4.4.1. To Determine the maximum force in rotavator tynes

4.4.2. To Determine the peak moment or torque (Td) in the rotavator shaft

4.4.3. Design of cutting blades for the rotavator

4.4.3.1 To Determine the byte length

4.4.3.2. To determine the number of blade on rotary

4.4.1. Determine the maximum force in rotavator tynes:- for design of rotavator it is necessary to take into account the maximum peripheral force of working blade sets and is determined by,

$$\textbf{Tractor power (Pt)} = \textbf{Kp X } u/(75\eta t * \eta r)$$

where, Pt = tractor power, hp

Kp = maximum peripheral force

U = rotavator tyne velocity, m/s

ηt = tractor transmission efficiency (0.9 for Concurrent revolution and 0.8-0.9 for reversed rotary)

ηr = Soil resistance to 0.7-0.8

4.4.2. Determine the peak moment or torque (Td) in the rotavator shaft

$$\textbf{Td} = \textbf{Kd X R}$$

Where R = Radius of rotary tyne

Kd = Design force for rotary tyne, Kgf

$$\textbf{Kd} = \textbf{Cs X Kp}$$

Considering overload factor (Cs) for peak peripheral force,

Cs= 1.5 for smooth stone less soil.

Cs= 2.0 for stony soil

4.4.3. Design of cutting blades for the rotavator:

4.4.3.1. Byte length: The byte length is the forward distance traveled in between successive cuts of soil by blades

$$\textbf{Byte length (mm)} = V \times \pi \times D/Vm$$

Where, V = Forward speed of the drive, m/s

Vm = Speed of rotary unit, m/s

D=outer diameter of the flange or disc of rotary, mm

4.4.3.2. Number of blade on rotary: The number of blades can be calculated from following expression

$$Z = 2\pi \times h / (Lb\,\lambda - 2A)$$

Where Z = number of blades

h = maximum depth of operation

Lb = byte length

A = blade thickness

λ = speed rate, $\lambda = Vc/Vf$

Where Vc = cutting speed, m/s

Vf = Forward speed, m/s

4.5. Dynamic Analysis:

Finite element method has been recently used for dynamic Analysis of rotavator. Figure below presents a flowchart of the main stages in the analysis procedure.

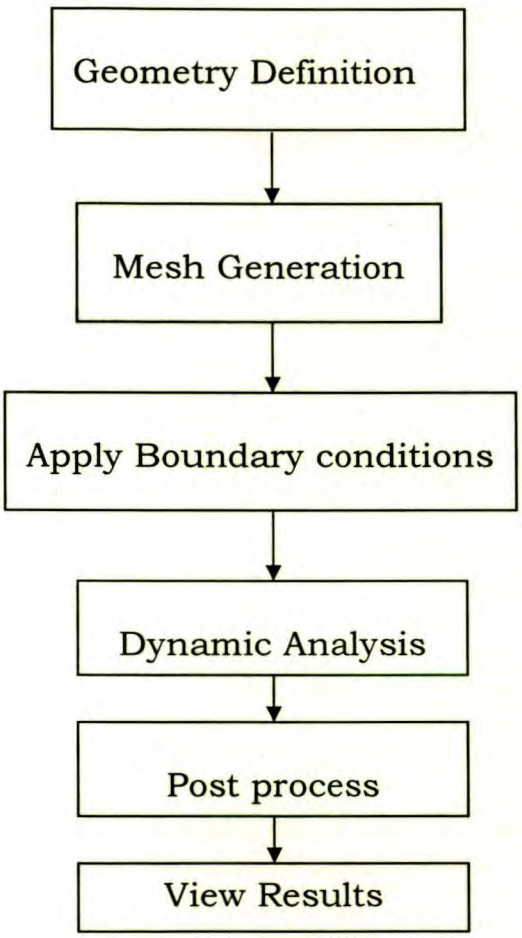

Figure 4.1 Procedure of dynamic analysis.

The first stage in the process is the geometry definition. This can be through engineering drawings, 3D CAD files. Many highly developed graphical pre-processing packages are now available for mesh generation. These pre-processors can use the outline geometry from a drawing or CAD model to form the starting point for the mesh.

The next step is to define the boundary conditions. Once calculated BC's are applied to the FE model using dedicated software, this software interfaces between the mesh generator, the load definition files and the FE solver/ analysis code, and outputs a complete data ready for analysis.

The output from this calculation interfaces directly with proprietary finite element post-processing packages, allowing the results to be presented in a variety of different ways e.g. color contour plots, deformed geometry, vectors, animations, graphs.

4.5.1. Solid modeling of rotavator

To carry out FEM analysis of any component, the solid model of the same is essential. It is also called body in white. So the solid model of Rotavator is require and this can be done in special CAD package like CATIA V5.

4.5.2. Solid models:

Following are the ways in which the solid model of Rotavator is created in CATIA V5

4.5.2.1. CSG: It is the constructive solid geometry process. In this case final model consists of union of various primitive objects such as brick, cube, sphere, cone, cylinder, etc. Depending upon the shape of final model Boolean operations are performed over these shapes to obtain the required geometry of solid model. Thus it builds a solid model from fundamental shapes.

4.5.2.2. B-REP: It is the boundary representation of solid objects. In this case final model is only represented by its boundary surfaces. The relations between surfaces are maintained so as to give required solid model. It is a quick process. This is used to get surface for auto mesh for the outer surface of rotavator

4.5.2.3. FBM: It is a feature based modeling. The features such as extrude, protrude, cut, revolve, copy, etc. are used to build a solid

model. Many CAD packages use FBM method. It is easy and gives 'model tree' for completed part, so that modification at any point at any branch can be passed through whole model. Thus FBM is suited for parameterization of model. It will be helpful to generate similar models from existing one just by changing the parameter values. It is proposed to use FBM using CATIA V5 because of its advantages over other methods and availability of parameterization functions.

4.5.3. Modeling details:

4.5.3.1. 2-D drawings: For generation of a 3-D model, 2-D orthographic views are required. The Rotavator is composed of following Component-

1. Independent top mast
2. Rotor with blade
3. Side gear box part
4. Frame and cover
5. Right side frame
6. Left side frame

The 2-D drawings of every individual part of Rotavator and their assembly are as shown below.

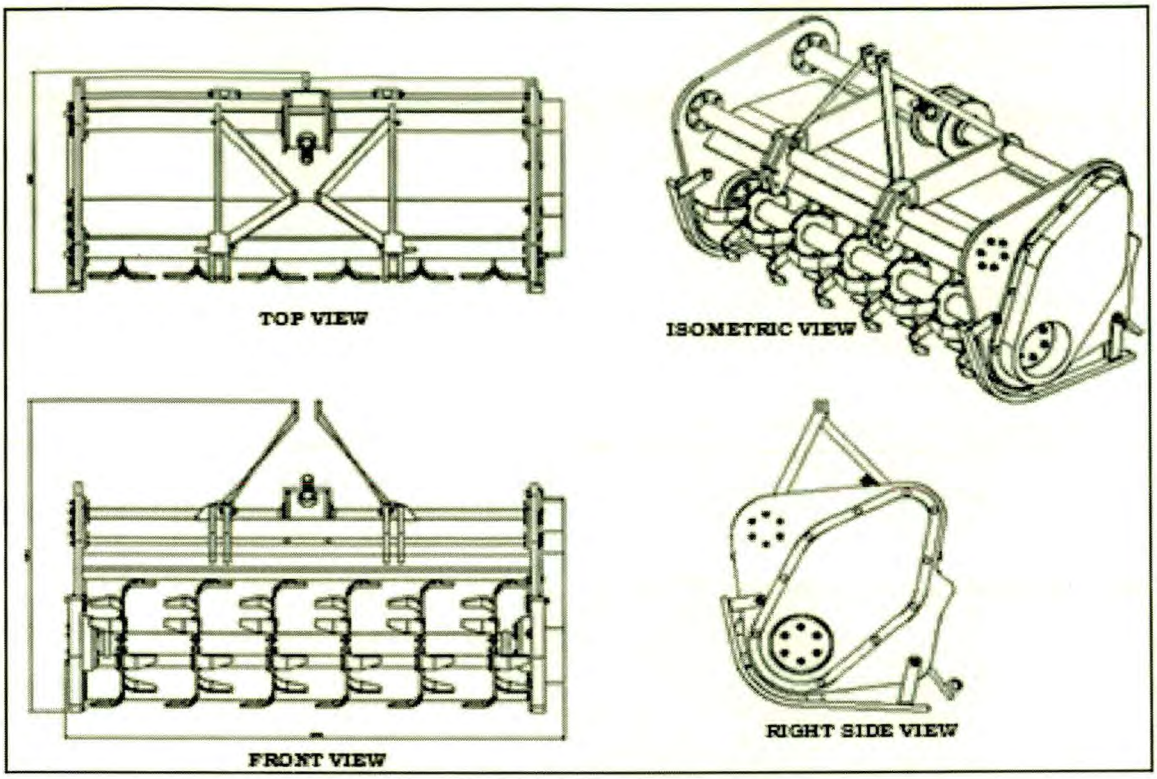

Fig 4.2:- 2D Drawing of Rotavator

4.5.3.2. 3-D Model: Using 2-D drawings one can prepare isometric views of a implement (Rotavator) and using that, solid model is generated. A feature based modeling technique is used for every individual part. These parts are assembled to get complete Rotavator. After the assembly, fine fillets and chamfer details at Blade and shaft etc. are created by surface generation techniques.

Using similar techniques complete Rotavator is generated in 3-D model. Fig. 4.3 shows a 3-D plot of the tractor operated Rotavator.

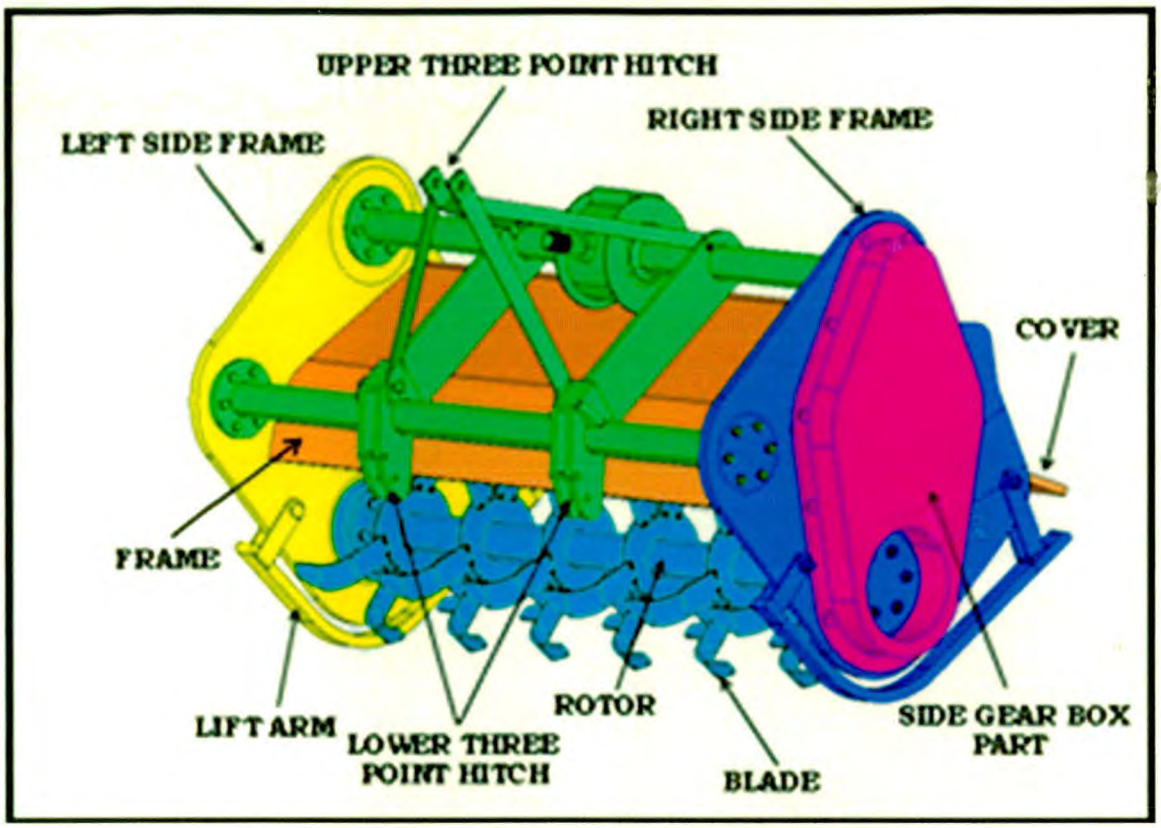

Fig 4.3 :- Solid Model of Rotavator

4.5.4. Building Clean Geometry

In short, clean geometry can be defined as a solid CAD model that maximizes the possibility for a' mesh which in turn captures the features required for correct results. Two key points are made in this statement. First, the geometric features must not prevent the mesh from being created and must also contain surfaces of consistent size and shape ratios to prevent forcing high, aspect ratio elements and/or transitions between element edges that may compromise accuracy. Second, simplification or manipulation of features in an attempt to clean up the geometry should not reduce the structural integrity of the part. The best mesh is the smallest model that yields correct data. Consequently, manipulation of the model, either by adjusting dimensions or suppressing features far from any area of interest, is acceptable, as effects local to the simplification will most likely not affect the

global behavior of the system. However, care should be taken when adjusting a model near an area of concern.

The best safeguard against the need to clean up geometry near an area of interest is to not create a problem in the first place. Many designers make dimensions and feature size choices based on convenience. Consequently, it is not surprising that short edges or sliver surfaces appear randomly in a model. If the feature choices are made with the knowledge of downstream needs, many of the modeling issues that plague the automeshers and analysts can' be avoided.

Essentially, automeshers pave or seed the outer surfaces of a part with triangles, and then fill towards the center of the volume. Unless local mesh refinement is employed the automeshers will try to space nodes on edges first and then within surfaces at the defined nominal element size. However, most meshers are constrained to use every point or edge on the part. Consequently, when a short edge is encountered, it will space the two legs of the triangle that are not on the offending edge to full element size and limit the edge length of the third to the physical geometric edge. This short edge will affect at least two elements in a Tet model and may affect more depending on your tool's algorithms for transitioning.

Limiting the size of small edges to no less than one-third of the expected nominal element size is good practice. This is great on paper, but difficult in practice. Educating geometry providers on the needs of FEA will help. Planning and evaluating features as they are created will also help in this case.

The primary causes of short edges are the misalignment of features and the proximity of fillet edges to other edges. Some commonly created short edges that could have been eliminated

with proper planning of geometry are shown in the three illustrations appearing in this section.

4.5.5. FE mesh generation for rotavator

After validation of the solid model next step is generation of Finite Element Mesh. For the Rotavator SOLID45 elements are used for meshing. A very fine mesh creates the hardware space problem because the computations become voluminous. As the number of nodes increases, the total degrees of freedom of the model increases Hence a designer has to model it optimally i.e. placing fine mesh only at critical area; and coarse mesh at other. So that the run time is less and also the accuracy is not much affected.

The solid model of complete assembly available in .IGES and .STEP format was imported into Hypermesh 9.0 for meshing

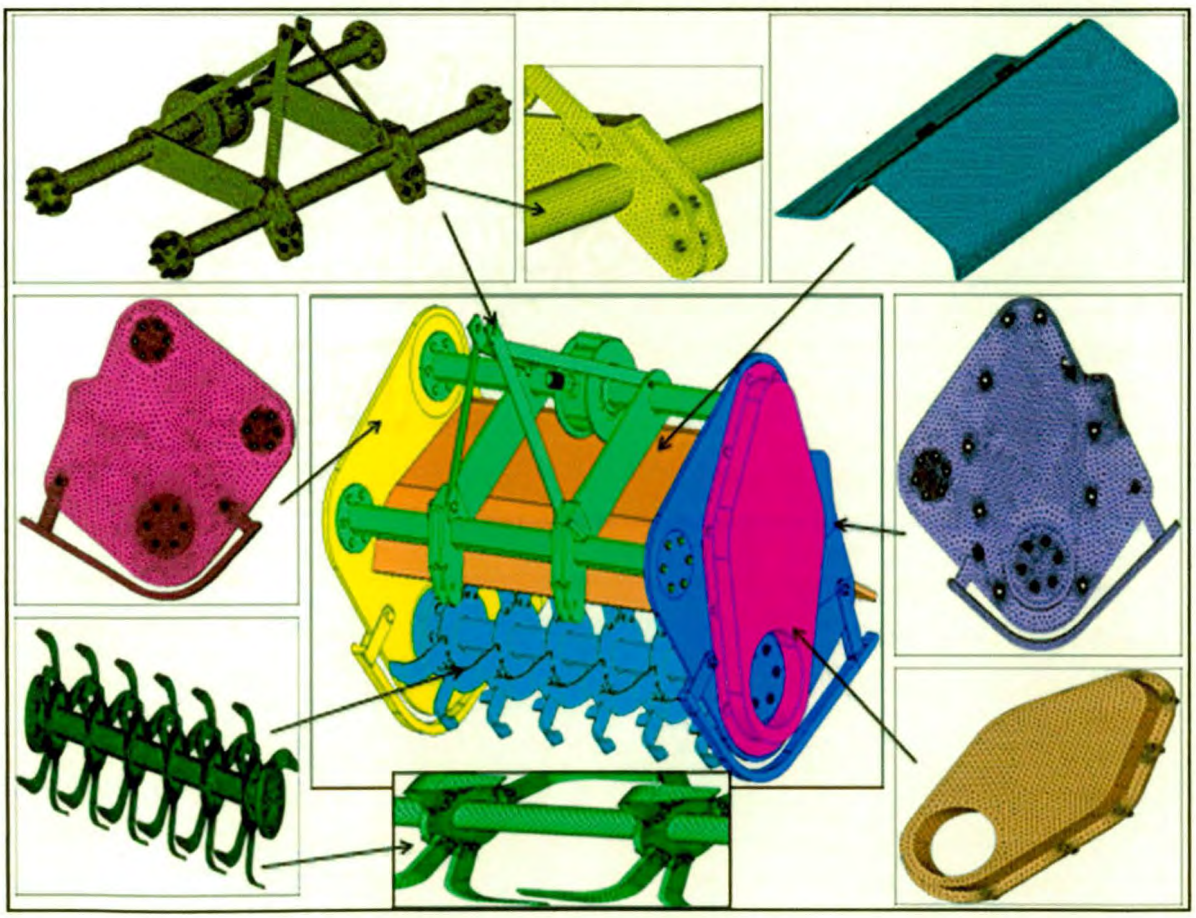

Fig 4.4: Mesh component of Rotavator

Fig 4.5: Isometric view of Rotavator

4.5.5.1 Element Description

4.5.5.1.1 SOLID 45

We done the solid meshing using SOLID-45 8 NODE 45 element, DOF: U_X, U_Y, U_Z

SOLID45 is used for the three-dimensional modeling of solid structures. Gokhale *et.al* (2008) The element is defined by eight nodes having three degrees of freedom at each node: translations in the nodal x, y, and z directions. The element has plasticity, creep, swelling, stress stiffening, large deflection, and large strain capabilities. A reduced integration option with hourglass control is available. A similar element with anisotropic properties is SOLID64. A higher-order version of the SOLID45 element is SOLID95.

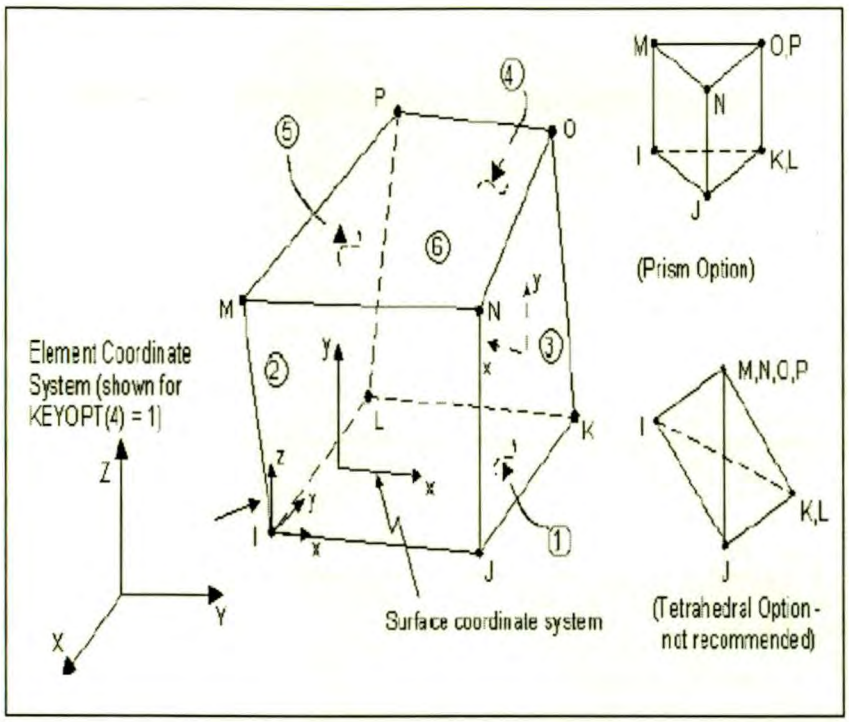

Fig. 4.6 (a): SOLID45 3-D 8-Node Tetrahedral Structural Solid

4.5.5.1.2 BEAM 188

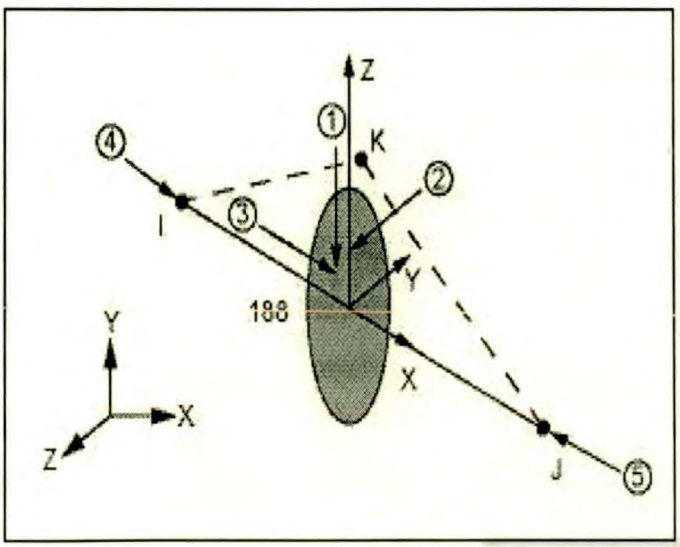

Fig 4.6 (b): Geometry of BEAM 188 element

BEAM188 is suitable for analyzing slender to moderately stubby/thick beam structures. Gokhale *et.al* (2008) The element BEAM 188 is based on Timoshenko beam theory. Shear deformation effects are included. BEAM188 is a linear (2-node) beam element in 3-D. BEAM188 has six or seven degrees of

freedom at each node, with the number of degrees of freedom depending on the value of KEYOPT(1). When KEYOPT(1) = 0 (the default), six degrees of freedom occur at each node. These include translations in the x, y, and z directions and rotations about the x, y, and z directions. When KEYOPT(1) = 1, a seventh degree of freedom (warping magnitude) is also considered. This element is well-suited for linear, large rotation, and/or large strain nonlinear applications. BEAM188 can be used with any beam cross section. A cross section associated with this element type can be a built-up section referencing more than one material.

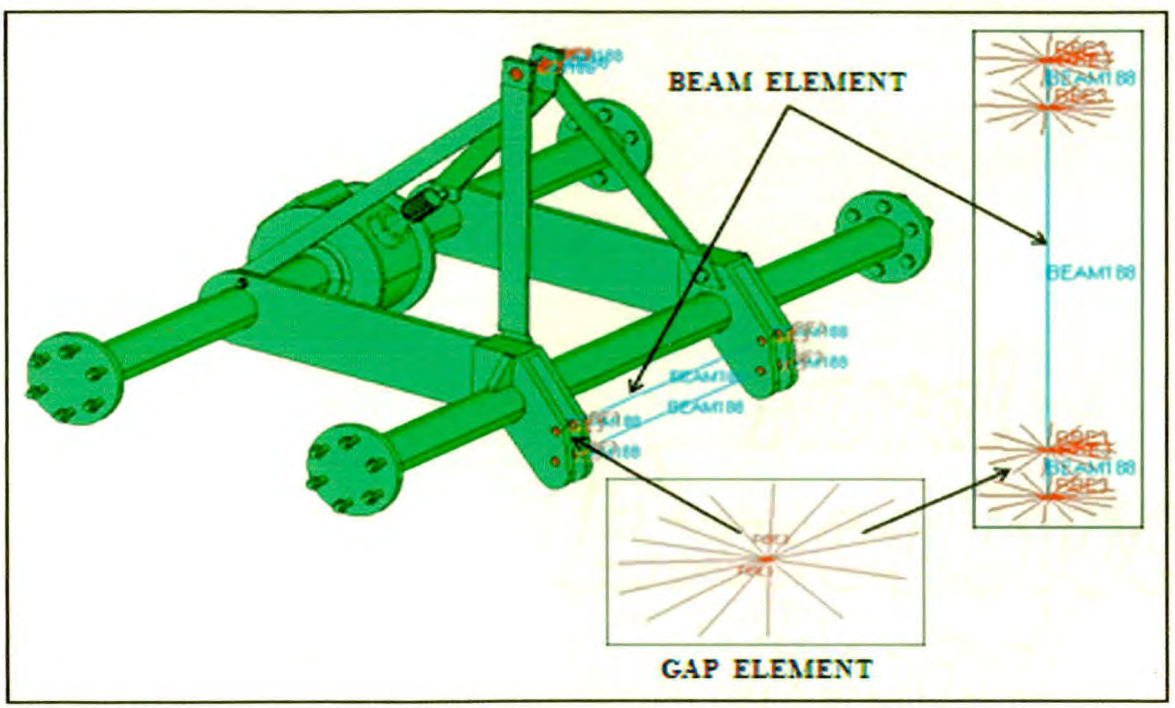

Fig 4.7: Beam and Gap Element

Following table shows the total number of 1-d, 2-d and 3-d element and total node present in FE model of rotavator.

Table 4.4: 1-d element reference

Sr. No.	Component Name	Element Type	Node Count	Element Count
1	Upper three point hitch	BEAM 188	12	9
2	Lower three point hitch			
3	Upper three point hitch	RBE 3	180	14
4	Lower three point hitch			

Table 4.5: 2-d & 3-d element reference

Sr. No.	Component Name	Element Name	Node Count		Element Count	
			2D	3D	2D	3D
1	Independent Top mast	Solid45	38098	59204	76252	231362
2	Rotor with Blade		47354	61463	94704	212411
3	Side Gear box part		6539	7292	13078	22763
4	Frame and cover		10255	10462	20518	30785
5	Left side Frame		12372	16754	24800	61187

Table 4.6: Total elements and node

NODE POPULATION COUNT		ELEMENT POPULATION COUNT	
2D	3D	2D	3D
120180	165773	256305	626628

4.6. Modal analysis:

Any physical system can vibrate. Analysis of vibration modes is a critical component of any design, but is often overlooked. The frequencies at which vibration naturally occurs, and the modal shapes which the vibrating system assumes are properties of the system, and can be determined analytically using Modal Analysis. Inherent vibration modes in structural components or mechanical support systems can shorten equipment life, and cause premature or completely unanticipated failure, often resulting in hazardous situations.

Detailed modal analysis determines the fundamental vibration mode shapes and corresponding frequencies. This can be relatively simple for basic components of a simple system, and extremely complicated when qualifying a complex mechanical device or a complicated structure exposed to periodic wind loading. These systems require accurate determination of natural frequencies and mode shapes using techniques such as Finite Element Analysis. Modal analysis is performed without the loads and without any constraint. And obtained the deformation plot for different frequency. In case of rotavator model analysis was done foe 10 different frequency range and obtained a deformation plot in Ansys solver.

The below mention table gave an idea about fundamental natural frequencies and higher natural frequencies in Hz. Section

4.1 contains the deformation plot for individual component and assembly for below mention 10 different natural frequencies

Table 4.7: Natural Frequency

Frequency No.	Frequency in (Hz)
1	0.035050
2	0.124740
3	0.136380
4	0.166260
5	0.189400
6	0.221610
7	16.64500
8	40.79900
9	56.55600
10	66.29900

4.6.1. Process for Modal analysis

4.6.1.1. Preprocessor

1. Define analysis type

   Solution > Analysis type > New analysis > Modal

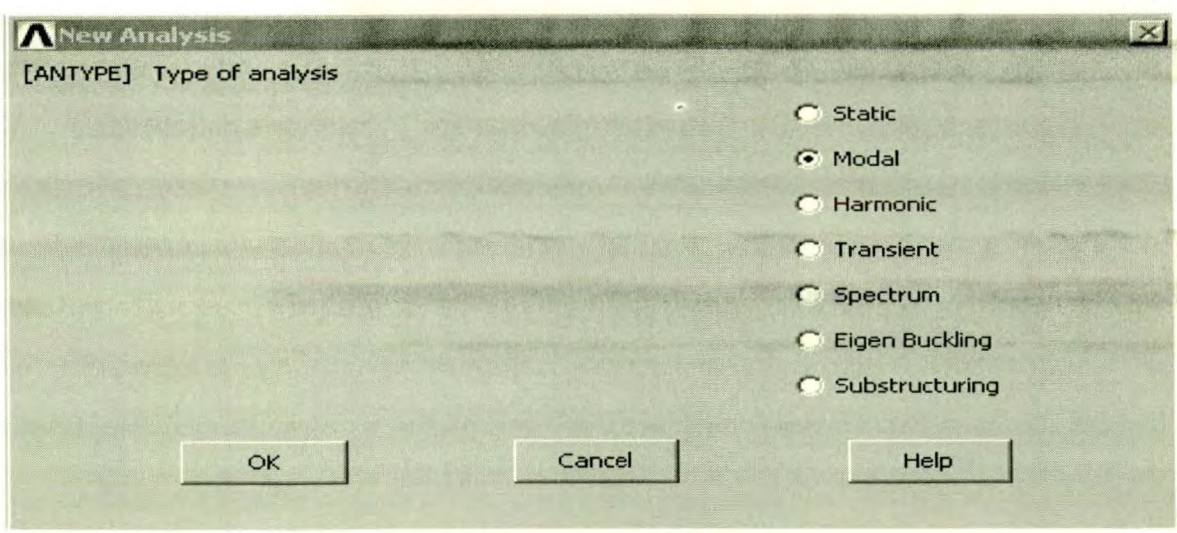

Fig 4.8: Modal Analysis window

2.control setting

Solution > Analysis type > Analysis options>set the no. of mode to extract.

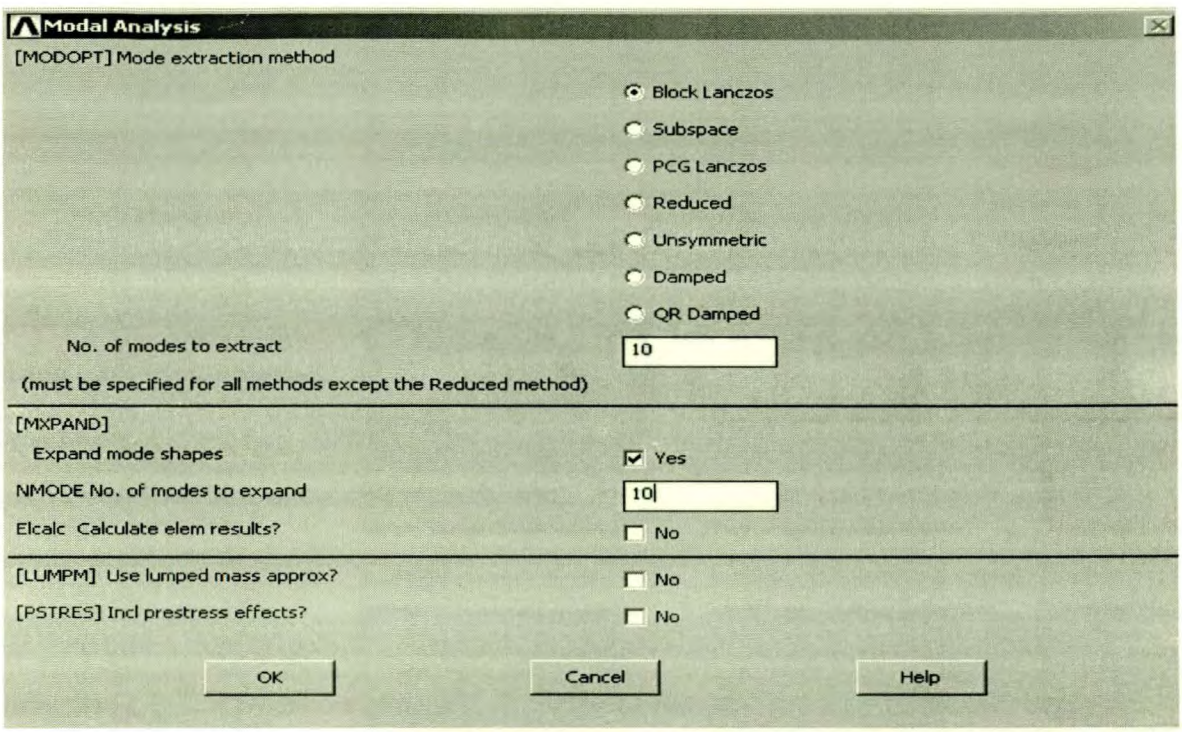

Fig 4.9: control setting window

Click ok, then following window will appear

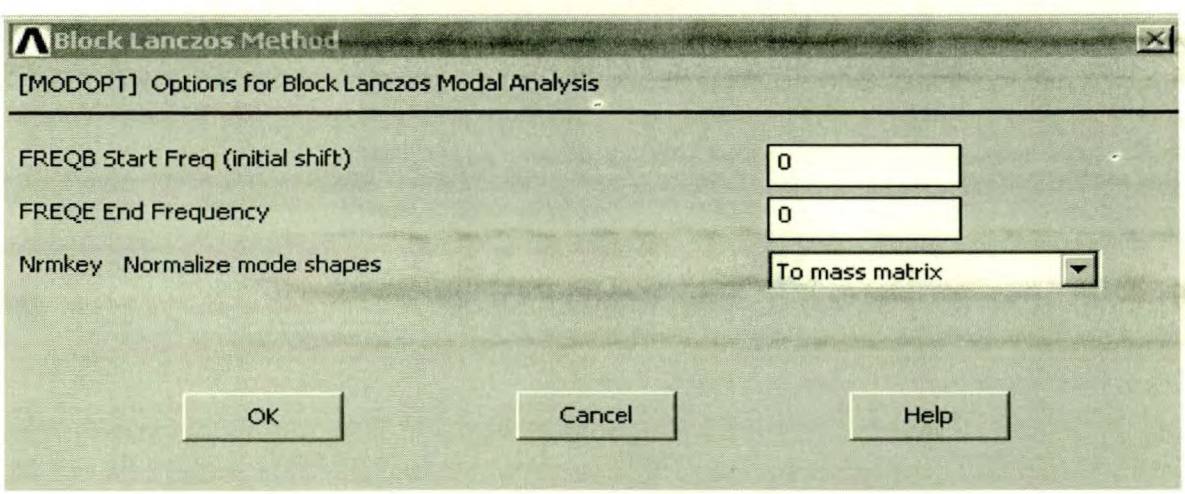

Fig 4.10: Block Lanczos window

Click ok

4.6.1.2. Solver

1.Solution>Solve>Current LS

SOLVE

4.6.1.3. Post processing

1. Verify extracted modes against theoretical predictions

Select: General postproc > Results summary...

The following window will appear

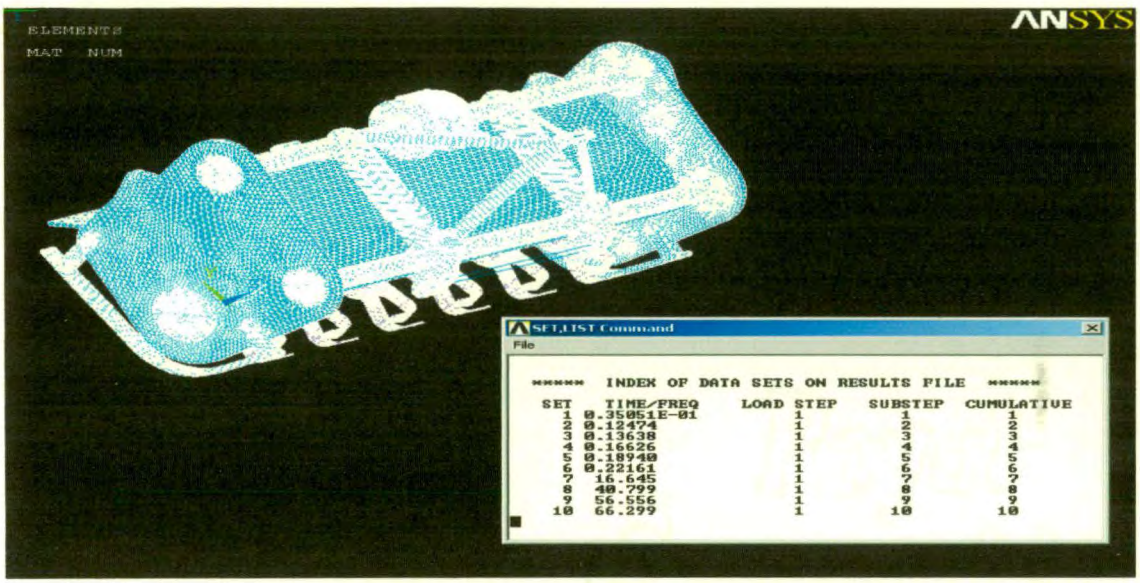

Fig 4.11: Result Summary window

2.View mode shapes

Select: General postproc > Read results > by pick

This selects the results for the first mode shape

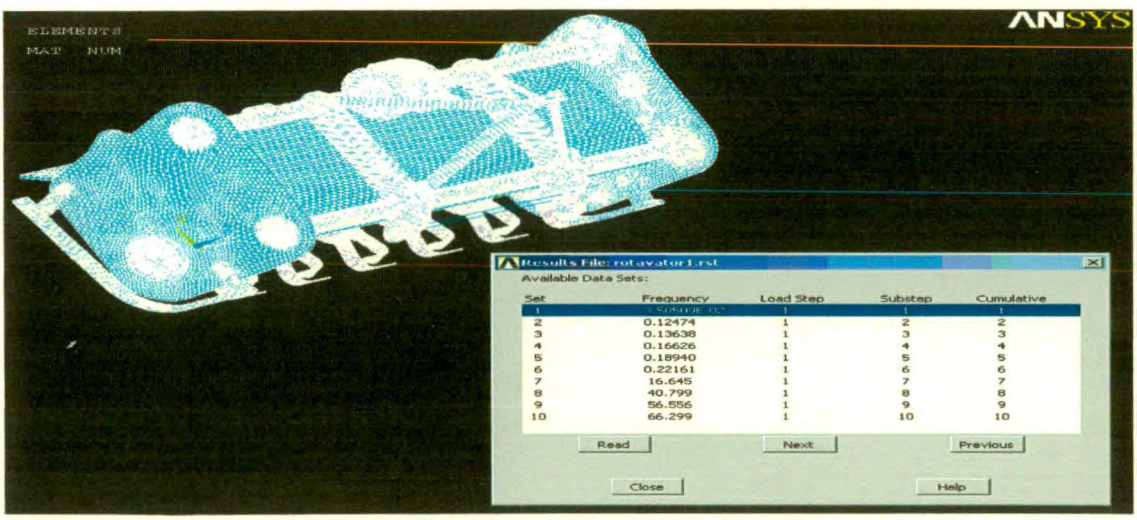

Fig 4.12: Mode Shape window

3.Plot result: Select General postproc > Plot results > Deformed shape. Select 'Def + undef edge'. The first mode shape will now appear in the graphics window.

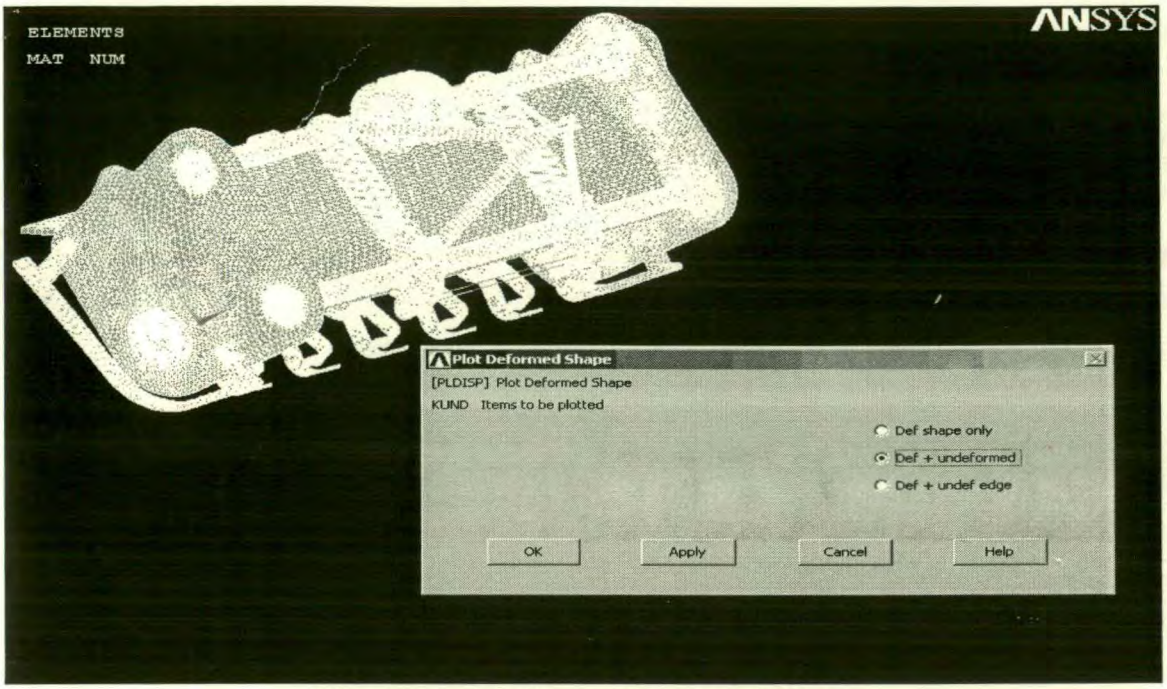

Fig 4.13: Deform shape window

4.7. General Procedure for Dynamic Analysis

4.7.1. Build FE modal: FE model building is very important step in FE analysis, irrespective of what kind of analysis to be performed. Selection of appropriate element is more important. The FAE group is provided with part surface data, which is required to be meshed with element to get the component mesh. When all the part in the assembly are meshed, they are all connected together using appropriate fastening elements. In general quad and Hex element should be preferred over Tria, Penta and Tetra. Important feature like fillets, holes, cutouts should be captured in the model appropriately. If load transfer is supposed to take place from one surface in a structure to the other, a contact set should be defined between them.

4.7.2. Applied load and boundary condition: No matter how good the FE mesh is, the results are not going to be accurate if FE model

is not constrained appropriately or load applied is not representative of intended loading. The mesh size and node location sometimes puts constrains on how and where load boundary conditions are applied to the model, it would not hurt to re-mesh the FE model locally at the location where to be applied to make sure loads and boundary conditions are represented best possible way.

4.7.3. Assign material properties: Material nonlinearity is defined in the FE model via this very important step. The response of the structure depends on the properties supplied to the FE model. The software manual should be referred to understand the input format of the material data card, as different software code may have different format. Analysis should required material suppliers to provide certified properties for the exact same material which is going to be used to build the part.

4.7.4. Run the analysis: the FE model is now ready to be run. The analysis run command may have options to specify solver version, memory size, and number of CPUs to better control execution

4.7.5. Review and interpret result: It is highly recommended that the analysis result should be carefully reviewed and checked for accuracy before making any conclusions based on simulations.

There are many way the FEA result can be checked, some of them are:

1. Observe for unexpected movements in the animation.
2. Compare the reaction forces against applied forces.
3. Check if stresses and strains are as per material properties supplied to the FE model.
4. Make quick hand calculation by simplifying the problem and compare it with the FE results.

4.8. Process for Dynamic Analysis:

4.8.1. Preprocessor

1. Analysis Type

Go to Solution>Analysis type>New analysis in the Main Menu. The Analysis type window wills pop-up.

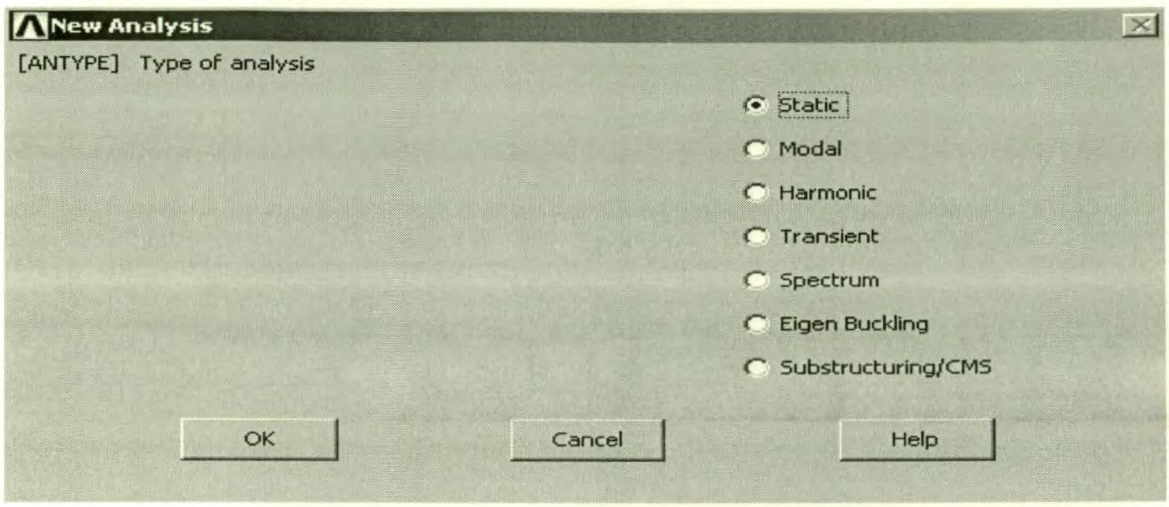

Figure 4.14: Analysis type window

Select Static and OK.

2. Apply constraints

Goto Solution>Define loads>Apply>Structural>Displacement>On node in the Main Menu. The apply F/M on node's window wills pop-up. Be sure that Pick, Box and Single are selected.

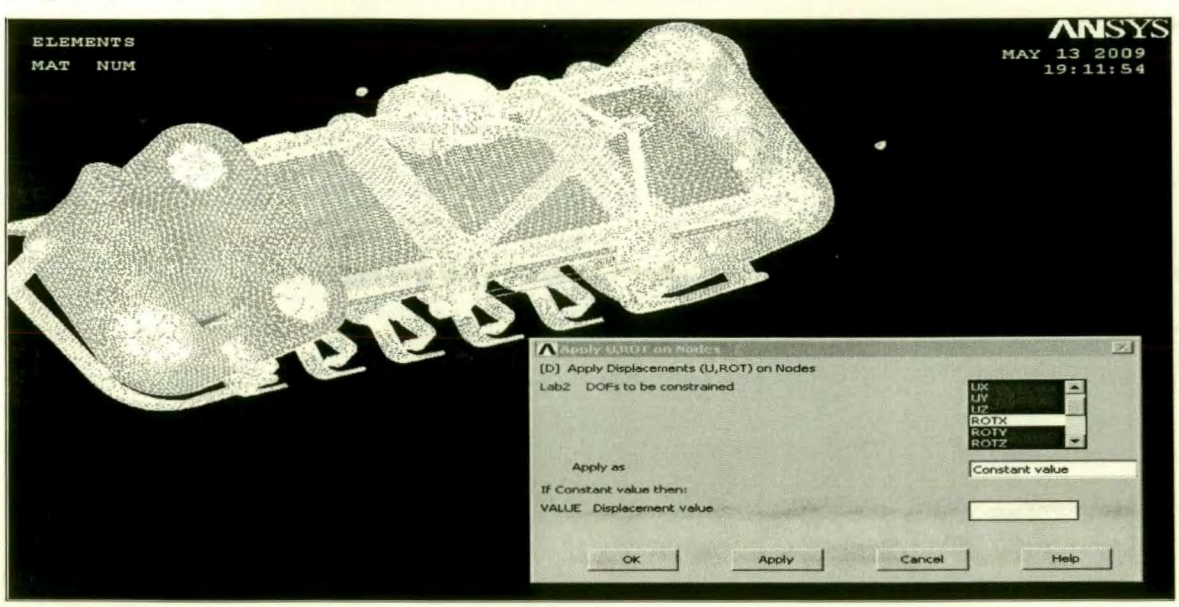

Figure 4.15: Define constraints window

3. Terminology used for constraints:

U_x: Translation in X direction

U_y: Translation in Y direction

U_z: Translation in Z direction

R_y: Rotation along Y direction

R_z: Rotation along Z direction

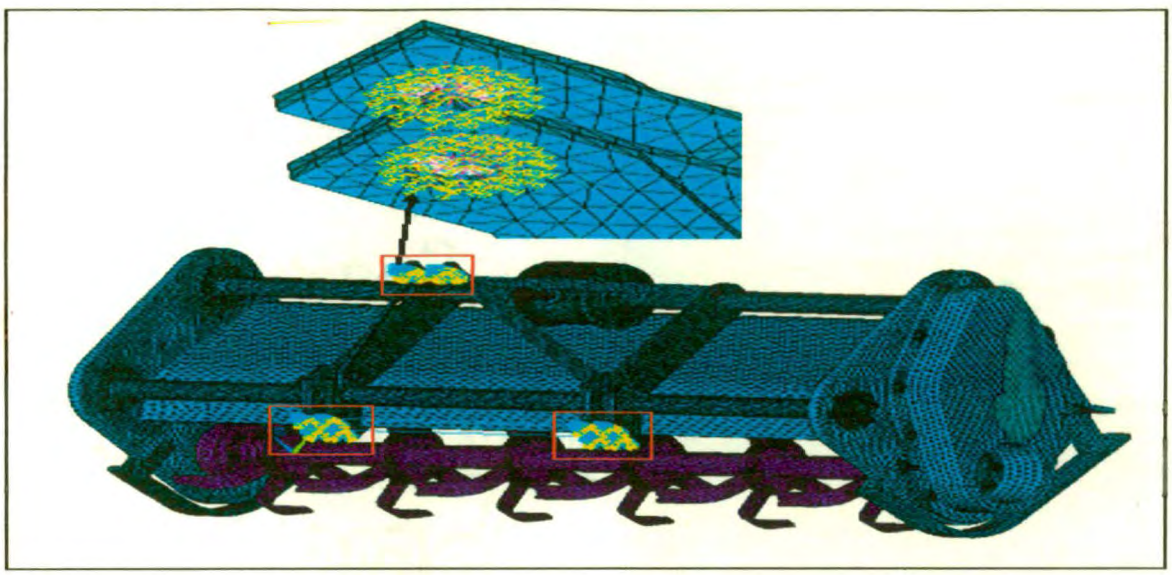

Fig 4.16: Displacement constrained at three point hitch

4. Apply Loads

Goto Solution>Define Loads>Apply>Structural>Force/Moment>On Node in the Main Menu. The Apply F/M on node's window wills pop-up. Be sure that Pick, Box and Single are selected.

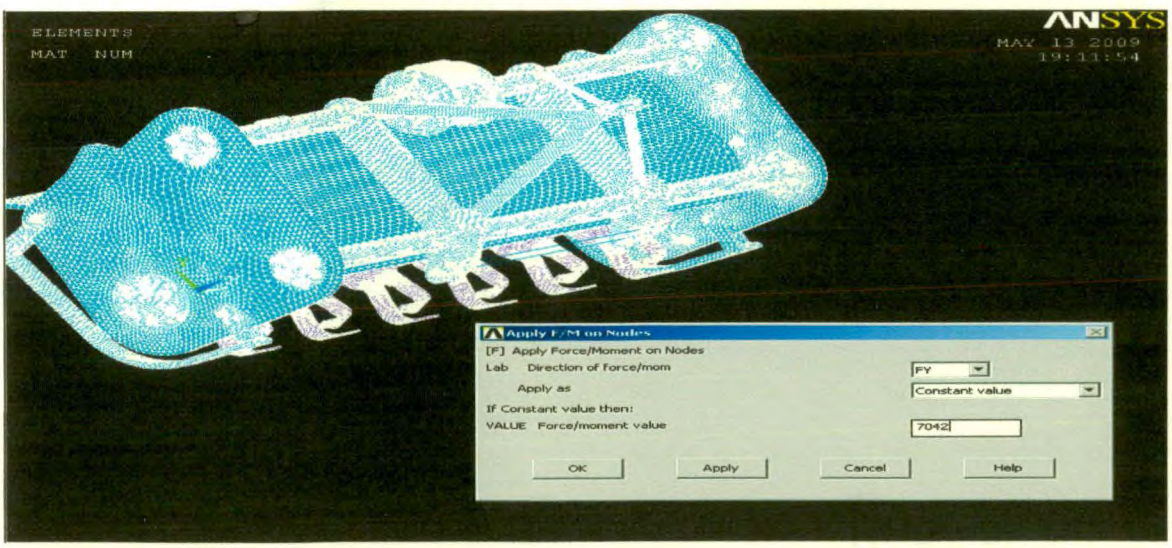

Fig 4.17: Apply Force on node window

Select the following:

a. FY

b. Apply as a constant

c. Magnitude = 7042

d. Select OK. This will close both the Define F/M and Apply F/M windows.

5 Force and Torque

1. Direction of Force: Y Direction
2. Applied force Value for 35 Hp Tractor: 6031 N
3. Applied force Value for 45 Hp Tractor: 7042 N
4. Torque Applied for 35 Hp Tractor: 270600 N-mm
5. Torque Applied for 45 Hp Tractor: 3099175 N-mm

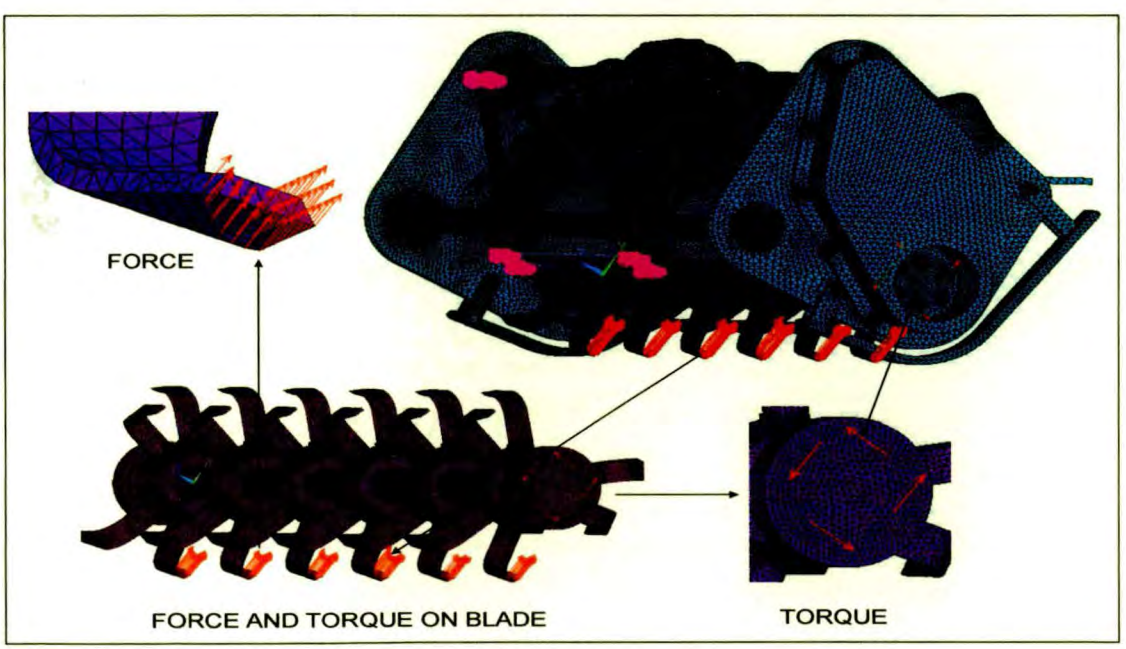

Fig 4.18: Apply Force and torque

4.8.2. Solver

1. Now your rotavator is fully constrained and loaded. You are now ready to have ANSYS actually solve the model.

Go to Solution>Solve>Current LS in the main menu.

The Solve current load step window will appear. Select OK.

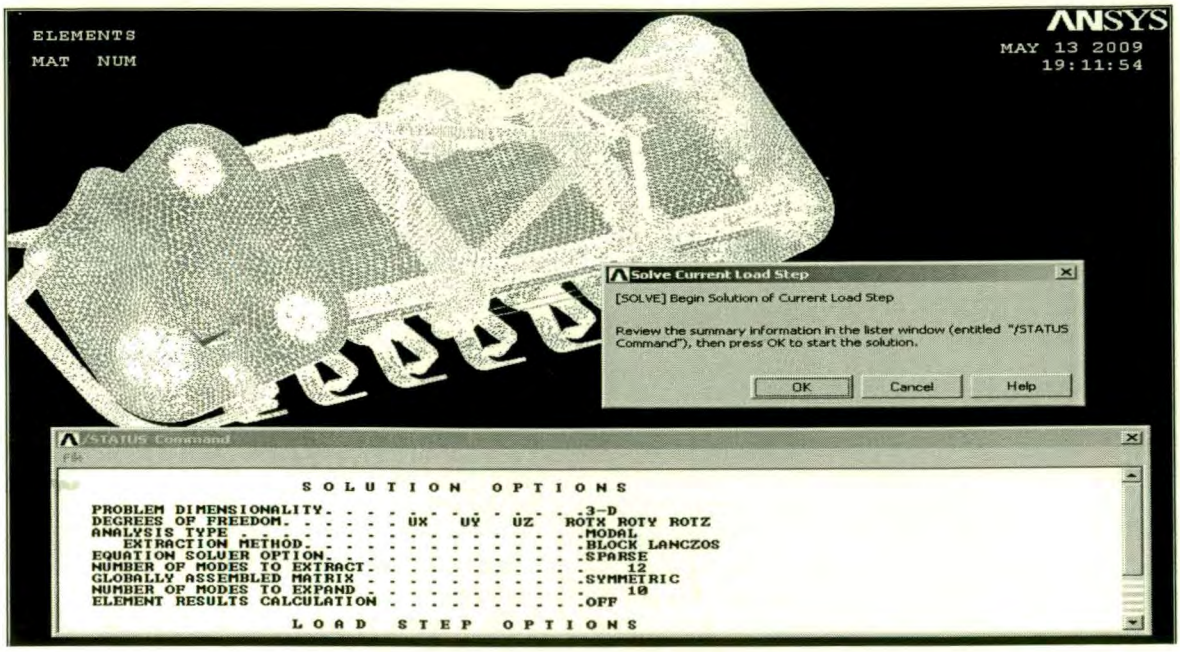

Figure 4.19: Solve current load step window

2. Then ANSYS will solve the rotavator analysis. It may take a few seconds before both of the following windows appear. You may close them both.

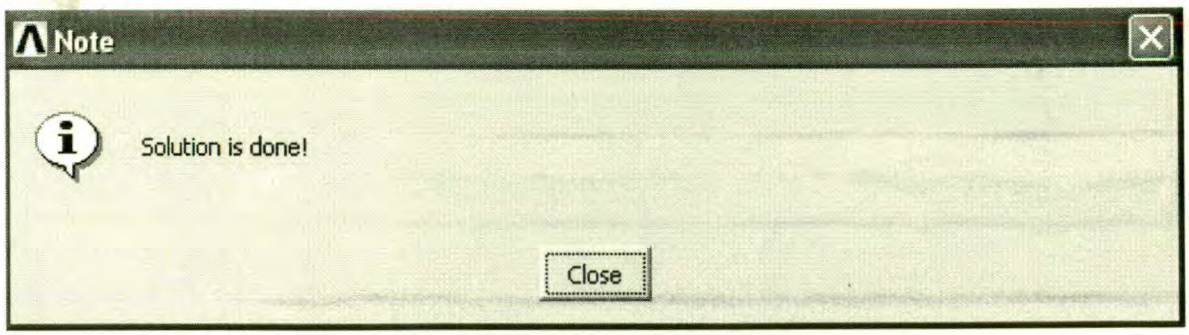

Figure 4.20: Solution windows.

This completes the solution phase. You are now ready for the final step, Post-processing.

4.5.1.3. Post processing

1. General postproce>Plot result>Contour plot>Nodal sol>DOF Sol

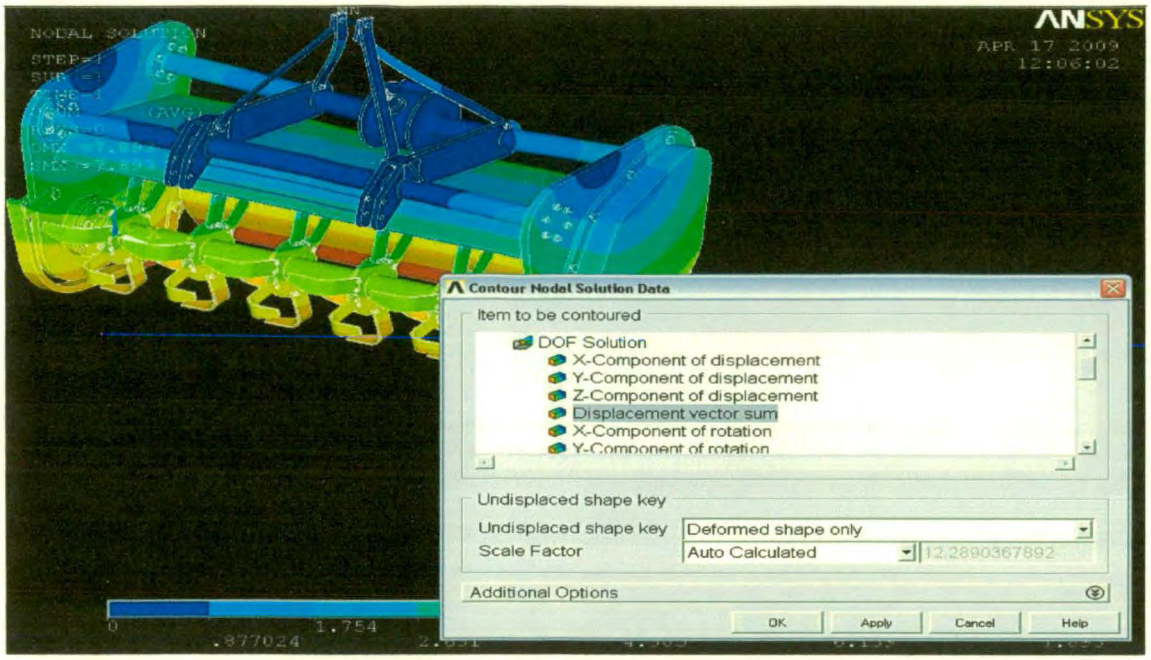

Fig 4.21: DOF solution

2. General postproce>Plot result>Contour plot>Nodal sol>DOF Sol

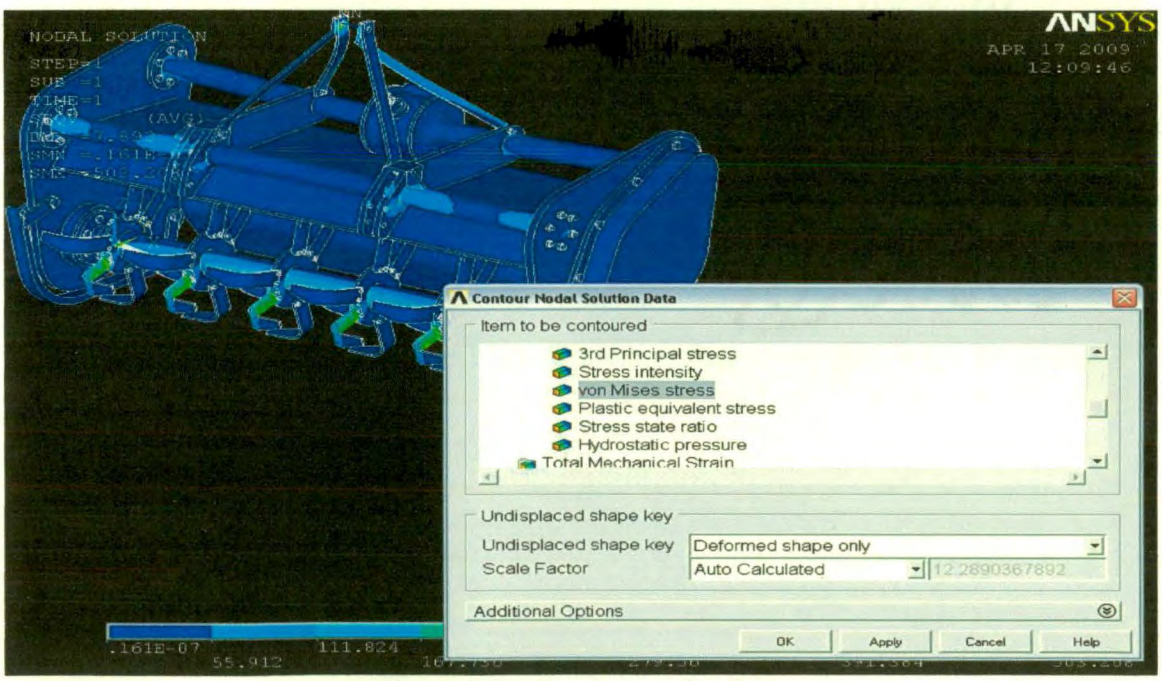

Fig 4.22: Stress solution

RESULTS AND DISCUSSION

CHAPTER V

RESULT AND DISCUSSION

5.1 Model Analysis

5.1.1 Deformation plots of all the rotavator components for different frequency (Hz) range

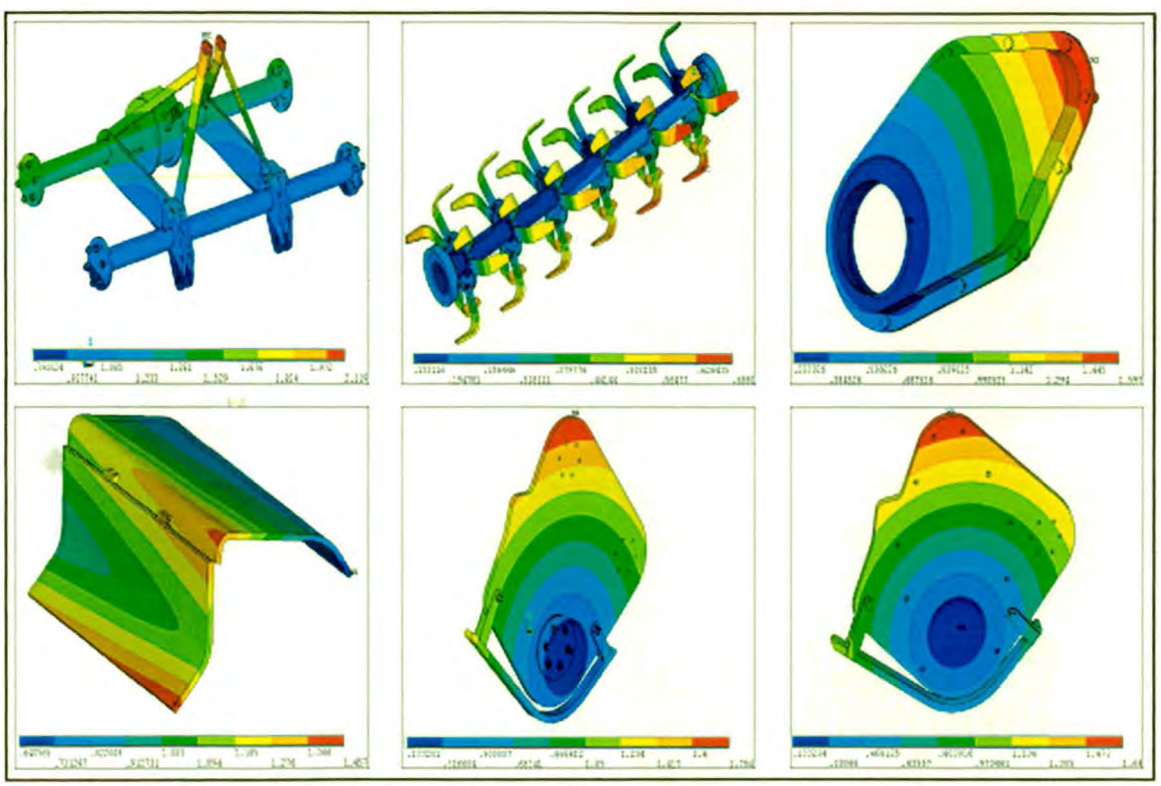

Fig 5.1: Diformation Plot for frequency 0.0350509 Hz

Deformation plots of all the individual components in mm.Blue colour shows the minimum deformation and red colour shows the maximum deformation location.

The deformation plots of all the components of Rotavator at the corresponding frequency are shown above. The maximum deformation of **2.119 mm** was observed in **Independent top mast** at the same frequency.

Table 5.1: Deformation at frequency 0.0350509 Hz

Sr. No.	Component Name	Max Deformation (mm)	Remark (Max deformation at)
1.	Independent top mast	2.119	Top
2.	Rotor with blade	0.688	Top right
3.	Side gear box part	1.597	Top
4.	Frame & Cover	1.457	Bottom front
5.	Left side frame	1.784	Top
6.	Right side frame	1.640	Top

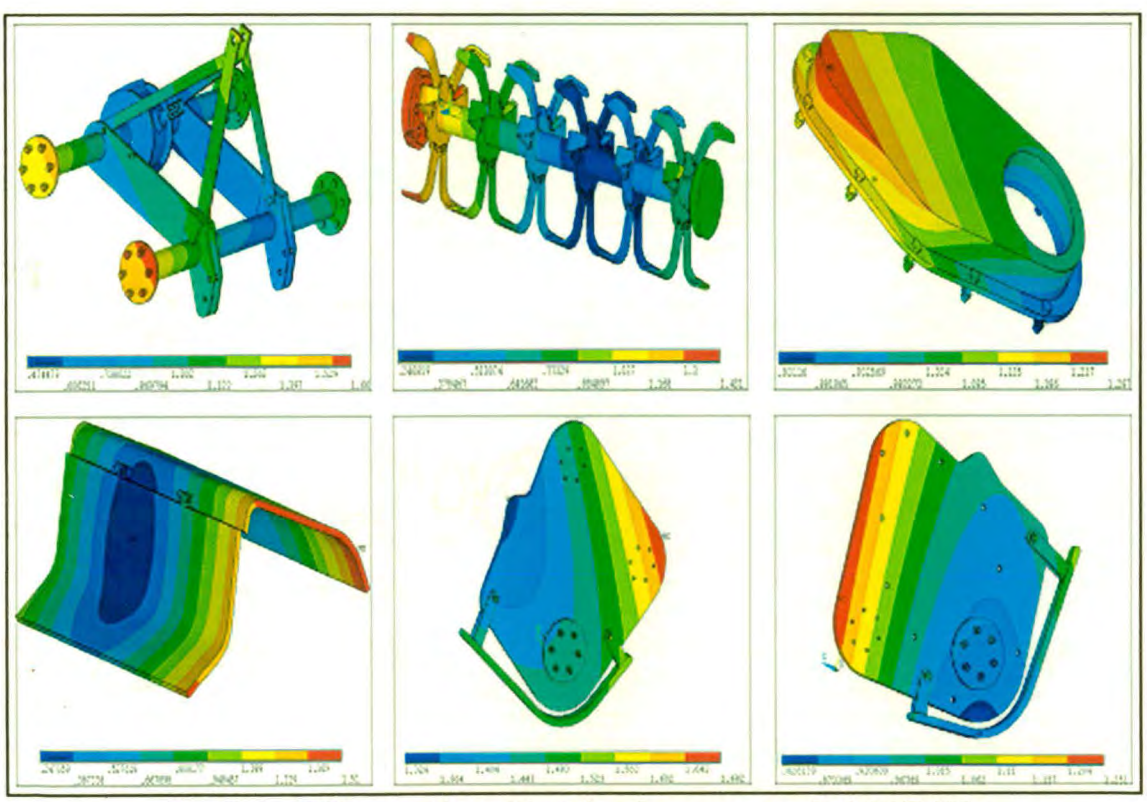

Fig 5.2: Diformation Plot for frequency 0.12474Hz

The deformation plots of all the components of Rotavator at the corresponding frequency are shown above. The maximum deformation of **1.682 mm** was observed in **Left side frame** at the same frequency.

Table 5.2: Deformation at frequency 0.12474 Hz

Sr. No.	Component Name	Max deformation (mm)	Remark (Max deformation at)
1.	Independent top mast	1.660	Bottom Left
2.	Rotor with blade	1.431	Left side
3.	Side Gear box bart	1.287	Top
4.	Frame & Cover	1.510	Front
5.	Left side frame	1.682	Right side center
6.	Right side frame	1.251	Top

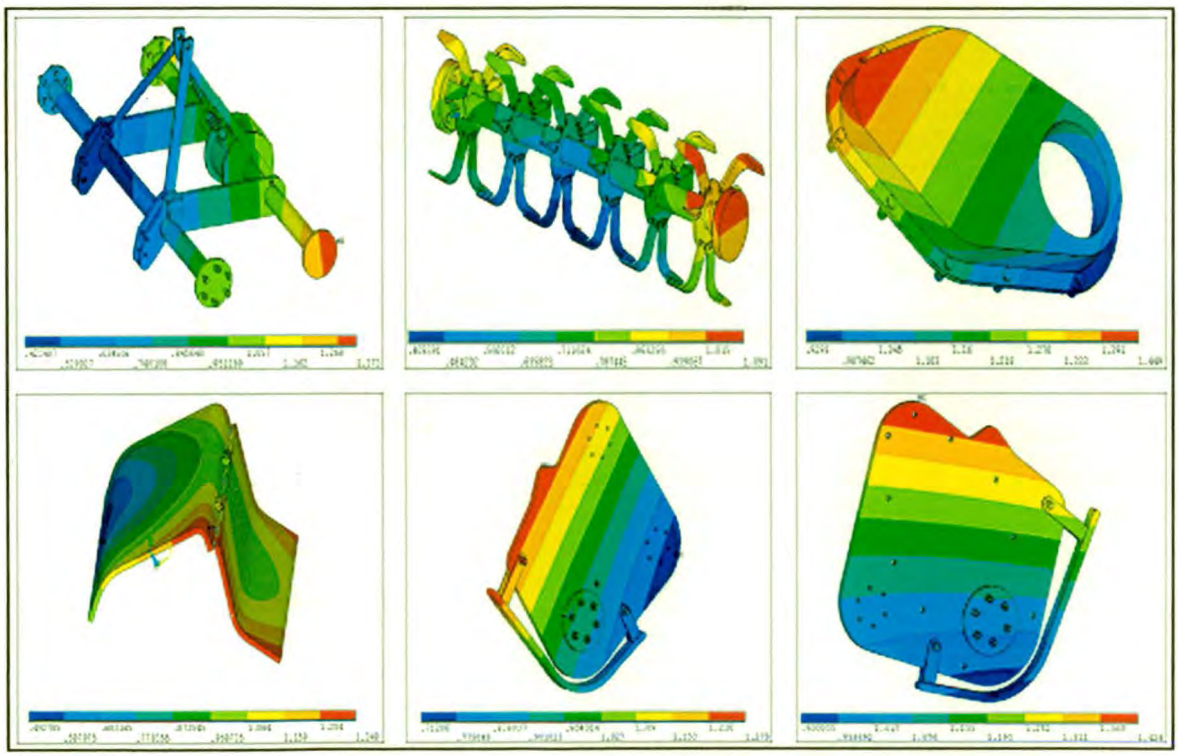

Fig 5.3: Diformation Plot for frequency 0.13638 Hz

The deformation plots of all the components of Rotavator at the corresponding frequency are shown above. The maximum deformation of **1.449 mm** was observed in **Side gear box part** at the same frequency

Table 5.3: Deformation at frequency 0.13638 Hz

Sr. No	Component Name	Max Deformation (mm)	Remark (Max deformation at)
1.	Independent top mast	1.373	Front right
2.	Rotor with Blade	1.091	Front
3.	Side Gear box part	1.449	Top
4.	Frame & Cover	1.349	Front
5.	Left side frame	1.279	Top
6.	Right side frame	1.428	Left

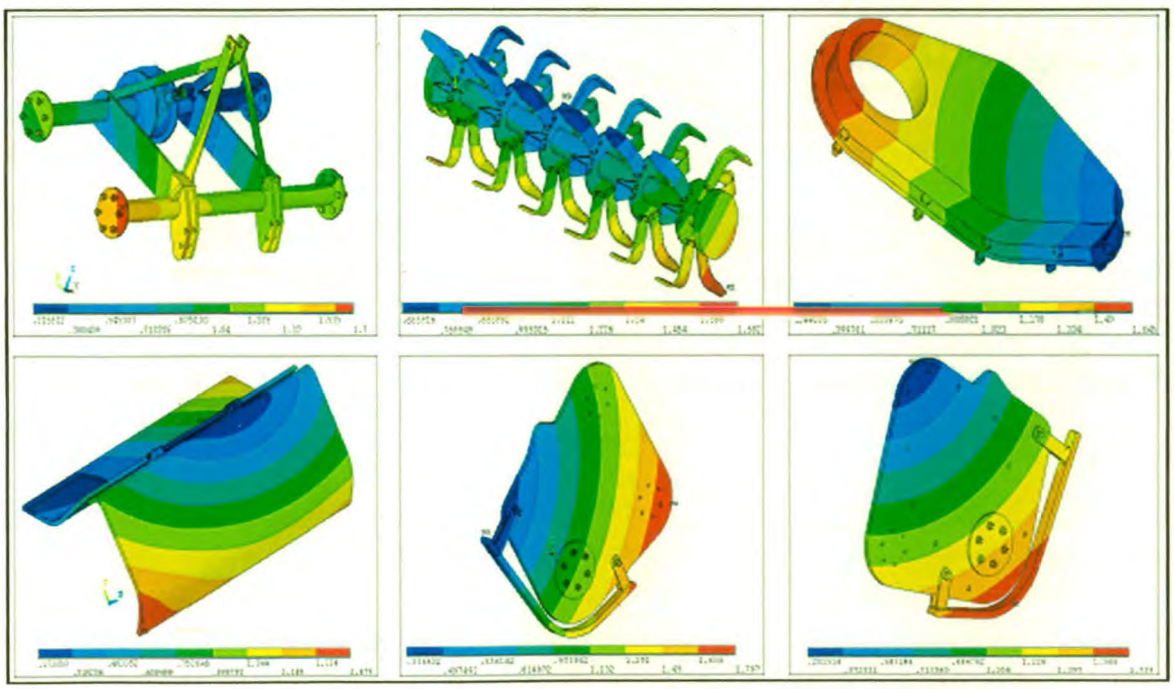

Fig 5.4: Deformation plots for frequency 0.16626 Hz

The deformation plots of all the components of Rotavator at the corresponding frequency are shown above. The maximum deformation of **1.767 mm** was observed in **Left side frame** at the same frequency

Table 5.4: Deformation at frequency 0.16626 Hz

Sr. No	Component Name	Max Deformation (mm)	Remark (Max deformation at)
1.	Independent top mast	1.70	Front Left
2.	Rotor with Blade	1.682	Front
3.	Side Gear box part	1.645	Top
4.	Frame & Cover	1.479	Bottom front
5.	Left side frame	1.767	Right Center
6.	Right side frame	1.739	Bottom

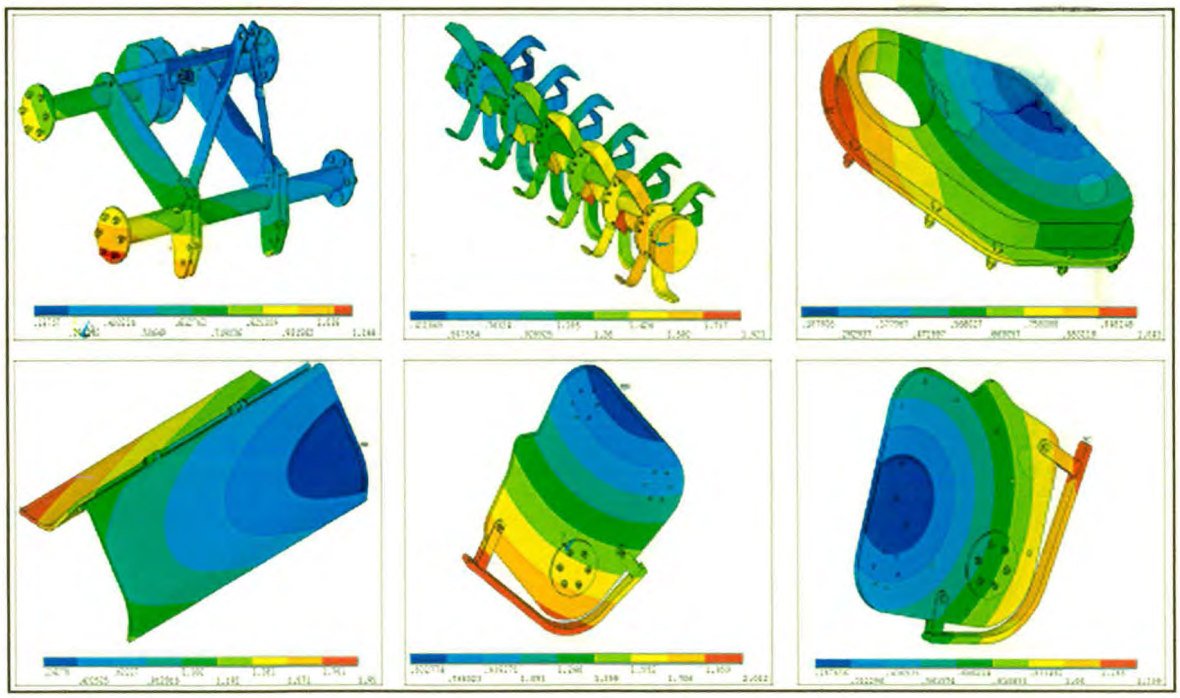

Fig 5.5: Deformation plots for frequency 0.18940 Hz

The deformation plots of all the components of Rotavator at the corresponding frequency are shown above. The maximum deformation of **2.012 mm** was observed in **Left side frame** at the same frequency

Table 5.5: Deformation at frequency 0.18940 Hz

Sr. No	Component Name	Max Deformation (mm)	Remark(Max deformation at)
1.	Independent top mast	1.144	Front
2.	Rotor with Blade	1.923	Front
3.	Side gear box part	1.043	Top
4.	Frame & Cover	1.95	Back
5.	Left side frame	2.012	Bottom
6.	Right side frame	1.309	Front Right

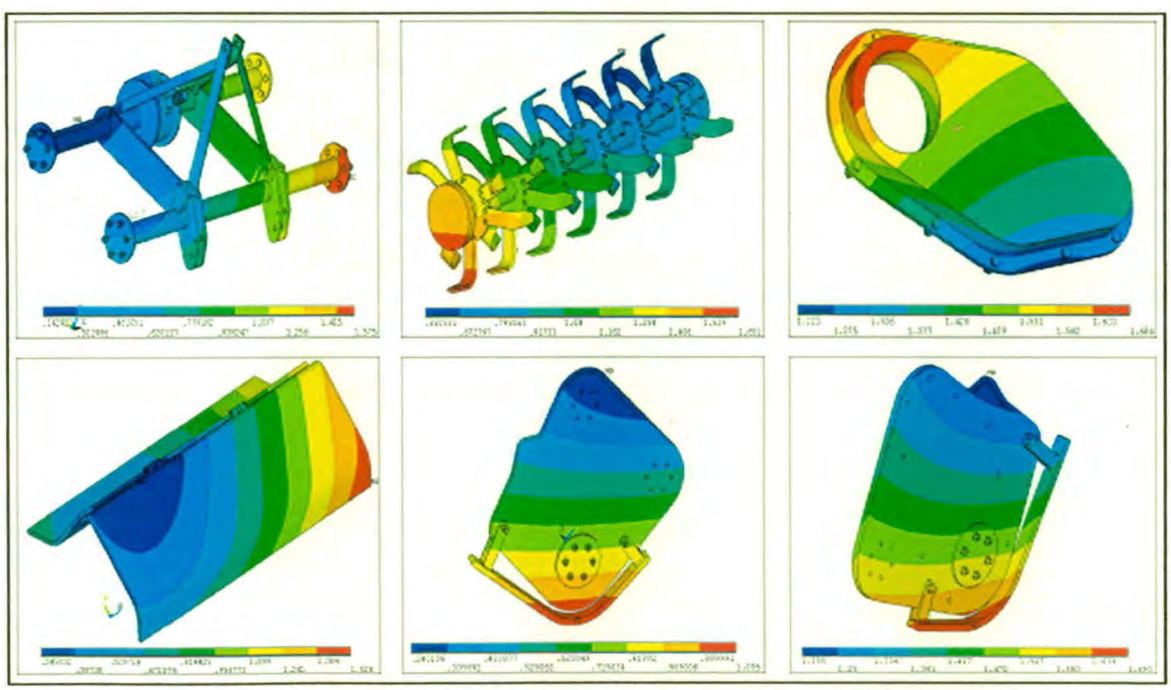

Fig 5.6: Deformation plots for frequency 0.22161 Hz

The deformation plots of all the components of Rotavator at the corresponding frequency are shown above. The maximum deformation of **1.693 mm** was observed in **Right side frame** at the same frequency

Table 4.6: Deformation at frequency 0.2216 Hz

Sr. No.	Component Name	Max Deformation (mm)	Remark (Max deformation at)
1.	Independent top mast	1.575	Right Front
2.	Rotor with Blade	1.651	Front
3.	Side gear box part	1.684	Top
4.	Frame & Cover	1.526	Bottom right
5.	Left side frame	1.095	Bottom
6.	Right side frame	1.693	Bottom

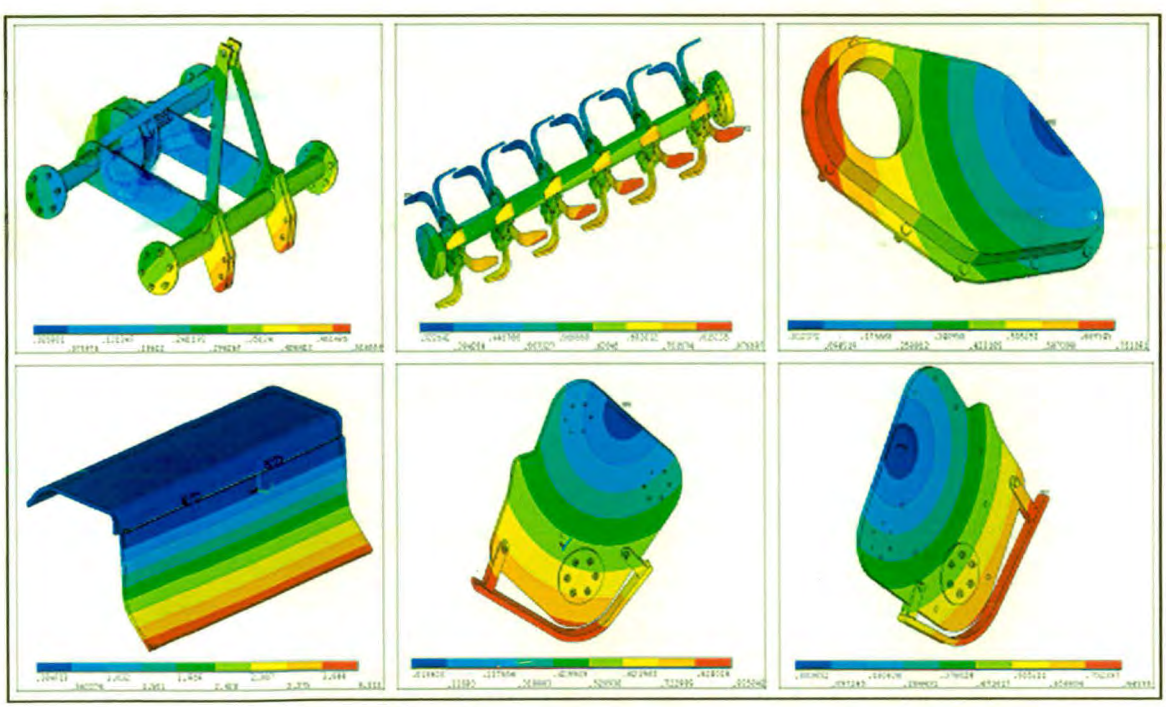

Fig 5.7: Deformation plots for frequency 16.645 Hz

The deformation plots of all the components of Rotavator at the corresponding frequency are shown above. The maximum deformation of **4.313 mm** was observed in **Frame and Cover** at the same frequency

Table 5.7: Deformation at frequency 16.645 Hz

Sr. No	Component Name	Max Deformation (mm)	Remark (Max deformation at)
1.	Independent top mast	0.516	Front
2.	Rotor with Blade	0.8766	Front
3.	Side gear box part	0.751691	Top
4.	Frame & Cover	4.313	Bottom front
5.	Left side frame	0.9250	Bottom
6.	Right side frame	0.845	Bottom

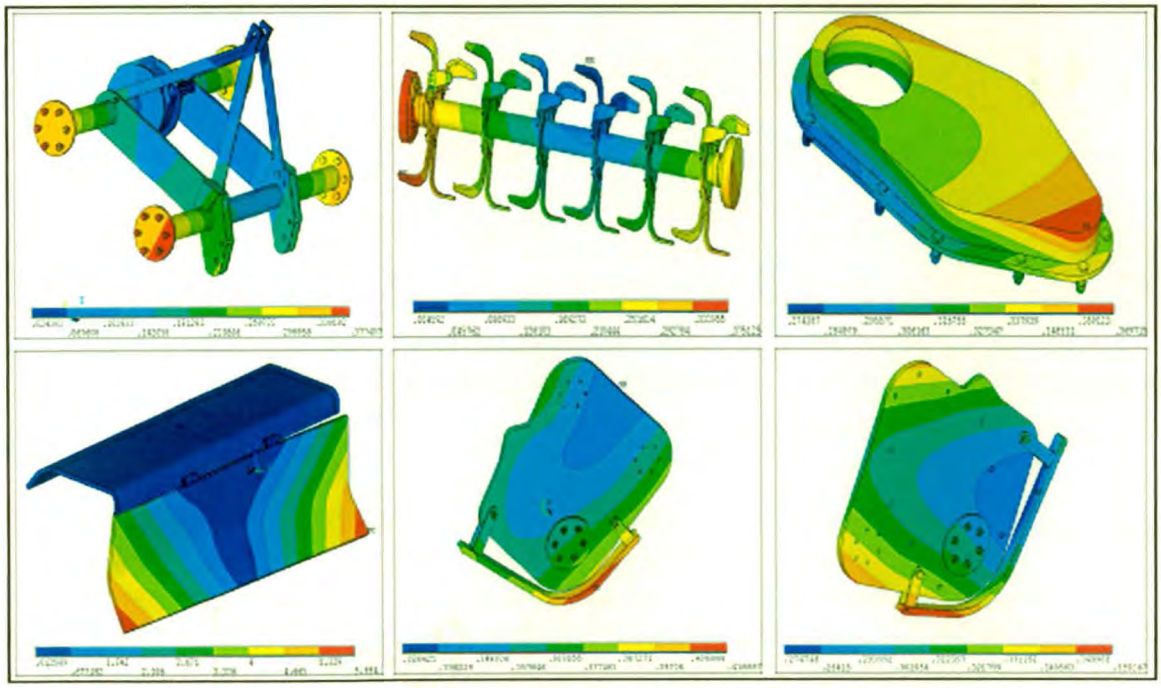

Fig 5.8: Deformation plots for frequency 40.799 Hz

The deformation plots of all the components of Rotavator at the corresponding frequency are shown above. The maximum deformation of **5.994 mm** was observed in **Frame and Cover** at the same frequency

Table 5.8: Deformation at frequency 40.799 Hz

Sr. No	Component Name	Max. Deformation (mm)	Remark(Max deformation at)
1.	Independent top mast	0.3774	Front
2.	Rotor with Blade	0.3751	Front Left
3.	Side gear box part	0.3697	Bottom
4.	Frame & Cover	5.994	Front corner
5.	Left side frame	0.4166	Bottom
6.	Right side frame	0.3593	Bottom

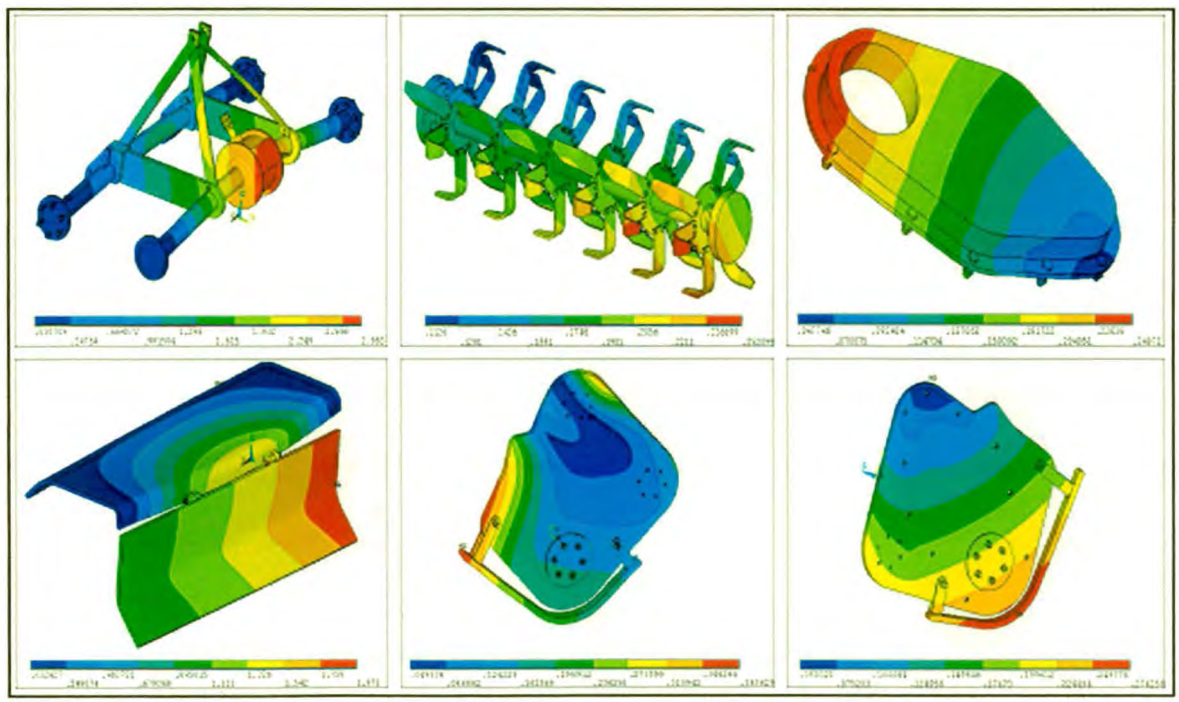

Fig 5.9: Deformation plots for frequency 56.556 Hz

The deformation plots of all the components of Rotavator at the corresponding frequency are shown above. The maximum deformation of **2.883 mm** was observed in **Independent top mast** at the same frequency

Table 5.9: Deformation at frequency 56.556 Hz

Sr. No	Component Name	Max Deformation (mm)	Remark (Max deformation at)
1.	Independent top mast	2.883	Front
2.	Rotor with Blade	0.252	Front
3.	Side gear box part	0.248	Top
4.	Frame & Cover	1.973	Front Right
5.	Left side frame	0.385	Left
6.	Right side frame	0.274	Bottom

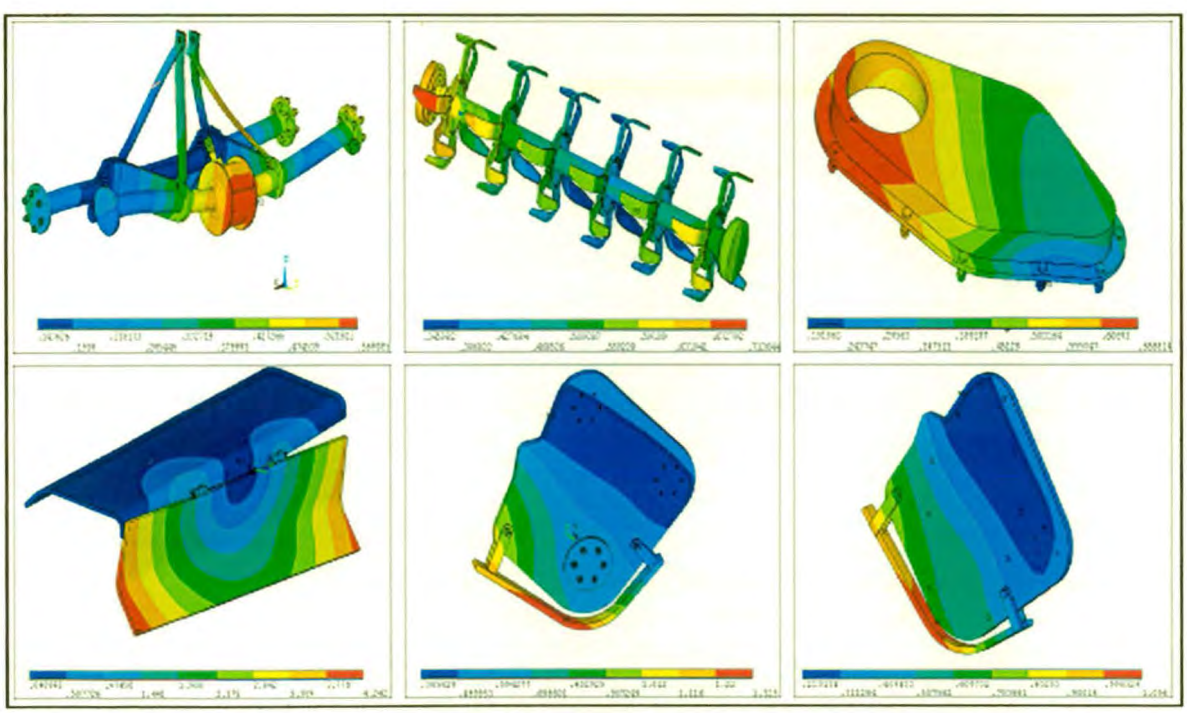

Fig 5.10: Deformation plots for frequency 66.299 Hz

The deformation plots of all the components of Rotavator at the corresponding frequency are shown above. The maximum deformation of **4.242 mm** was observed in **Frame and Cover** at the same frequency

Table 5.10: Deformation at frequency 66.299 Hz

Sr. No	Component Name	Max Deformation (mm)	Remark (Max deformation at)
1.	Independent top mast	0.569	Front
2.	Rotor with Blade	0.713	Top left
3.	Side gear box part	0.658	Top
4.	Frame & Cover	4.242	Side corner
5.	Left side frame	1.325	Bottom
6.	Right side frame	1.096	Bottom

5.1.2. Deformation plots Rotavator Assembly at all Frequency

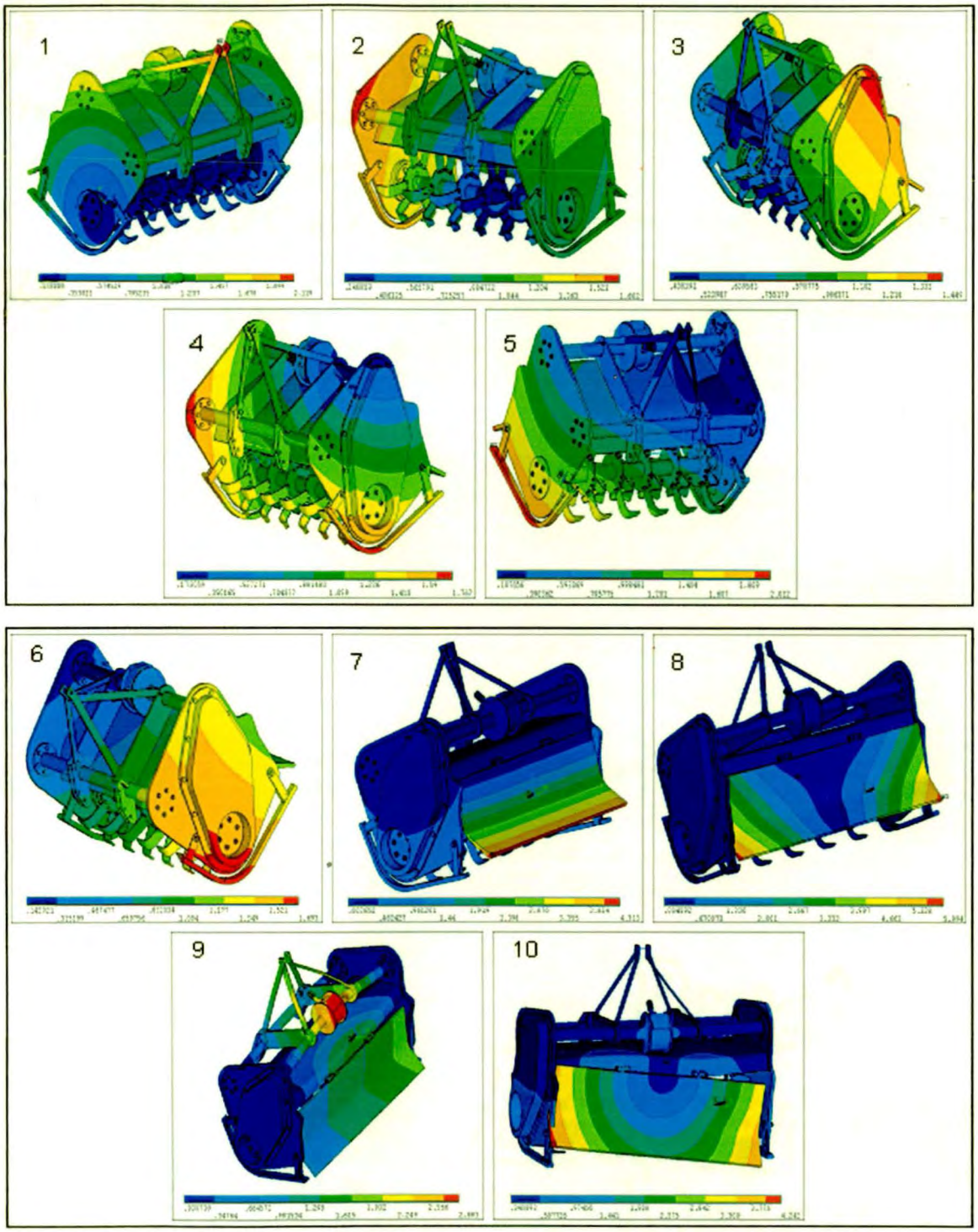

Fig 5.11: Deformation plot for rotavator assembly

Table 5.11: frequency wise Deformation of rotavator assembly

Sr. No.	Frequency Hz	Max Deformation (mm)	Remark (Max deformation at)
1.	$3.50509e^{-2}$	2.119	Top
2.	0.12474	1.682	Front left
3.	0.13638	1.449	Top Front
4.	0.16626	1.767	Front left
5.	0.18940	2.012	Bottom front
6.	0.22161	1.693	Bottom front
7.	16.645	4.313	Front
8.	40.799	5.994	Front corner
9.	56.556	2.883	Top front
10.	66.299	4.242	Bottom front

5.2 Displacement and Stress plot for 35 and 45 Hp tractor

5.2.1 Displacement vector sum plot for 35 Hp tractors

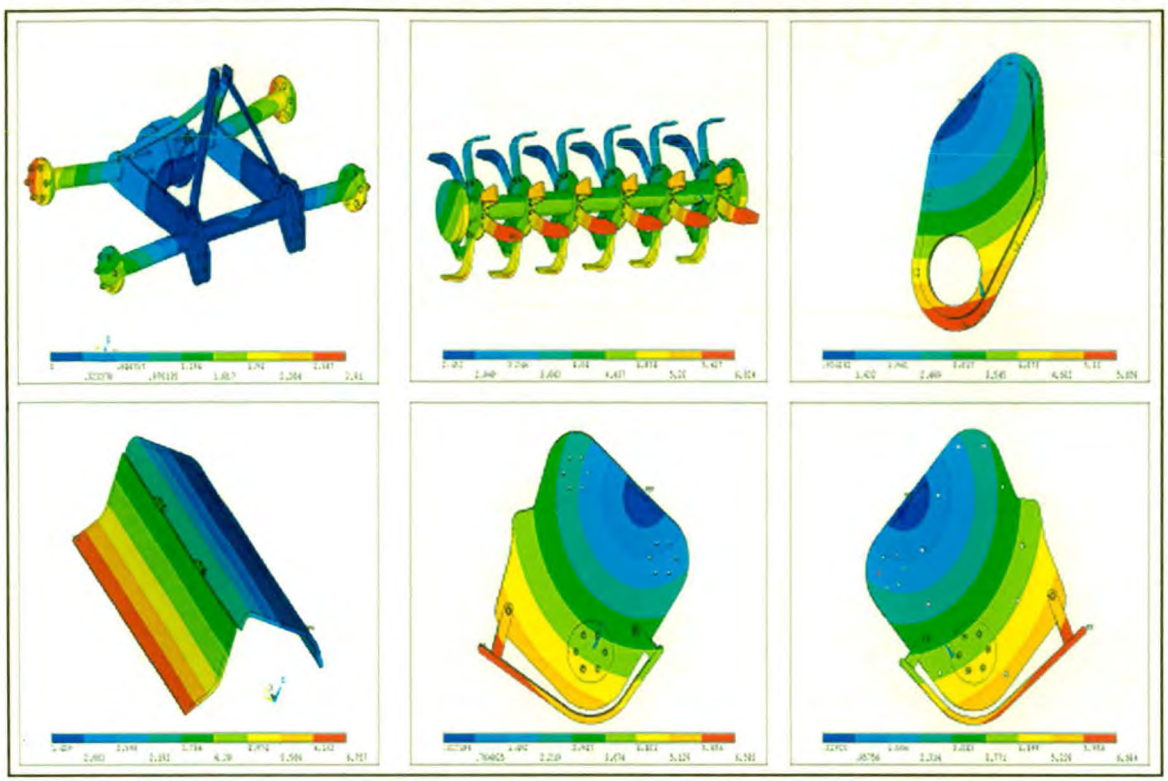

Fig 5.12: Displacement Vector Sum for 35 Hp Tractors

Table 5.12: Displacement of rotavator for 35 hp tractor

Sr. No	Component Name	Displacement in mm			
		X axis	Y axis	Z axis	D.V.S.
1	Rotavator assembly	1.012	6.172	3.48	6.757
2	Independent top mast	1.012	1.731	2.791	2.91
3	Rotor with Blade	-0.036	6.016	1.008	6.757
4	Side gear box part	-0.0497	5.626	2.939	5.658
5	Frame and Cover	0.0147	5.945	3.48	6.057
6	Left side frame	0.2466	5.994	3.423	6.526
7	Right side frame	0.2637	6.172	3.273	6.684

5.2.2 Displacement vector sum plot for 45 Hp tractor

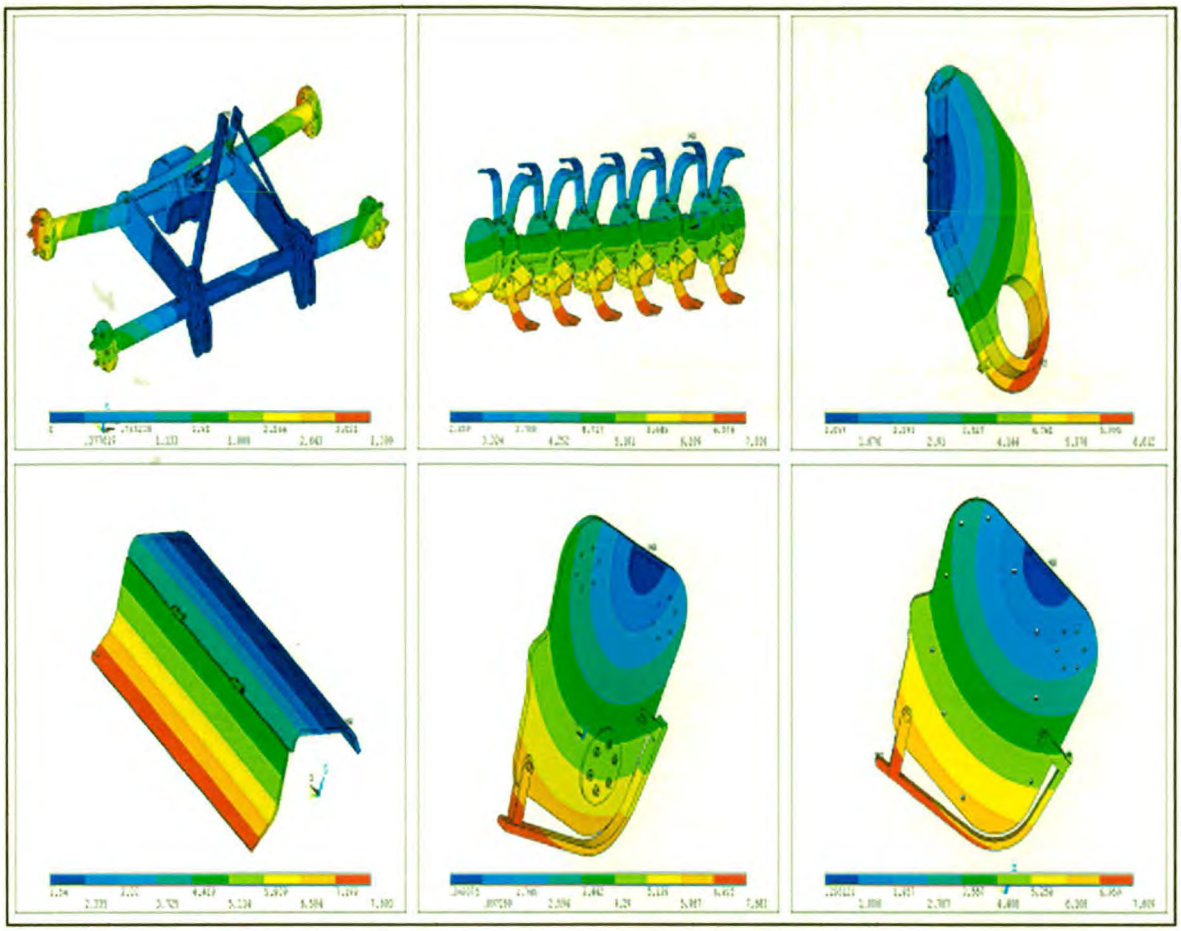

Fig 5.13: Displacement Vector Sum for 45 Hp Tractors

Table 5.13: Displacement of rotavator for 45 hp tractor

Sr. No	Component Name	Displacement in mm			
		X axis	Y axis	Z axis	D.V.S.
1	Rotavator assembly	1.18	7.213	4.065	7.893
2	Independent top mast	1.18	2.026	3.268	3.399
3	Rotor with Blade	-0.043	7.028	1.179	7.893
4	Side gear box part	-0.0591	6.574	3.43	6.612
5	Frame and Cover	0.0162	6.946	4.065	7.893
6	Left side frame	0.284	6.993	3.999	7.683
7	Right side frame	0.308	7.213	3.82	7.609

4.2.3 Von mises stress plot for 35 Hp tractor

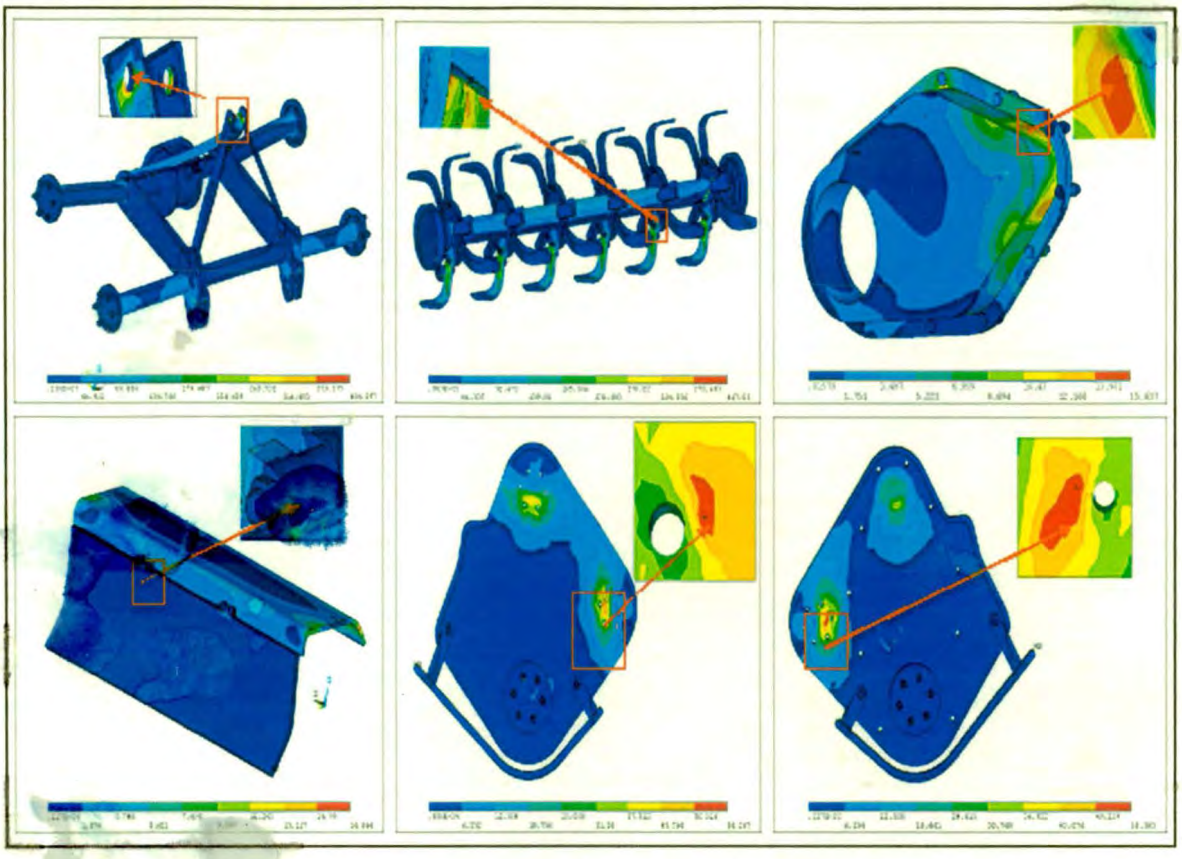

Fig 5.14: Von mises stress for 35 Hp tractor

Table 5.14: Stress of rotavator component for 35 hp tractor

Sr. No	Component Name	Von Mises Stress in Mpa			
		X axis	Y axis	Z axis	D.V.S.
1	Rotavator assembly	183.947	440.334	268.441	417.03
2	Independent top mast	172.669	135.735	268.441	404.29
3	Rotor with Blade	183.947	440.334	253.896	417.03
4	Side gear box part	11.139	8.867	9.896	15.637
5	Frame and Cover	23.191	8.403	7.89	16.864
6	Left side frame	22.517	33.905	39.758	56.267
7	Right side frame	25.181	40.016	52.561	55.383

4.2.4 Von mises stress Plot for 45 Hp tractors

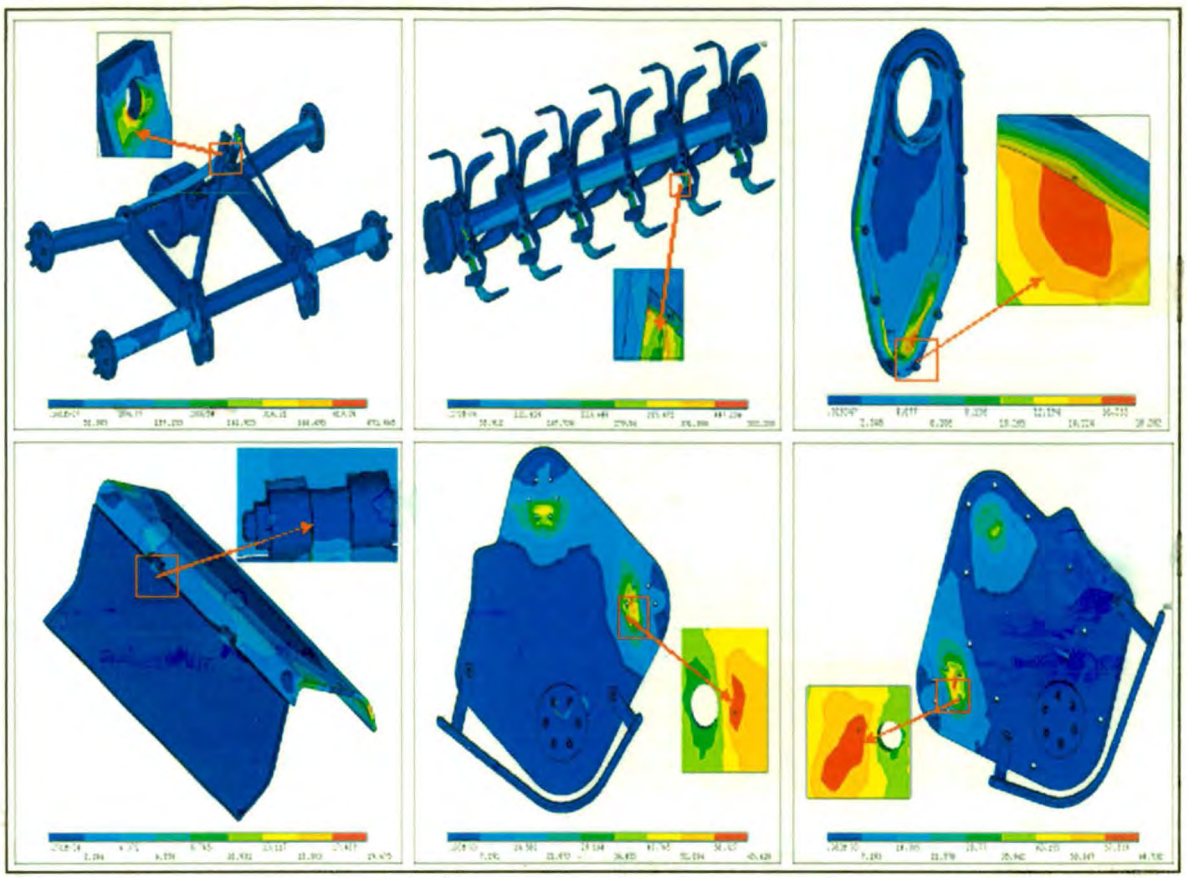

Fig 5.15: Von mises stress for 45 Hp tractors

Table 5.15:Stress of rotavator component for 45 hp tractor

Sr. No	Component Name	Von Mises Stress in Mpa			
		X axis	Y axis	Z axis	D.V.S.
1	Rotavator assembly	223.288	529.775	313.835	503.20
2	Independent top mast	201.453	158.683	313.835	471.47
3	Rotor with Blade	223.288	529.775	304.364	503.21
4	Side gear box part	13.021	10.3589	11.561	18.282
5	Frame and Cover	27.055	9.808	9.207	19.675
6	Left side frame	26.265	39.513	61.351	65.618
7	Right side frame	29.431	46.814	46.453	64.732

5.2.5 Deformation and Stress in rotavator assembly for 35 Hp tractor

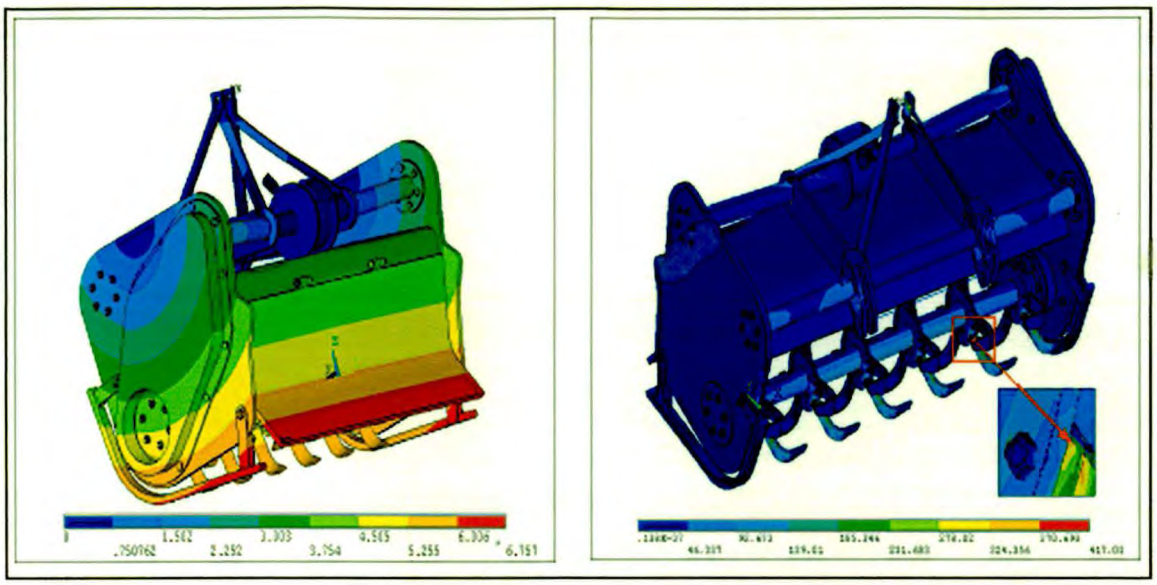

Fig 5.16 : Deformation and Stress plot for 35 hp tractor

5.2.6 Deformation and Stress in rotavator assembly for 45 Hp tractor

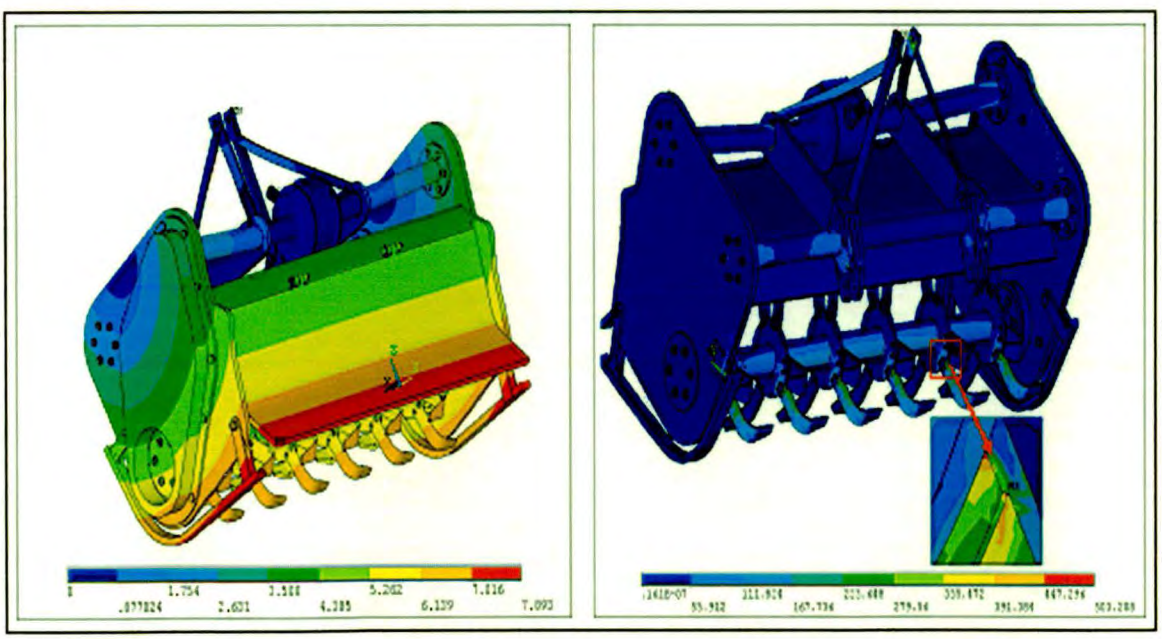

Fig 5.17: Deformation and Stress plot for 45 hp tractor

Table 5.16: Maximum deformation of rotavator parts at different frequency level

Sr. No	Frequency in Hz	Deformation in mm	Component Name
1	0.0350509	2.119	Independent top mast
2	0.12474	1.682	Left side frame
3	0.13638	1.449	Side gear box part
4	0.16626	1.767	Left side frame
5	0.18940	2.012	Left side frame
6	0.22161	1.693	Right side frame
7	16.645	4.313	Frame and Cover
8	40.799	5.994	Frame and Cover
9	56.556	2.883	Independent top mast
10	66.299	4.242	Frame and Cover

Table 5.17: Maximum resultant displacement and Von mises stress of rotavator parts for 35 hp and 45 hp tractor

Sr. No	Component Name	Resultant displacement (mm)		Von mises stress (Mpa)	
		35 hp Tractor	45 hp Tractor	35 hp Tractor	45 hp Tractor
1	Independent top mast	2.19	3.399	404.297	471.465
2	Rotor with Blade	6.757	7.893	417.03	503.208
3	Side gear box part	5.658	6.612	15.637	18.282
4	Frame and Cover	6.526	7.893	16.864	19.675
5	Left side frame	6.583	7.683	56.267	65.618
6	Right side frame	6.684	7.609	55.383	64.732

5.1.2.7 Structural analysis for single rotavator blade

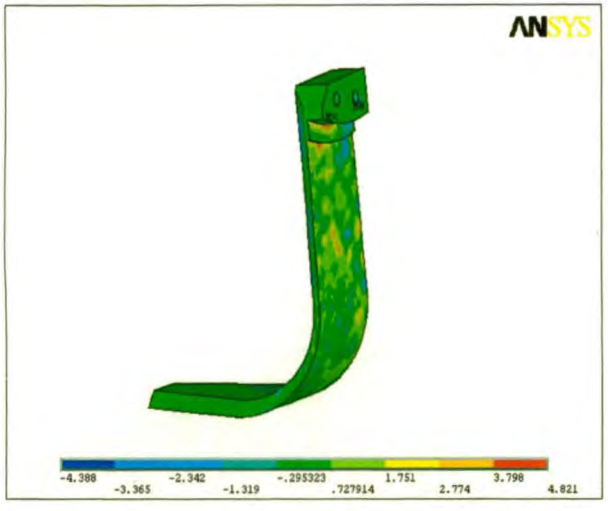

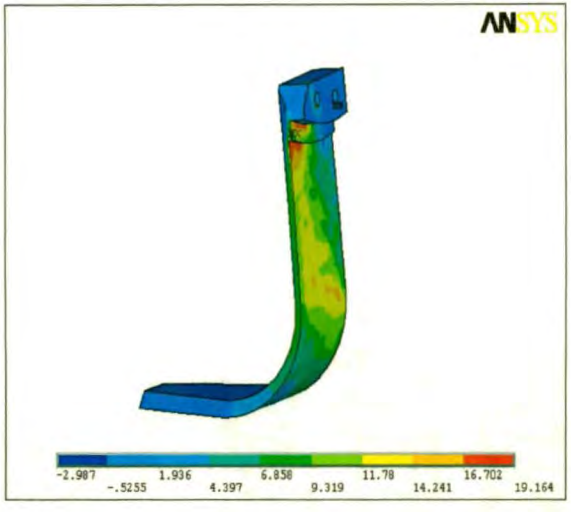

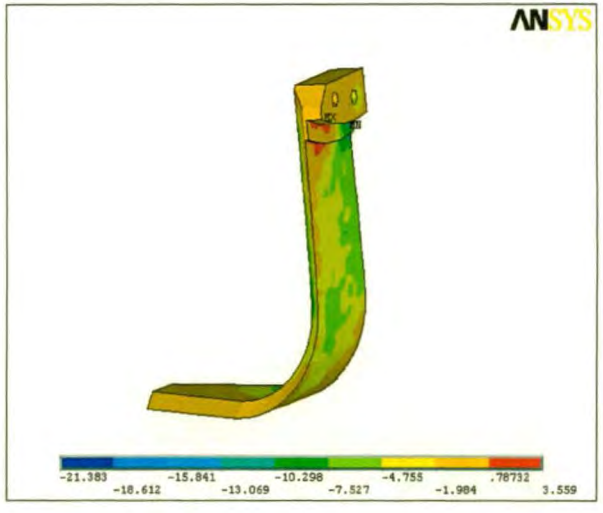

Fig 5. 18: Principle stress along X axis **Fig 5. 19: Principle stress along Y axis** **Fig 5. 20: Principle stress along Z axis**

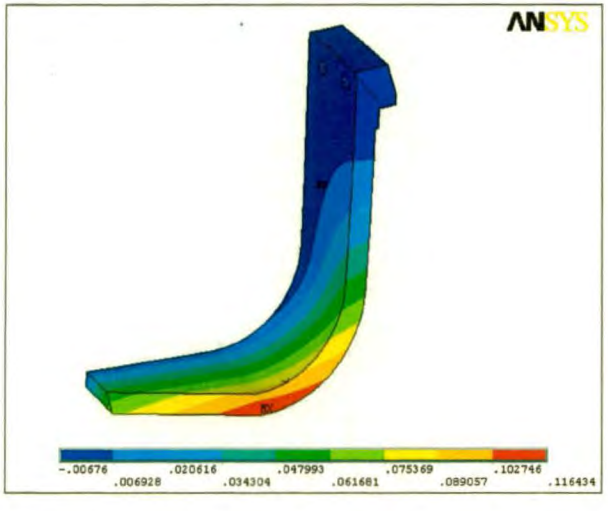

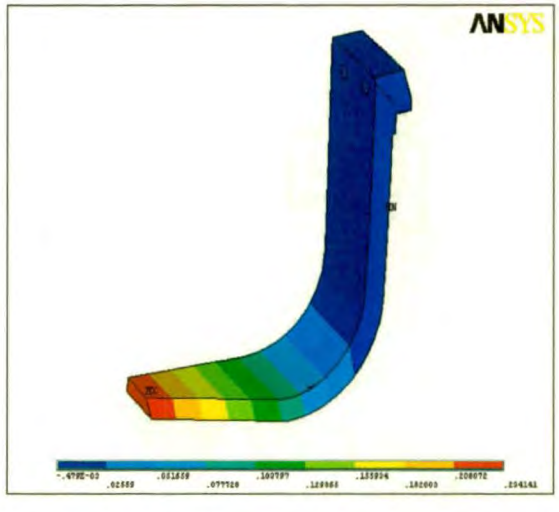

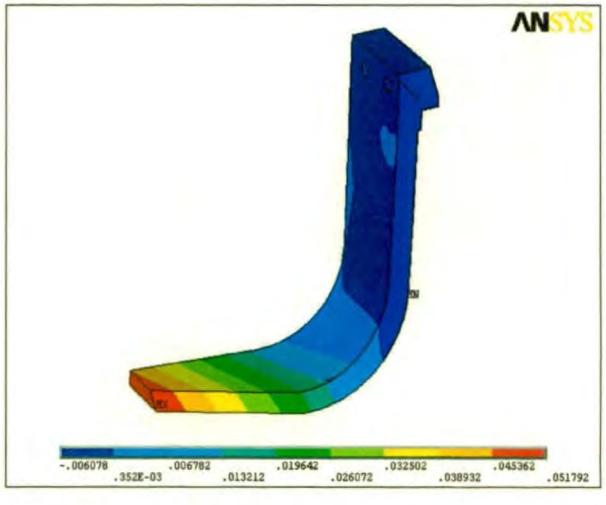

Fig 5. 21: Displacement along X axis **Fig 5. 22: Displacement along Y axis** **Fig 5. 23: Displacement along Z axis**

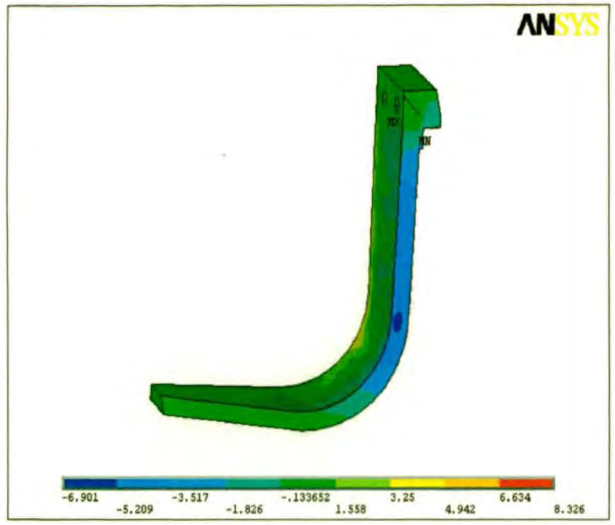

Fig 5. 24: Shear stress along XY axis

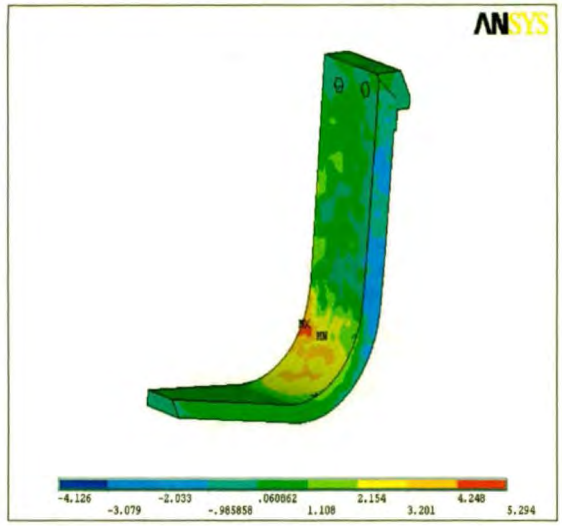

Fig 5. 25: Shear stress along XZ axis

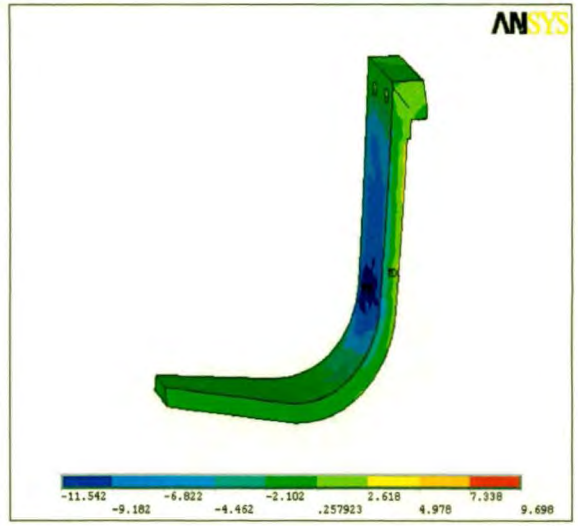

Fig 5. 26: Shear stress along YZ axis

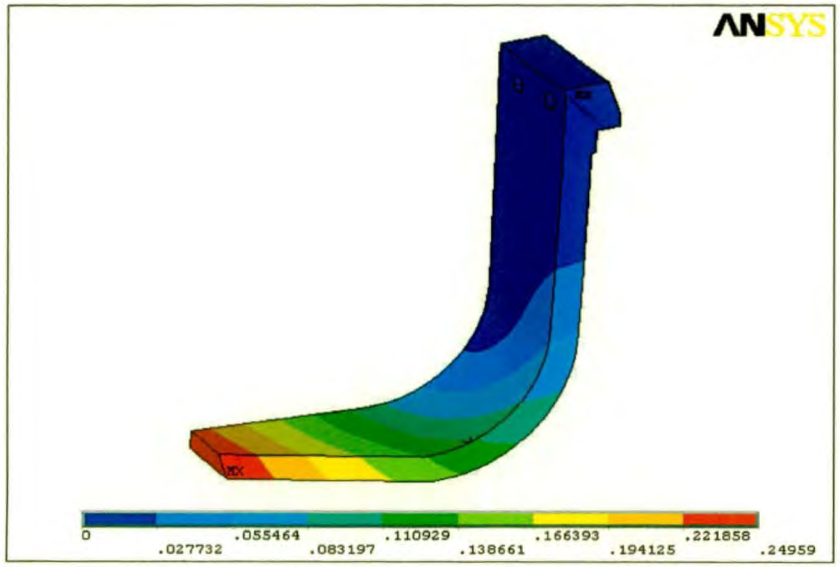

Fig 5. 27: **Displacement vector sum**

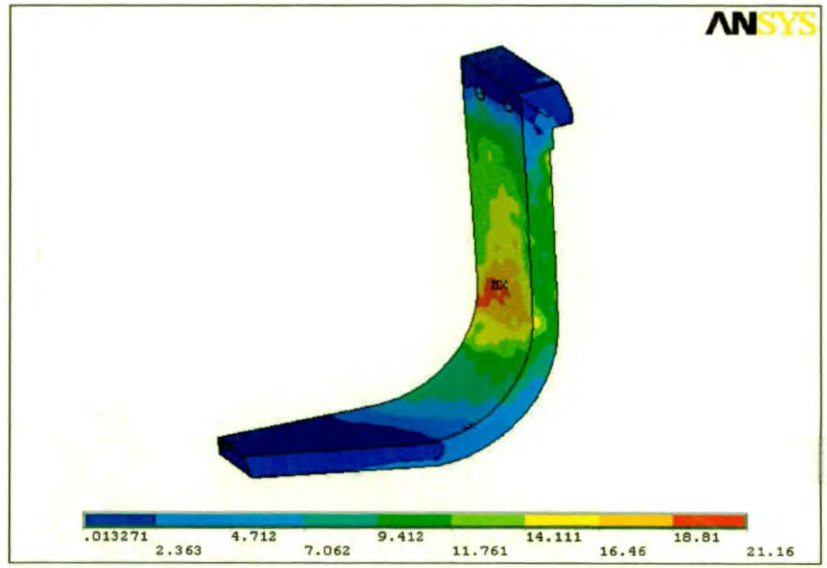

Fig 5. 28: **Von mises stress**

Table 5.18:- Principle stresses for single rotavator blade

Sr. No	Component Name	Principle stress in Mpa		
		X axis	Y axis	Z axis
1	Blade	4.821	19.164	3.559

Table 5.19:- Displacement for single rotavator blade

Sr. No	Component Name	Displacement in mm			
		X axis	Y axis	Z axis	D.V.S.
1	Blade	0.116434	0.234141	0.051792	0.24959

Table 5.20:- Shear stress for single rotavator blade

Sr. No	Component Name	Shear stress in Mpa		
		XY axis	XZ axis	YZ axis
1	Blade	8.326	5.294	9.698

Table 5.21:- Component stress for single rotavator blade

Sr. No	Component Name	Component stress in mm			
		X axis	Y axis	Z axis	V.M.S.
1	Blade	6.586	17.265	9.408	21.16

SUMMARY AND CONCLUSION

CHAPTER-VI

SUMMARY AND CONCLUSION

A rotary tillage tool such as rotavator is designed in computer aided design software. The rotary motion and soil surface interaction is considered with respect to the soil v/s. tillage tool dynamics by considering the following factors effecting the tillage operation such as tractor power (hp), maximum peripheral force (N), rotavator tyne velocity (m/s), tractor transmission efficiency (0.9 for concurrent revolution and 0.8-0.9 for reversed rotary), soil resistance to 0.7-0.8, radius of rotary (mm)

The software executes the structural analysis in terms of the type of forces interacting at soil and tillage tool interface. The selected rotavator is designed with accurate dimensions and geometry. Here each and every assembled part of rotavator is effectively subject to rotary action as well as linear tillage operation.

The design analysis procedure is carried with the following estimated parameters such as

For **35** hp tractor:

- Maximum peripheral force on rotary blade= **6031.08975** N
  and Torque= **270600** N-mm (see appendix-I)

For **45** hp tractor:

- Maximum peripheral force on rotary blade =**7041.17** N
  and Torque= **315920** N-mm (see appendix-I)

The effect of high power, forces on cutter blade and soil parameters interfaces with each other causes deformations

Especially for the individual effect and the assembled effect together is determined by simulation to understand and correct the design of Rotavator by failure diagnosis with FEM method.

In this study, rotary tiller which was designed as three-dimensional solid geometry in the parametric design software according to its operating condition and simulated under traditional designing method with the effective changes for its design optimization.

Modal analysis

The modal analysis as per above stated condition is done and the results obtained from the table 1 in Appendix VI, it is observed that

1. The maximum and minimum deformation of 1.923mm and 0.252mm respectively was observed in blade section.

Structural analysis

The structural analysis as per above stated condition is done and the results obtained from the table 2 in Appendix VI, it is observed that

1. The displacement Vector Sum and Von Mises Stress is maximum at blade section such as 6.757 mm and 417.03 Mpa respectively for 35 hp tractor
2. The displacement Vector sum and Von mises stress is maximum at blade section such as 7.893 mm and 503.21 Mpa respectively for 45 hp tractor

Conclusion

The Design analysis of rotavator results with an output file generated by simulation with respect to yield stress and deformation obtained by using condition in the Post processor.

The following observations obtained after applying the input parameters and the simulation for the field performance under ideal condition

1. The maximum displacement vector sum in rotavator for **35** hp tractor was observed in Blade section.

2. The maximum displacement vector sum in rotavator for **45** hp tractor is **7.893** mm was observed in Blade section.

3. The maximum von mises stress in rotavator for **35** hp tractor is **417.03** Mpa was observed in Blade section.

4. The maximum von mises stress in rotavator for **45** hp tractor is **503.20** Mpa was observed in Blade section.

5. The maximum principle stress for **35 hp** tractor is **490 Mpa** was observed in blade section. This stress value is less than yield stress of blade material i.e **690 Mpa**

6. The maximum principle stress for **45 hp** tractor is **577 Mpa** was observed in blade section. This stress value is less than yield stress of blade material i.e **690 Mpa**

Hence it is concluded that there is sufficient tolerance in changing the dimensions of raotavator frame sections and side gear box for removing the excess weight in the solid section and also there is a scope in changing the dimensions to increase the strength by adding the weight in blade section.

SUGGESTIONS FOR FUTURE WORK

CHAPTER-VII

SUGGESTIONS FOR FUTURE WORK

1. The Solid model developed in the CAD software is a standard model of rotavator from which various types of design changes can be made and analyzed for its design optimization.

2. The service function of rotavator is most important aspect in design and development of agricultural tillage tool which changes according to farmer's need. Hence the research can be further extended for producing different redesigns according to operational needs and the farmer's degree of acceptance.

3. The software needs knowledge of application from the field which is a inputs resource in expectation of the useful results for its redesigning process or several kinds of experiments for its optimization.

4. Optimization is performed to reduce the weight and manufacturing cost by changing its material for e.g. Micro alloyed steel is having higher yield strength and endurance limit hence the weight of rotavator can be further reduced.

5. The designer/researcher/user may create a material library and the various custom rotavator's designing parameters within software.

LITERATURE CITED

LITERATURE CITED

Akinci, I., D. Yilmaz, and M. Canakci. (2005). Failure of a Rotary Tiller Spur Gear. Engineering failure analysis, 12(3): 400- 404.

Altair Engineering. Inc, "Hypermesh Users Guide", 2003

Anonymous, (1971). Design data book. PSG college of Tech. Kalaikathir Publications, Coimbatore.

Ansys Inc, "ANSYS 8.1 Documentation, Structural Analysis Guide", Swansos Analysis System, United state, 2004

Balock, J.M. (1986). "Performance of power tiller blades". . Agric. Mech. in Asia, Africa and Latin America, 17 (1): 22-26.

Bax, A. J., and S. V. Kooi. (2007). "Nonlinear Stress Analysis and Optimization of a welded plate Steel Pro-Engineer Assembly".

Bechly, M. E., and P. D. Clausent. (1997). "Structural Design of a Composite wind turbine blade using Finite Element Analysis". Computers & Structures Vol. 63. No. 3, pp. 639-616.

Beeny, J.M., and D. C. Khoo. (1970). "Preliminary investigations in to the performance of different shaped blades for the rotary tillage of wet rice soil". J. Agric. Engg. Res, 15 (1):27-33.

Ben Yahia, Logue, and M. Khelifi. (1999). "Optimum settings for rotary tools used for on-the-row mechanical cultivation in corn". Transactions of ASAE, 15(6): 615-619.

Biswas, H.S. (1993). "Performance Evaluation and optimization of straight blades for shallow tillage and weeding in black soils", Agric. Mech. in Asia, Africa and Latin America, 24(4) 19-22.

Borovkov, A. I., and A. A. Michailov. (2007). "Finite Element 3D Structural and Model Analysis of Three Layered Finned coninal Shells". Computational Mechanics Lab., St. Petersburg State Technical University, Russia

David Roylance (2001). "Finite Element Analysis Methode". Department of Materials Science and Engineering Massachusetts Institute of Technology Cambridge, MA 02139 February 28

Davies, G.R. (1967). Abration test on plastics, elestomers and ferrous metal. J. Agric. Engg. Res. 12(1); 55-60.

Fielke, J.M, T.W. Reiley; M.G. Slattery and R.W. Fitzpatt. (1993). "Comparision of tillage forces and wear rates of pressed and cast cultivator shares". Soil and Tillage Research, 25; 317-328.

Ghosh, B.N. (1967). "The power requirement of a rotary cultivator". J. Agric. Engg. Res., 12 (1): 5-12.

Gill, W.R., and G.E. Vanden Berg. (1996). "Design of tillage tool. In soil dynamics in tillage and traction". 211-294. Washington, D.C.,U.S.GPO

Godwin, R.J. (1982). "Force measurement on tillage implements". 9th Conference of the International soil Tillage Research organization, Osijek,

Godwin, R.J., and S.M. Miller. (1987). "Instrumentation to study the forces systems and vertical behavior of Soil-engaging Implements". Journal of Agricultural Engg.36, 301-310

Gokhale, N. S., S. S. deshpande, and A. N. Thite. (2008). "Practical Finite Element Analysis".

Gupta, C.P., and R. Viswvanathan. (1993). "Power requirement of a rotary tiller in satured soil". Transactions of ASAE, 36 (4):1009-1012.

Gupta, J .P., and K.P. Pandey. (1991). "Performance of spiral and straight edge tynes of rotary tiller under wet land condition". Journal of Agricultural Engineering 1991, 28; 1-4, 211-216.

Gupta, J.P., and K.P. Pandey. (1996). "Performance of rotary tines blade under wetland condition". Agric. Mech. in Asia, Africa and Latin America, 27 (1): 16-20.

Gurswamy, T. (1988). "Effect of blade shape on the performance of blade hoe". Agricultural Engineering Today, 12 (2); 25-27.

Hamdy, M.Y., R.E. Stewart, and W. H. Johnson. (1996) "Theoretical Analysis of Centrifugal Threshing and separation". ASAE 25(1), 65-73

Hendrick James G, and R. Gill William. (1971a). "Rotary – Tiller Design parameters – Direction of rotation". Transactions of ASAE, 669-674.

Hendrick James G, and R. Gill William. (1971b). "Rotary – Tiller Design parameters – Depth of Tillage". Transactions of ASAE, 675-683.

Hendrick James G, and R. Gill William. (1971c). "Rotary – Tiller Design parameters – Ratio of peripheral and forward velocities". Transactions of ASAE, 684-688.

Jain, S.C., and Philip (2003). "Farm machinery an approach", standard publishers distributors Delhi pp. 5-7, 21, 27.

Jonathan Raub (2008). "Modeling Diesel Engine Cylinder Head Gaskets using the Gasket Material option of the SOLID185 Element".

Khomane, S., and D. K. Mahanty. (2007). "Analysis and Weight Reduction of a Tractor's Front Axle".

Kumar V.J.F (1987). "Effect of Weeder Design on operating force", Agric. Mech. in Asia, Africa and Latin America, 18(4), 75-79.

Koichi Iwasaki, Y. Miyabe, and K. Sumitaka. (1993). "Dynamic analysis of rotary tiller, (Measurement of stress on chain tightener)". Journal of Agricultural Engineer, 22 (5), 112-118

Kosutic, S., D Filipovic, and Z Gospodaric. (1996). "Rotary Cultivator Energy Requirement Influenced by Different Constructional Characteristics, Velocity and Depth of Tillage". Poljoprivredna-Znanstvena-Somatra, vol 61, nos 3-4, 1996, p 239.

Kosutic, S., D. Filipovic and Z. Gospodaric (1997). "Agro technical and energetic characteristic of a rotary cultivator with spike tins in seedbed preparation". International-Agricultural-Engineering-Journal, 6:3-4, 137-144.

Krutz, G., L. Thompson and C. Poul (1984). "Design of Agricultural Machines". John Willey and Sons, New Delhi. pp. 32-36.

Leacher, F.G., and H.F.McColly. (1959). "Abrasive wear resistance of hard facing material using on agricultural tillage tools". Transactions of ASAE 2(1); 55-57.

Mehmet topakchi, Kursat H., Celik D., and Akinchi (2008). "Stress Analysis on Transmission gears of rotary tiller using Finite Element Method". Akdeniz University, Faculty of Agriculture, Department of Agricultural Machinery, Antalya, Turkey Accepted 12 August 2008

Miu, P. I., and H. D. Kutzbach. (2008). "Modeling and simulation of Grain threshing and separation in threshing units- Part- I". Computer and Electronics in Agriculture 60 (2008):96-104

Monsouri, Y.S., and M.S. Daraudi (2002). "Design and development of a rotary tiller as attachment to Ashtad two wheel tractor". Journal of Agricultural Sciences-Islamic Arad University 8:2 Ar.33-Ar 53, 4-5.

Mootaz Abo-Elnor, Hamilton R., and J. T. Boyle. (2004). "Simulation of soil–blade interaction for sandy soil using advanced 3D finite element analysis". Soil & Tillage Research 75 (2004) 61–73

Murali, M. R. (2002). "Finite Element Topography and Shape Optimization of Jounce Bumper". SAE Inc, Dana corp.

Nishiwaki, H., S. Nishiwaki, and T. Amago (2008). "A New Type of Computer Aided Engineering Integration for Design Engineers – First Order". Analysis Linked with ANSYS Toyota Central R&D Labs., Inc.Noboru Kikuchi the University of Michigan

Niyamapa, T.S. Thampatpong, C. Rangdang, V.M. Salokhe, and G. Singh (1994). "Laboratory investigation on design parameters of rotary tiller". International agricultural engineering conference. Processing of a conference held in Bangkok, Thailand, Volume I., 206-214.

Noguchi, N. (1998). "Internet CAD system for Agricultural Machinery- Cad program Applied to Rotary Blade Design", Institute of Agricultural and Forest Engineering, University of Tsukuba, 1-1-1 Tennodai 305, Japan

Omprash, V., and V. Ramamurti. (1989). "Dynamic Stress analysis of Rotating Turbo Machinery Bladed Disk systems". computers & secures Vol. 32, No. 2. pp. 477-488,

Oni K.C (1990). "Performance Analysis of Ridge profile rotary weeders". Agric. Mech. in Asia, Africa and Latin America, 21 (1), 43-50.

Pawar, R.B. (2004). "Design and development of Hydro-rotavator". Unpublished M.Tech. (Agril. Engg) Thesis. M.A.U., parbhani.

Potekar, J. M., and D.D. Tekale (2004). "Comparative performance of tractor drawn implements tillage system with Rotavator Tillage System". Karnataka J. Agril. Sci., 17(1):(76-80)

Quinn, T.F.J., (1977). "The importance of selecting materials for wear". Materials Engineering, 85(4); 58-61.

Reddy, J. N. (2003). "An Introduction to finite element method", Tata McGraw Hill, New Delhi

Richardson, R.C.D., (1967). "The wear of metallic materials by soil practical phenomena". J. Agric. Engg. Res. 12(1); 22-39.

Saimbhil, V. S.; D.S. Wadhwa and P.S. Grewal (2004). "Development of a Rotary Tiller Blade using Three-dimensional Computer Graphics". Biosystems Engineering 89 (1), 47–58

Sakurai, H., and J. Sakai (1989). "Study on the Mathematical model of Japanese Rotary Blade for Computer Aided Design (CAD) (Part-I)", J of JSAM, 51(1), 29-35

Salokhe,V.M., and N. Ramalingam. (2003). "Effect of rotation direction of a rotary tiller on draft and power requirements in a Bangkok clay soil". Journal of Terramechanics 39,195–205

Salokhe, V. M., W. Chuenpakaranant, and T. Niyampa (1999). "Effect of enamel coating on the performance of a tractor drawn rotavator". Journal of Terramechanics 36 (1999) 127-138

Salokhe, V.M. (1993). "Effect of blade type on power requirement and paddling quality of rotavator in wet clay soil". J. Terramechanics, 30 (5) 337-350.

Sharma, D. N., and S. Mukesh (2008). "Farm Machinery Design Principles and Problem". page no 13, 97,100,197.286-290.

Shrivastava, A. K., and R.K. Datta (2006). "Effect of different size and orientation of rectangular rotary blades on quality of paddling". Journal of Terramechanics 43 191–203

Singh, S., and A. Sharda (2000). "Effect of Selected Parameters on Field Performance of Rotary Tiller".

Song Jessica (2007). "Chair Analysis and Simulation using ANSYS software"

Sorensen, C. G., and V. Nielsen (2005). "Operational Analyses and Model Comparison of Machinery Systems for Reduced Tillage". Biosystems Engineering (2005) 92 (2), 143–155

Tanya Niyamapa, Chairat Rangdang, and Somyot Thampatpong (1993). "Rotary tiller. Bangkok (Thailand), 39 leaves".

Teruo Takahashi, Bekki E., and Taiitsu Takeda (1981). "Consideration on dynamic behavior of rotary tillers attached to tractor". Journal of Agricultural engineering 32(2), 45-52

Thakur T.C., (1991). "Design aspects of soil engaging hand tools". Agricultural Engineering Today.21:15-18.

Viector and Verma (2003). "Design and Development of Power operated Rotary weeder for Wetland paddy". Agricultural Mechanization in Asia, Africa and Latin America, 34(4):27-29

Yibin, Y., Yun,Z., and Juanqin J. (2004). "Computer Aided Analysis of Forces Acting on a Trailed plough", 96-100 Agriculture publishing House of China.

Zhang, J., and R.L.K Khuswala, (1996). "Wear and draft of cultivator sweeps with hardened edges". Canadian Agricultural Engineering, 37(1); 41-47.

http://www.finitetoinfinite.com

http://www.extencore.com

APPENDICES

APPENDIX-I

Strength calculations:

For design of rotavator it is necessary to take into account the maximum peripheral force of working blade sets and is determined by

$$\textbf{Tractor power } (P_t) = K_p \, X \, u/(75\eta_t * \eta_r)$$

where, P_t = tractor power, hp

K_p = maximum peripheral force

U = rotavator tyne velocity, m/s

η_t = tractor transmission efficiency (0.9 for concurrent revolution and 0.8-0.9 for reversed rotary)

η_r = soil resistance to 0.7-0.8

or

$$K_p = (P_t \, X \, 75 \, X \, \eta_t \, X \, \eta_r) \, / \, u$$

For 45 Hp tractor

u/v = 3

Also tractor is operated in 3rd gear, v=1.1m/s

Therefore, u = 3 X 1.1

= 3.3m/s and

Therefore,

Kp= (45 X 75 X 0.9 X 0.78) / (3.3) = 718 Kg = 7041.1747 N

Kp = 718 Kg = 7041.1747 N

Now, Torque **(Td)= Kd X R**

But Kd=Cs X Kp = 2 X 718 = 1436 Kg

Therefore Td= Kd X R, where R = radius of Rotary = 22cm

= 1436 X 22 = 31592 Kg-cm = 315920 N-mm

Td= 315920 N-mm

For 35 Hp tractor

$$u/v = 3$$

Also tractor is operated in 3rd gear, v=1.0m/s

Therefore, u = 3 X 1.0

= 3m/s and

Therefore,

Kp= (35 X 75 X 0.9 X 0.78) / (3) = 615 Kg = 6031.08975 N

Kp= 615 Kg = 6031.08975 N

Now, Torque (Td)= Kd X R

But Kd=Cs X Kp = 2 X 615 = 1230 Kg

Therefore Td= Kd X R, where R = radius of Rotary = 22cm

= 1230 X 22 = 27060 Kg-cm = 270600 N-mm

Td= 270600 N-mm

APPENDIX II

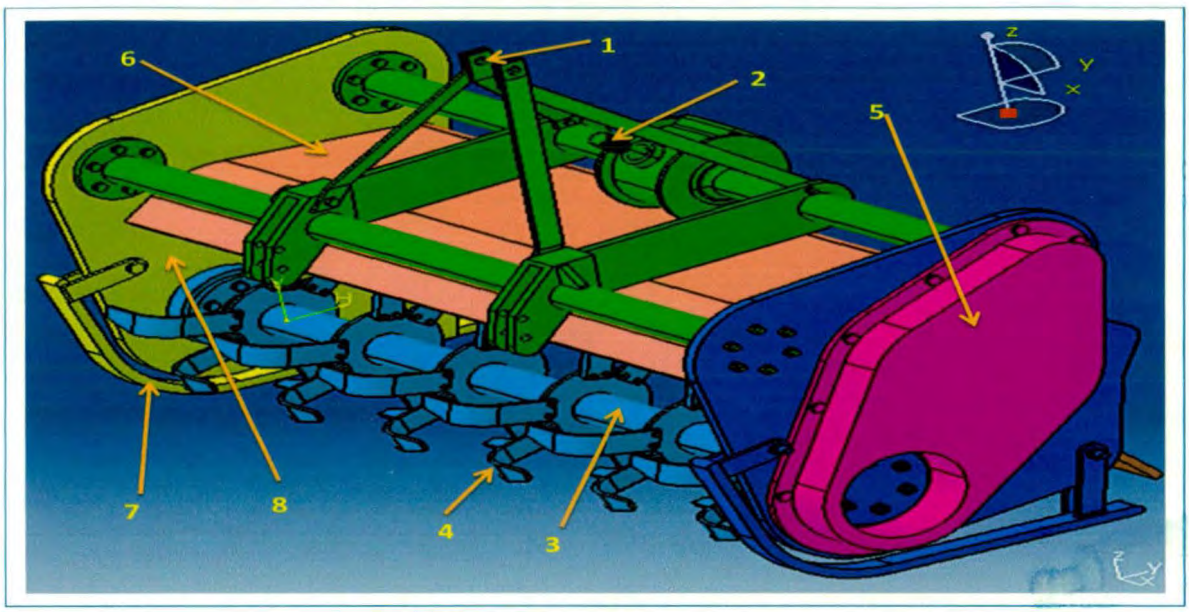

Solid Model of Rotavator

1. Independent Top Mast
2. Single / Multi Speed Gear Box
3. Chain / Gear Cover
4. Blades
5. Chain / Gear Cover Part
6. Frame and Cover
7. Adjustable depth skids
8. Central & offset able positions

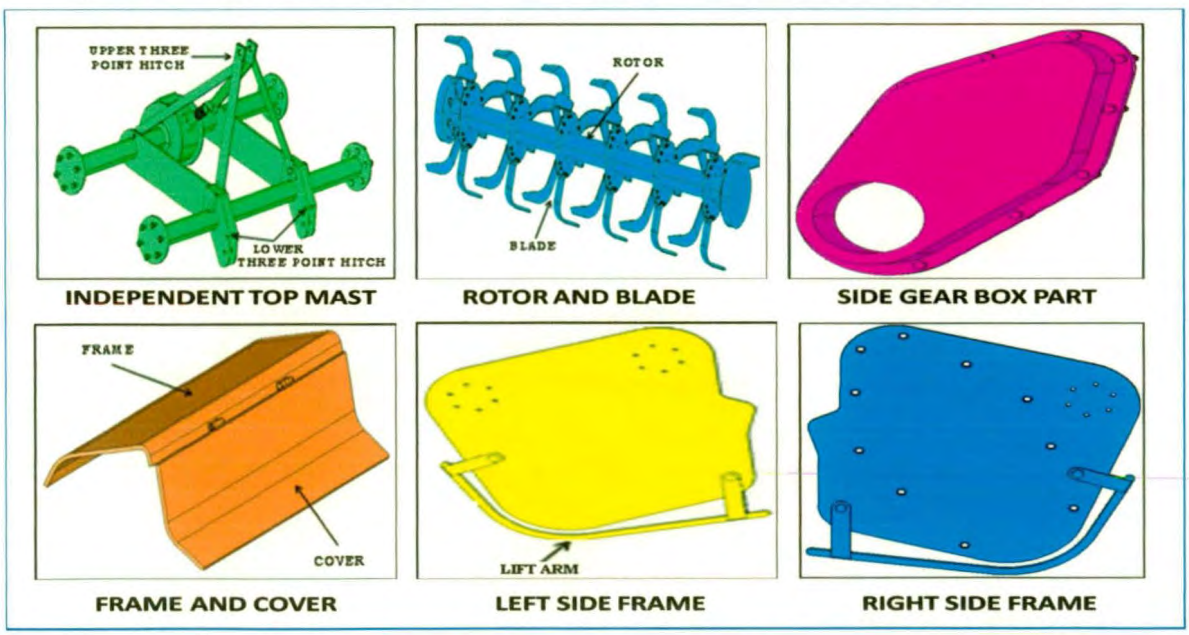

Rotavator Part's

View's of Rotavator (Solid Model and Wireframe Model)

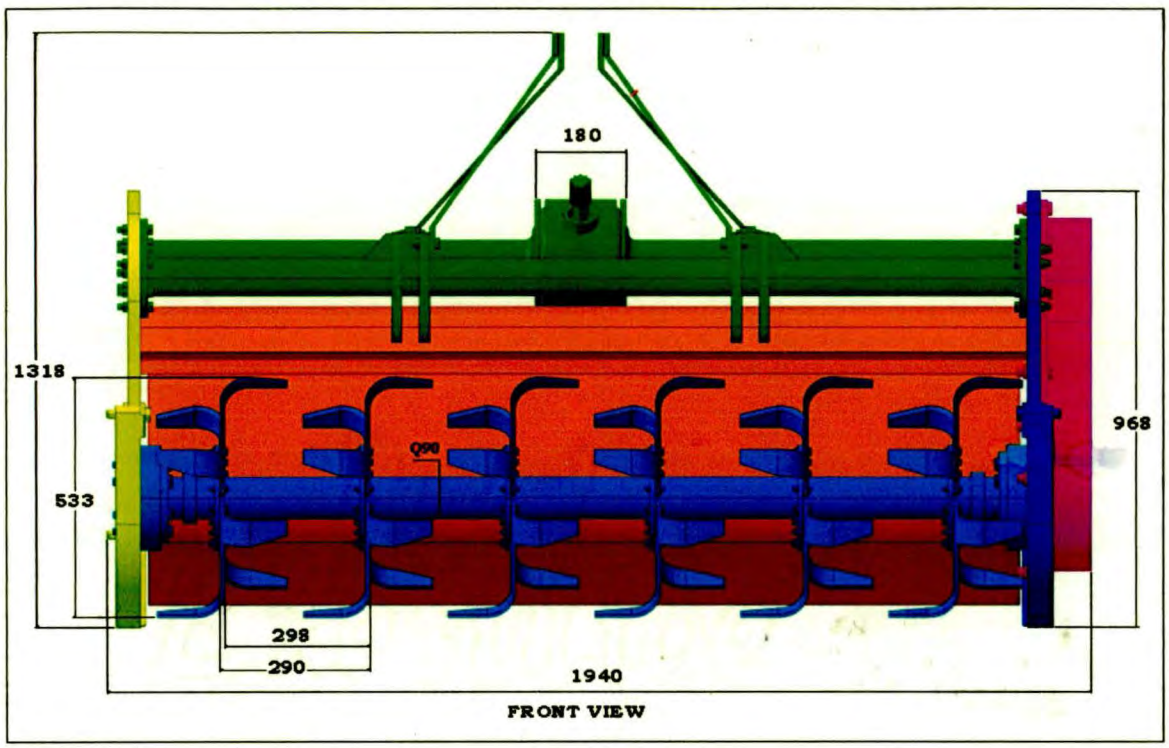

Front View

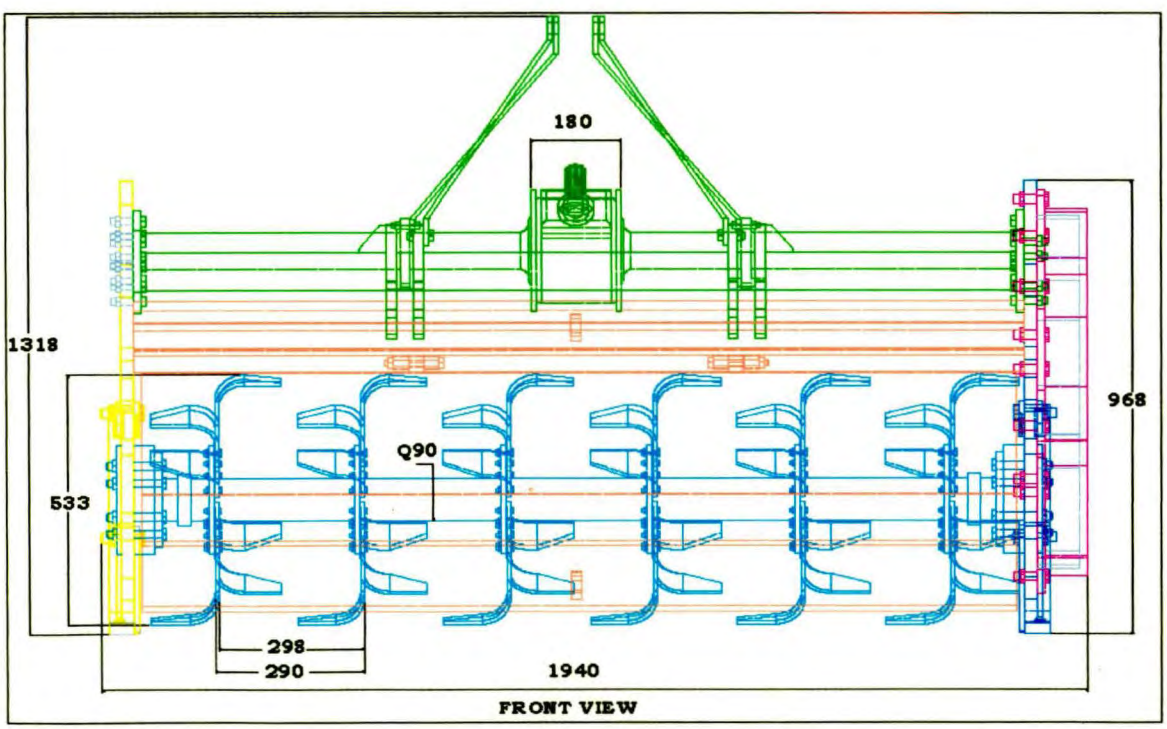

Front View

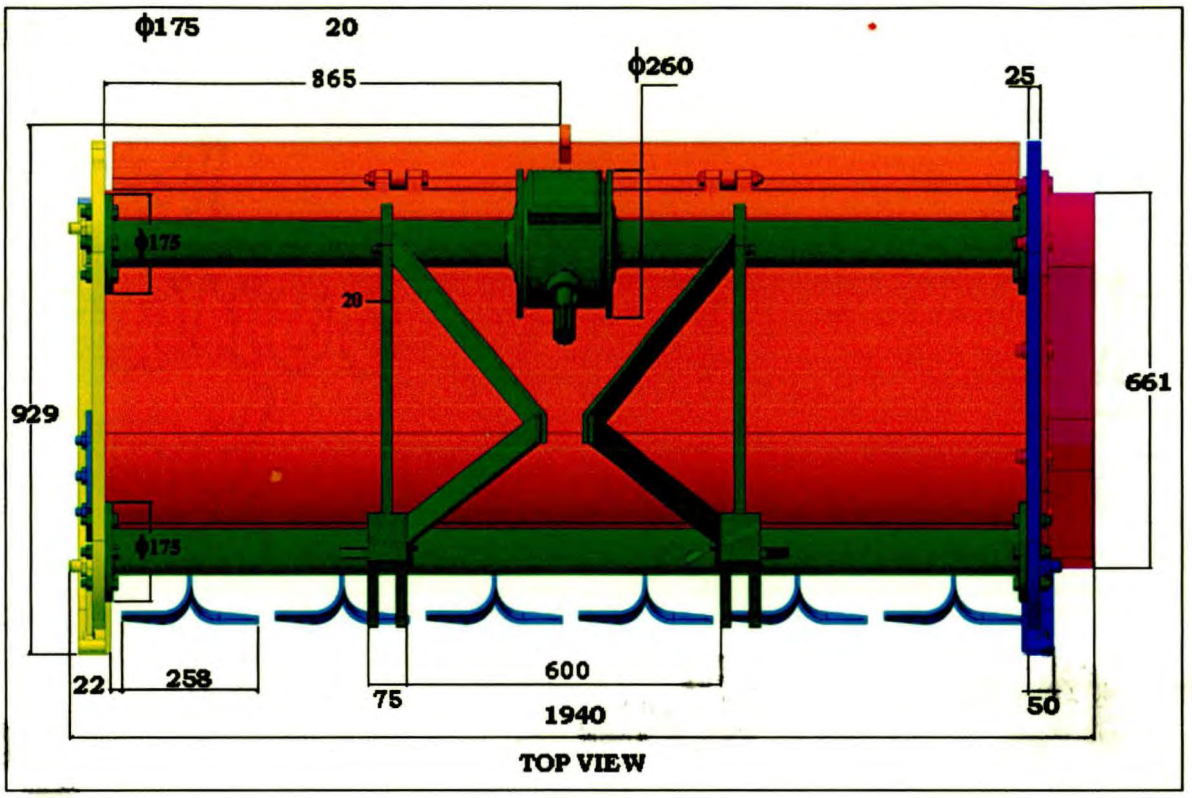

Top view

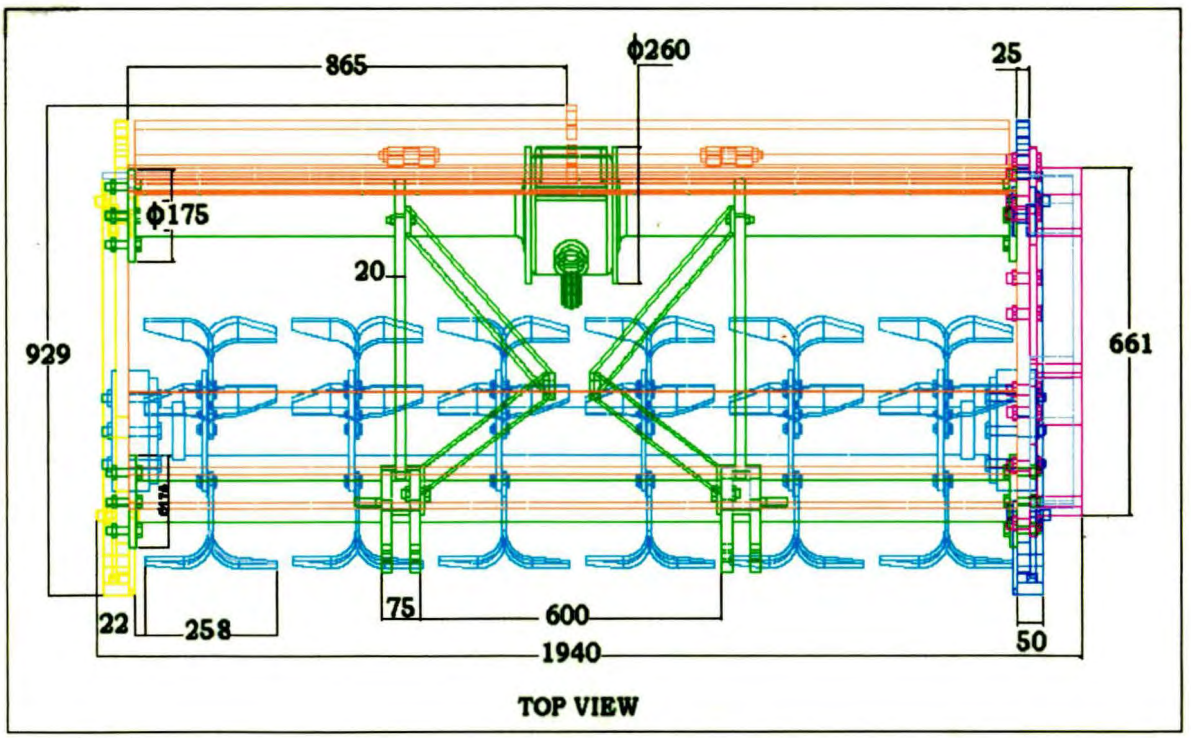

Top view

APPENDIX-III

Output file generated in Ansys for Modal Analysis

```
RESUME ANSYS DATA FROM FILE
NAME=C:\DOCUME~1\ADMINI~1\DESKTOP\MODAL\rotavator1.db

*** ANSYS GLOBAL STATUS ***
TITLE =
ANALYSIS TYPE = MODAL
NUMBER OF ELEMENT TYPES =     2
 626614 ELEMENTS CURRENTLY SELECTED.  MAX ELEMENT NUMBER =  5351939
 165773 NODES CURRENTLY SELECTED.    MAX NODE NUMBER =      634517
   10 COMPONENTS CURRENTLY DEFINED
MAXIMUM LINEAR PROPERTY NUMBER      =     2
ACTIVE COORDINATE SYSTEM            =     0 (CARTESIAN)
MAXIMUM CONSTRAINT EQUATION NUMBER  =    72
CURRENT LOAD CASE =     0 OF     0
LOAD SET  =     1
SUBSTEP   =    10
TIME/FREQ =   66.299

INITIAL JOBNAME = rotavator
CURRENT JOBNAME = rotavator

            S O L U T I O N   O P T I O N S
 PROBLEM DIMENSIONALITY. . . . . .3-D
 DEGREES OF FREEDOM. . . . . UX  UY  UZ  ROTX ROTY ROTZ
 ANALYSIS TYPE . . . . . .MODAL
   EXTRACTION METHOD. . . . . .BLOCK LANCZOS
 EQUATION SOLVER OPTION. . . . . .SPARSE
 NUMBER OF MODES TO EXTRACT. . . . . 10
 GLOBALLY ASSEMBLED MATRIX . . . . . .SYMMETRIC
 NUMBER OF MODES TO EXPAND . . . . . 10
 ELEMENT RESULTS CALCULATION . . . . . .OFF

                L O A D   S T E P   O P T I O N S
 LOAD STEP NUMBER. . . . . 1
 PRINT OUTPUT CONTROLS . . . . . .NO PRINTOUT
 DATABASE OUTPUT CONTROLS. . . . . .ALL DATA WRITTEN
Element Formation Element= 98000 Cum.  Iter.= 1 CP= 41.188
 Load Step= 1 Mode= 1.
Element Formation Element= 198000 Cum.  Iter.= 1 CP= 52.000
 Load Step= 1 Mode= 1.
Element Formation Element= 297000 Cum.  Iter.= 1 CP= 62.719
 Load Step= 1 Mode= 1.
Element Formation Element= 397000 Cum.  Iter.= 1 CP= 73.578
 Load Step= 1 Mode= 1.
Element Formation Element= 497000 Cum.  Iter.= 1 CP= 84.125
 Load Step= 1 Mode= 1.
Element Formation Element= 597000 Cum.  Iter.= 1 CP= 95.000
 Load Step= 1 Mode= 1.

      **** CENTER OF MASS, MASS, AND MASS MOMENTS OF INERTIA ****
```

```
 CALCULATIONS ASSUME ELEMENT MASS AT ELEMENT CENTROID
                    MOM. OF INERTIA       MOM. OF INERTIA
 CENTER OF MASS     ABOUT ORIGIN          ABOUT CENTER OF MASS
 XC =   790.84      IXX =  0.2265E+06     IXX =  0.1251E+06
 YC =   185.45      IYY =  0.1227E+07     IYY =  0.5082E+06
 ZC =   250.30      IZZ =  0.1193E+07     IZZ =  0.5041E+06
                    IXY = -0.1521E+06     IXY =  1131.
                    IYZ = -0.4960E+05     IYZ = -1111.
                    IZX = -0.2048E+06     IZX =  1948.

  *** ELEMENT MATRIX FORMULATION TIMES
 TYPE  NUMBER   ENAME     TOTAL CP  AVE CP
    1  626605  SOLID45     66.578  0.000106
    2       9  BEAM188     0.000  0.000000
Time at end of element matrix formulation CP= 98.21875.


 FREQUENCIES AT CURRENT LANCZOS CYCLE
   1 0.22658319E+00   2 0.20311580E+00   3 0.17327964E+00
   4 0.13994274E+00   5 0.13512951E+00   6 0.39107119E-01
   7 0.66298699E+02   8 0.56555954E+02   9 0.40799465E+02
  10 0.16644995E+02
   number of steps     :     6
   eigenvalues found   :    10
   total no. eigenvalues:    10

 LANCZOS CYCLE NUMBER =  2
    new shift:  1.9210D+05     modes still needed:       0
curEqn=    24  totEqn= 497283 Job CP sec=   173.062
    Factor Done=  0% Factor Wall sec=     0.000 rate=    0.0 Mflops

 MODE    FREQUENCY      PERIOD   PARTIC.FACTOR     RATIO     EFFECTIVE MASS     MASS
FRACTION
    1   0.391071E-01   25.571     0.11014        0.179305     0.121302E-01    0.116116E-01
    2   0.135130        7.4003    0.52742        0.858651     0.278174        0.277892
    3   0.139943        7.1458   -0.61424        1.000000     0.377296        0.639058
    4   0.173280        5.7710   -0.44437        0.723438     0.197463        0.828078
    5   0.203116        4.9233    0.20870E-01    0.033976     0.435544E-03    0.828495
    6   0.226583        4.4134    0.42328        0.689104     0.179164        1.00000
    7    16.6450       0.60078E-01 -0.30607E-07   0.000000     0.936819E-15    1.00000
    8    40.7995       0.24510E-01  0.13300E-05   0.000002     0.176896E-11    1.00000
    9    56.5560       0.17682E-01 -0.48079E-06   0.000001     0.231162E-12    1.00000
   10    66.2987       0.15083E-01 -0.25595E-05   0.000004     0.655111E-11    1.00000

Solution is done!
 *** ANSYS BINARY FILE STATISTICS
 BUFFER SIZE USED= 16384
   2095.812 MB WRITTEN ON ELEMENT SAVED DATA FILE: rotavator.esav
    184.000 MB WRITTEN ON ASSEMBLED MATRIX FILE: rotavator.full
     91.750 MB WRITTEN ON MODAL MATRIX FILE: rotavator.mode
    152.312 MB WRITTEN ON RESULTS FILE: rotavator.rst

 FINISH SOLUTION PROCESS
```

APPENDIX-IV

Output file generated in Ansys for 35 Hp tractor for dynamic analysis

***** ANSYS SOLVE COMMAND *****

*** SELECTION OF ELEMENT TECHNOLOGIES FOR APPLICABLE ELEMENTS ***

---GIVE SUGGESTIONS ONLY---

ELEMENT TYPE 2 IS BEAM188 . KEYOPT(1)=1 IS SUGGESTED FOR NON-CIRCULAR CROSS SECTIONS AND KEYOPT(3)=2 IS ALWAYS SUGGESTED.

SOLUTION OPTIONS

PROBLEM DIMENSIONALITY. 3-D

DEGREES OF FREEDOM. . . . . UX UY UZ ROTX ROTY ROTZ

ANALYSIS TYPE . . . . . .STATIC (STEADY-STATE)

GLOBALLY ASSEMBLED MATRIX . . . . . .SYMMETRIC

LOAD STEP OPTIONS

LOAD STEP NUMBER. 1

TIME AT END OF THE LOAD STEP. 1.0000

NUMBER OF SUBSTEPS. 1

STEP CHANGE BOUNDARY CONDITIONS . . . . . NO

PRINT OUTPUT CONTROLS . . . . . .NO PRINTOUT

DATABASE OUTPUT CONTROLS. . . . . .ALL DATA WRITTEN

FOR THE LAST SUBSTEP

SOLUTION MONITORING INFO IS WRITTEN TO FILE= rotavator1.mntr

Element Formation Element= 88000 Cum. Iter.= 1 CP= 112.062

Time= 1.0000 Load Step= 1 Substep= 1 Equilibrium Iteration= 1.

Element Formation Element= 184000 Cum. Iter.= 1 CP= 122.875

Time= 1.0000 Load Step= 1 Substep= 1 Equilibrium Iteration= 1.

Element Formation Element= 280000 Cum. Iter.= 1 CP= 133.719

Time= 1.0000 Load Step= 1 Substep= 1 Equilibrium Iteration= 1.

Element Formation Element= 376000 Cum. Iter.= 1 CP= 144.516

Time= 1.0000 Load Step= 1 Substep= 1 Equilibrium Iteration= 1.

Element Formation Element= 474000 Cum. Iter.= 1 CP= 155.406

Time= 1.0000 Load Step= 1 Substep= 1 Equilibrium Iteration= 1.

Element Formation Element= 570000 Cum. Iter.= 1 CP= 166.297

Time= 1.0000 Load Step= 1 Substep= 1 Equilibrium Iteration= 1.

**** CENTER OF MASS, MASS, AND MASS MOMENTS OF INERTIA ****

CALCULATIONS ASSUME ELEMENT MASS AT ELEMENT CENTROID

```
 TOTAL MASS =  1.0447
                    MOM. OF INERTIA       MOM. OF INERTIA
 CENTER OF MASS        ABOUT ORIGIN      ABOUT CENTER OF MASS
 XC =  790.84      IXX =  0.2265E+06    IXX =  0.1251E+06
 YC =  185.45      IYY =  0.1227E+07    IYY =  0.5082E+06
 ZC =  250.30      IZZ =  0.1193E+07    IZZ =  0.5041E+06
                   IXY = -0.1521E+06    IXY =  1131.
                   IYZ = -0.4960E+05    IYZ = -1111.
                   IZX = -0.2048E+06    IZX =  1948.
Range of element maximum matrix coefficients in global coordinates
 Maximum= 4.98818329E+12 at element 4932609.
 Minimum= 73184.7093 at element 5121202.
  *** ELEMENT MATRIX FORMULATION TIMES
 TYPE  NUMBER   ENAME     TOTAL CP  AVE CP
   1  626605  SOLID45     69.250  0.000111
   2       9  BEAM188      0.016  0.001736
 Time at end of element matrix formulation CP= 172.609375.
  *** ELEMENT RESULT CALCULATION TIMES
 TYPE  NUMBER   ENAME     TOTAL CP  AVE CP
   1  626605  SOLID45     65.266  0.000104
   2       9  BEAM188      0.000  0.000000
  *** NODAL LOAD CALCULATION TIMES
 TYPE  NUMBER   ENAME     TOTAL CP  AVE CP
   1  626605  SOLID45      3.875  0.000006
   2       9  BEAM188      0.000  0.000000
 *** LOAD STEP     1   SUBSTEP     1  COMPLETED.   CUM ITER =      1
 *** TIME =  1.00000       TIME INC =  1.00000     NEW TRIANG MATRIX
Solution is done!
 *** ANSYS BINARY FILE STATISTICS
 BUFFER SIZE USED= 16384
    2095.812 MB WRITTEN ON ELEMENT SAVED DATA FILE: rotavator1.esav
     131.250 MB WRITTEN ON ASSEMBLED MATRIX FILE: rotavator1.full
    1269.250 MB WRITTEN ON RESULTS FILE: rotavator1.rst
```

APPENDIX-V

Output file generated in Ansys for 45 Hp tractor for dynamic analysis

***** ANSYS SOLVE COMMAND *****

*** SELECTION OF ELEMENT TECHNOLOGIES FOR APPLICABLE ELEMENTS ***
---GIVE SUGGESTIONS ONLY---
ELEMENT TYPE 2 IS BEAM188 . KEYOPT(1)=1 IS SUGGESTED FOR NON-CIRCULAR CROSS SECTIONS AND KEYOPT(3)=2 IS ALWAYS SUGGESTED.

SOLUTION OPTIONS
PROBLEM DIMENSIONALITY. 3-D
DEGREES OF FREEDOM. . . . . UX UY UZ ROTX ROTY ROTZ
ANALYSIS TYPE . . . . . .STATIC (STEADY-STATE)
GLOBALLY ASSEMBLED MATRIX . . . . . .SYMMETRIC

LOAD STEP OPTIONS
LOAD STEP NUMBER. 1
TIME AT END OF THE LOAD STEP. 1.0000
NUMBER OF SUBSTEPS. 1
STEP CHANGE BOUNDARY CONDITIONS . . . . . NO
PRINT OUTPUT CONTROLS . . . . . .NO PRINTOUT
DATABASE OUTPUT CONTROLS. . . . . .ALL DATA WRITTEN
FOR THE LAST SUBSTEP

**** CENTER OF MASS, MASS, AND MASS MOMENTS OF INERTIA ****
CALCULATIONS ASSUME ELEMENT MASS AT ELEMENT CENTROID
TOTAL MASS = 1.0447

CENTER OF MASS	MOM. OF INERTIA ABOUT ORIGIN	MOM. OF INERTIA ABOUT CENTER OF MASS
XC = 790.84	IXX = 0.2265E+06	IXX = 0.1251E+06
YC = 185.45	IYY = 0.1227E+07	IYY = 0.5082E+06
ZC = 250.30	IZZ = 0.1193E+07	IZZ = 0.5041E+06
	IXY = -0.1521E+06	IXY = 1131.
	IYZ = -0.4960E+05	IYZ = -1111.
	IZX = -0.2048E+06	IZX = 1948.

*** MASS SUMMARY BY ELEMENT TYPE ***

TYPE	MASS
1	1.04163
2	0.303311E-02

Range of element maximum matrix coefficients in global coordinates
Maximum= 4.98818329E+12 at element 4932609.
Minimum= 73184.7093 at element 5121202.

*** ELEMENT RESULT CALCULATION TIMES

TYPE	NUMBER	ENAME	TOTAL CP	AVE CP
1	626605	SOLID45	54.844	0.000088
2	9	BEAM188	0.000	0.000000

```
 *** NODAL LOAD CALCULATION TIMES
TYPE  NUMBER   ENAME     TOTAL CP  AVE CP

   1  626605  SOLID45      3.172   0.000005
   2       9  BEAM188      0.000   0.000000
*** LOAD STEP    1   SUBSTEP    1  COMPLETED.   CUM ITER =      1
*** TIME =   1.00000        TIME INC =   1.00000      NEW TRIANG MATRIX

*** NOTE ***                      CP =     232.328   TIME= 11:48:05
Solution is done!

*** ANSYS BINARY FILE STATISTICS
 BUFFER SIZE USED= 16384
   2095.812 MB WRITTEN ON ELEMENT SAVED DATA FILE: rotavator1.esav
    131.250 MB WRITTEN ON ASSEMBLED MATRIX FILE: rotavator1.full
   1269.250 MB WRITTEN ON RESULTS FILE: rotavator1.rst

PRODUCE ELEMENT PLOT IN DSYS =   0

FINISH SOLUTION PROCESSING
```

APPENDIX-VI

Table 1 maximum deformation for different frequency ranges

Sr. No.	Component Name	Maximum Deformation (mm) for different frequency range (Hz)									
		0.0350509	**0.12474**	**0.13638**	**0.16626**	**0.18940**	**0.22161**	**16.645**	**40.799**	**56.556**	**66.299**
1	Independent top mast	2.119	1.660	1.373	1.70	1.144	1.575	0.516	0.3774	2.883	0.569
2	Blade	0.688	1.431	1.091	1.682	1.923	1.651	0.8766	0.3751	0.252	0.713
3	Side gear box part	1.597	1.287	1.449	1.645	1.043	1.684	0.751691	0.3697	0.248	0.658
4	Frame & Cover	1.457	1.510	1.349	1.479	1.95	1.526	4.313	5.994	1.973	4.242
5	Left side frame	1.784	1.682	1.279	1.767	2.012	1.095	0.9250	0.4166	0.385	1.325
6	Right side frame	1.640	1.251	1.428	1.739	1.309	1.693	0.845	0.3593	0.274	1.096

Table 2 Displacement and stress plot for 35 Hp tractor

Sr. No	Component Name	Displacement (mm)				Stress (Mpa)			
		X axis	Y axis	Z axis	D.V.S.	X axis	Y axis	Z axis	V.M.S.
1	Independent top mast	1.012	1.731	2.791	2.91	172.669	135.735	268.441	404.29
2	Blade	-0.036	6.016	1.008	**6.757**	183.947	440.334	253.896	**417.03**
3	Side gear box part	-0.0497	5.626	2.939	5.658	11.139	8.867	9.896	15.637
4	Frame & Cover	0.0147	5.945	3.48	6.057	23.191	8.403	7.89	16.864
5	Left side frame	0.2466	5.994	3.423	6.526	22.517	33.905	39.758	56.267
6	Right side frame	0.2637	6.172	3.273	6.684	25.181	40.016	52.561	55.383

Table 3 Displacement and stress plot for 45 Hp tractor

Sr. No	Component Name	Displacement (mm)				Stress (Mpa)			
		X axis	Y axis	Z axis	D.V.S.	X axis	Y axis	Z axis	V.M.S.
1	Independent top mast	1.18	2.026	3.268	3.399	201.453	158.683	313.835	471.47
2	Blade	-0.043	7.028	1.179	**7.893**	223.288	529.775	304.364	**503.21**
3	Side gear box Part	-0.0591	6.574	3.43	6.612	13.021	10.3589	11.561	18.282
4	Frame & Cover	0.0162	6.946	4.065	7.893	27.055	9.808	9.207	19.675
5	Left side frame	0.284	6.993	3.999	7.683	26.265	39.513	61.351	65.618
6	Right side frame	0.308	7.213	3.82	7.609	29.431	46.814	46.453	64.732

APPENDIX-VII

Deformation plots for different frequency ranges

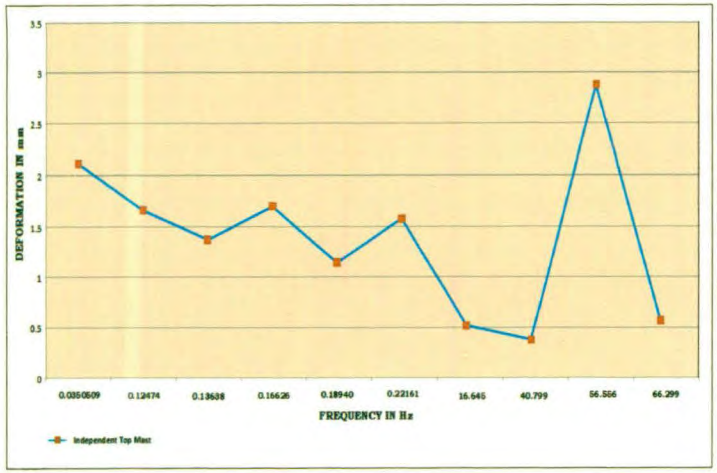

Deformation in independent top mast

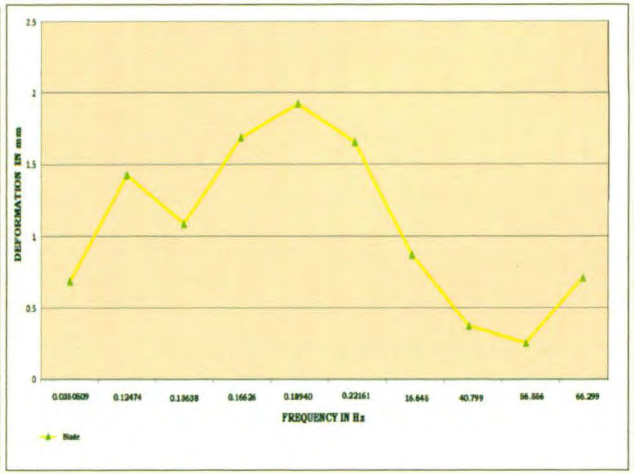

Deformation in Blade

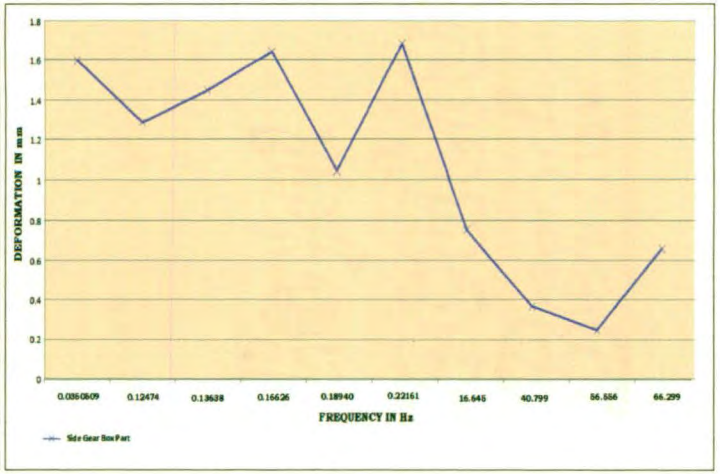

Deformation in side gear box part

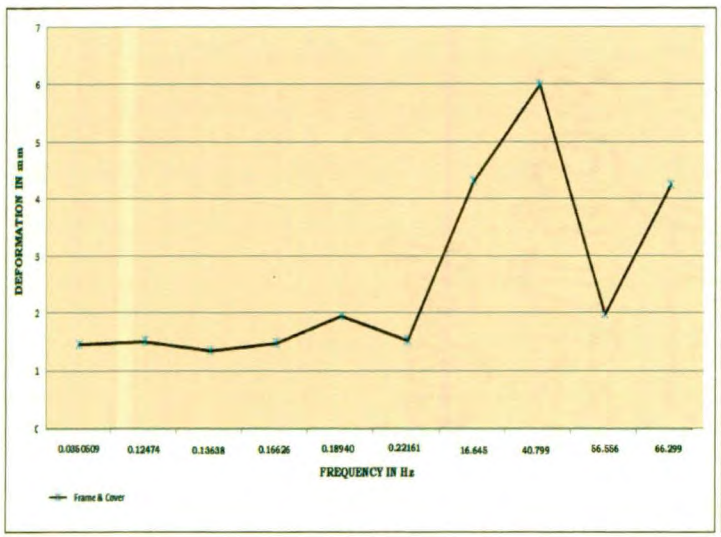

Deformation in frame & cover

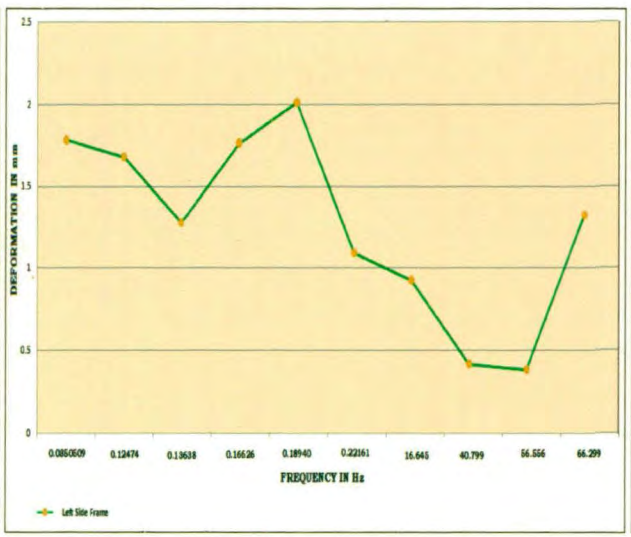

Deformation in left side frame

Deformation in right side frame

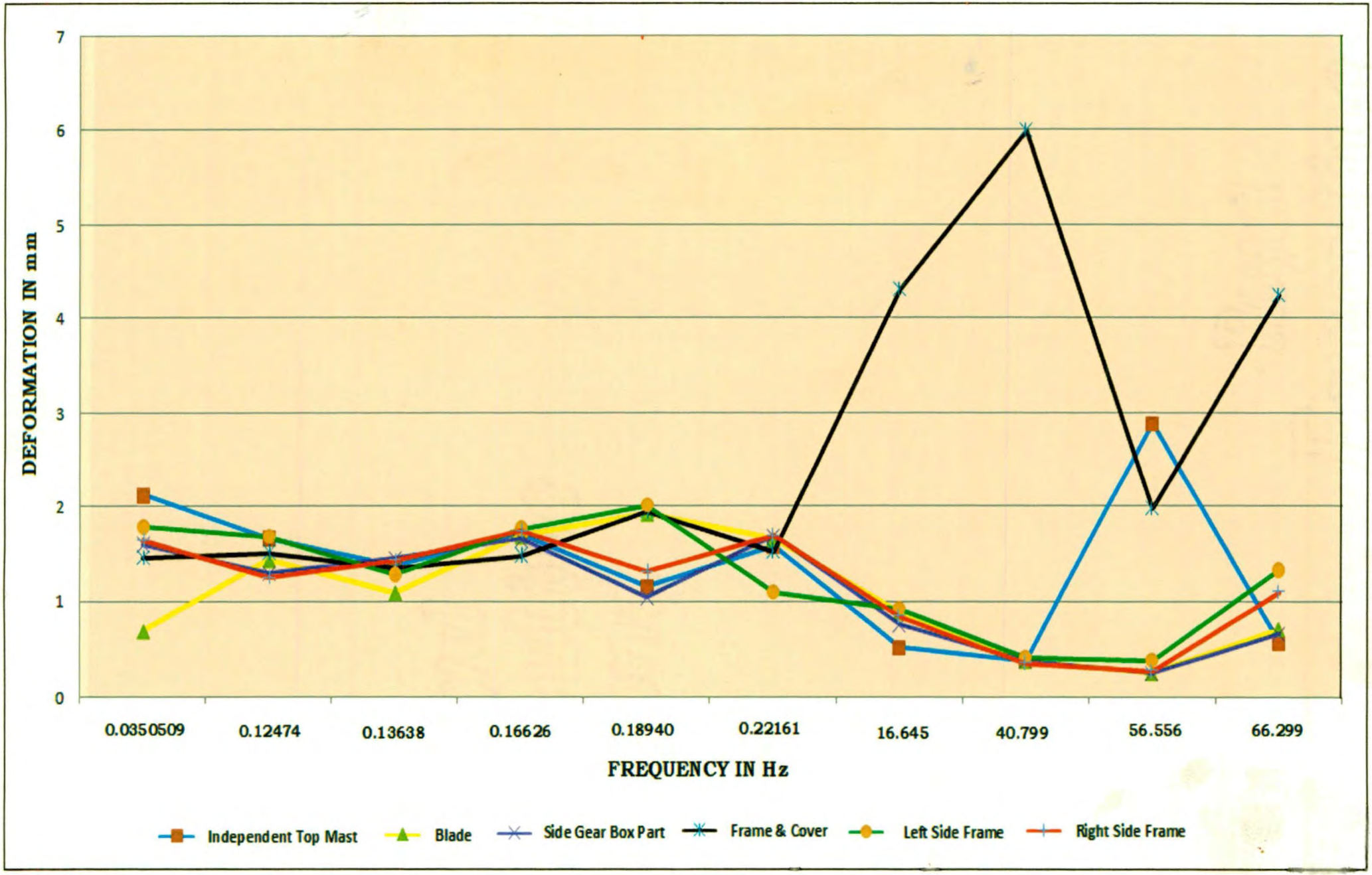
DEFORMATION IN mm
7
6
5
4
3
2
1
0
0.0350509
0.12474
0.13638
0.16626
0.18940
0.22161
16.645
40.799
56.556
66.299
FREQUENCY IN Hz
Independent Top Mast
Blade
Side Gear Box Part
Frame & Cover
Left Side Frame
Right Side Frame